DOE/CE/15401--T13

CeramPhysics, Inc.
921 Eastwind Drive, Suite #110, Westerville, Ohio 43081
Telephone (614) 882-2231 FAX (614) 882-1437

DOE/CE/15401--T13
DE92 001884

FINAL TECHNICAL REPORT

Dept. of Energy Contract No. DE-FG01-88CE15401

A Miniature Inexpensive, Oxygen Sensing Element

by

R.W. Arenz RWA

October 7, 1991

Distribution

J. Aellen - DOE
Calvin Lee - DOE
OSTI - DOE
J. Ryan - DOE
R. Tostevin - GBC
W. N. Lawless - CPI
C. F. Clark - CPI

TABLE OF CONTENTS

PAGE

I. SUMMARY.....1

II. INTRODUCTION.....2

III. THEORY.....4

IV. ORIGINAL PROPOSED CONCEPT AND ENVISIONED AREAS OF DEVELOPMENT.....8

V. SENSOR HEATING AND RELATED DESIGN MODIFICATIONS.....11

VI. THERMAL EXPANSION STUDIES.....16

VII. SEALING MATERIALS AND METHODS SEARCHES.....18
- A. Search of Commercially Available Ceramic Adhesives/Sealants.....19
- B. Braze Sealing.....25
- C. "Soft" Seals.....26
- D. Glass Seals.....27

VIII. FINAL REDESIGN.....29

IX. FINAL SEAL MATERIALS AND CHARACTERISTICS.....31

X. ELECTRODING AND LEAD ATTACHMENT STUDIES.....34

XI. IONIC CONDUCTIVITY STUDIES.....38

XII. MATERIALS DEVELOPMENT AND OS-3 PARTS PRODUCTION.....40

XIII. ASSEMBLY PROCEDURES.....43

XIV. SENSOR TESTS AND RESULTS.....47

XV. AMPEROMETRIC SENSOR STUDIES.....56

XVI. CONCLUSIONS AND AREA FOR FUTURE DEVELOPMENT.....65

REFERENCES

APPENDIX A. PHOTOGRAPHS

APPENDIX B. THEORETICAL DISCUSSION OF AMPEROMETRIC OXYGEN SENSING

FIGURES

I. SUMMARY

An exhaustive study was conducted to determine the feasibility of Nernst-type oxygen sensors based on ceramics containing Bi_2O_3 (having oxygen ionic conductivities ~ 30-50 times larger than ZrO_2:Y_2O_3). The basic sensor design consisted of a ceramic sensing module sealed into a metal tube. The module (which underwent several design changes) accommodated an internal heater and thermocouple; modules were fabricated under subcontract by GBC Materials Corp. using dry-pressing production methods.

Thermal-expansion-matched metals, adhesives, and seals were researched and developed, consistent with sequential firings during sensor assembly. Significant effort was devoted to heater design/testing and to materials' compatibility with Pt electrodes. A systematic approach was taken to develop all sensor components which led to several design modifications.

Prototype sensors were constructed and exhaustively tested side-by-side with a zirconia Nernst sensor. Prototype sensors were successfully operated as low as 600 °C; however, the full Nernst output voltage was never achieved (nor could it be determined experimentally why this was the case). Three other problem areas were discovered: (1) Long-term signal instabilities; (2) Erratic, non-reproducible phenomena; and (3) A completely leak-tight seal was closely approached but never fully realized.

The exhaustive studies in this program led to more problems than solutions for this type of sensor, and it is concluded that development of Nerst-type oxygen sensors based on Bi_2O_3 will require much further effort and application of specialized technologies.

However, during the course of this 3-year program much progress was reported in the literature on amperometric-type oxygen sensors, and a minor effort was devoted here to this type of sensor based on

Bi_2O_3. These studies were made on Bi_2O_3-based ceramic samples in a multilayer-capacitor-type geometry (available from a previous program), and amperometric-type oxygen sensing was demonstrated at very low temperatures (~ 160 °C). A central advantage here is that these types of sensors can be mass-produced very inexpensively (~ 20-50 cents per unit). Research is needed, however, to develop an optimum diffusion-limiting barrier coating.

In summary, the original goals of this program were not achieved due to unforeseen problems with Bi_2O_3-based Nernst sensors. However, a miniature amperometric sensor base on Bi_2O_3 was demonstrated in this program, and it is now seen that this latter sensor is far superior to the originally proposed Nernst sensor (i.e., much lower operating temperature, no need for a reference gas, simple design, and mass-producible at very low-cost).

II. INTRODUCTION

This Final Report details the work performed by CeramPhysics, Inc. (CPI) of Westerville, Ohio, and GBC Materials, Inc. (GBC) of Latrobe, Pennsylvania, toward the development of a miniature, inexpensive oxygen sensor based on solid oxygen-conducting electrolytes proprietary to CPI ("OS" materials). The goals at the beginning of this program were to produce a number of self-contained, prototype sensing units for rigorous testing, and to bring the technology/methodology of producing those units up to the manufacturing level should the prototypes test satisfactorily.

The novelty of our proposed sensor concept was that the formability, raw material and fabrication costs, and other properties of the OS materials would lead to the production of miniature, accurate, versatile devices with many advantages over extant zirconia sensors: cost would be less than $20 per unit compared to greater than approximately $50 per zirconia unit, operating temperatures would be ~ 150 °C lower, and the OS sensors would be more rugged,

i.e. less susceptible to thermal shock. The small size and the ceramic forming technology available through GBC would allow the inclusion of a small heater and a tiny thermocouple directly into the sensor. (These elements are often added separately in systems utilizing generally larger zirconia components; the sensing element must be heated and the resultant temperature must be known when using all sensors of the type under discussion.) We felt sensors with these advantages could readily be incorporated into home heating controls to further promote the efficiency of natural gas combustion in appliances such as furnaces and water heaters.

Though we still have this vision, we have not been able to achieve our goals in the course of this contract. That is, we have not produced large numbers of proven devices for exhaustive test and we have not worked out some fabrication details to the extent which would be required for manufacturing. However, our researches have demonstrated that complex shapes may be fabricated from the OS materials and that these materials do conduct oxygen at the same levels as zirconia at temperatures at least 100 °C lower than zirconia. Our researches have given good indication that with expert assistance sealed structures of metal and OS materials may be realized and that self-contained miniature sensors of low cost are not out of the question.

Further, our researches have discovered that tiny multilayer structures of OS materials ($\sim< 0.125$ cm^3) may be of use as amperometric oxygen sensors and these may function at temperatures as low as $\sim$ 200 °C. This development is a further leap toward realization of a device with utility in the home heating market, as these devices are even simpler, lower in cost, more rugged, and pose fewer constraints for use than the Nernst sensor configuration we originally proposed and which has been the prime focus of this contract study.

III. THEORY

One of the most common configurations used in chemical species sensors is that of the "Nernst cell". Nernst cells consist of an electrolyte barrier separating two "regions" which differ in concentration of the chemical species to be detected. The electrolyte itself is of a material which selectively conducts ions of the species. The difference in the species concentrations gives rise to a chemical potential which tends to re-establish equilibrium, driving ions of the species through the electrolyte from the higher concentration side to the lower.

In practice the electrolyte is electroded on each of the faces in contact with the regions. This electroding plays a triple role: First it catalyzes the conversion of molecules/atoms of the species into the ions for transport through the electrolyte; Second, it aids transfer of the ions into the electrolyte; and third, as ions are produced and as the chemical potential drives them through the electrolyte, the electrodes supply and collect the various transferred electrical charges.

As charge carriers are re-arranged within the system, an electrical potential is created which opposes the driving chemical potential. If the electrodes on the electrolyte are not shorted by an external circuit, an equilibrium will be achieved such that the chemical potential is opposed and balanced by the electrical potential, and the electrical potential will be directly related to the causal imbalance in species concentrations.

The "Nernst Equation" is the mathematical relationship describing the interrelationships at equilibrium. The resultant electrical potential (EMF) which is established in a gaseous system is given by:

$$EMF = t_i(RT/nF)\ln(P_{ref}/P_{unk}) \qquad (1)$$

where R is the gas constant, T is the absolute temperature of the system, n is the number of electrons involved in the electrode reaction, F is the Faraday constant, and P_{ref} and P_{unk} are the partial pressures of oxygen on each of the two sides of the electrolyte. t_i is the ionic "transference number"; we will describe this parameter further below.

In application to the oxygen detecting Nernst Cell, "n" in the equation is 4, i.e. each oxygen molecule at one electrode captures four electrons during catalysis to become two oxygen (charge -2) ions. Further, the oxygen partial pressure on one side of the electrolyte (P_{ref}) must somehow be controlled or otherwise known absolutely, so that the measurement of the EMF may be related to one unknown (P_{unk}). Generally, the gas used on the reference side of the sensor is air, and P_{ref} becomes the nearly constant atmospheric oxygen partial pressure 0.209 atm. (For most accuracy this value for atmospheric oxygen content should be corrected for the reductive effect of humidity. Such corrections, however, were not made during the course of this study due to a lack of hygrometry equipment.) [1]

The "transference number" in the Nernst Equation is a ratio describing the nature of the electrolyte itself. That is, we have discussed the model as though only ions are transferred through the electrolyte and free electrons might travel only through an external path (e.g. a wire) connecting the opposing electrodes. In reality this is not the case, and the electrolyte, though preferrentially conducting ions, also has some conductivity to electrons. The transference number ratio is the relative comparison of the conductivity of the electrolyte to ions to the total conductivity (ions plus electrons) of the electrolyte. In useful oxygen conducting materials, such as the OS materials and zirconia, this transference ratio is very near 1.0 under most circumstances, i.e. there is very little electronic conduction through the electrolyte.

Transference ratio not near 1.0 for zirconia and the OS materials does occur in situations in which at least one face of the electrolyte is exposed to reducing gases with very low oxygen partial pressures ~ 10^{-25}. These reducing atmospheres attack and reduce the electrolyte, and the membrane increasingly becomes electronically conductive as the stoichiometry of the material changes. Electrons begin to migrate along with the ions, at least partially canceling the charge separation which normally occurs, and the EMF generated is less than would be expected. [2]

Ionically conductive electrolytes do NOT conduct ions uniformly with temperature; as is generally true, conduction of charge through a solid is a temperature dependent phenomenon. The ionic conduction of zirconia and of the OS materials is described by the Arhenius-type equation:

$$\sigma T = \sigma_0 \exp(-\theta/T) \qquad (2)$$

where T is absolute temperature, the σ's are conductivities, and $\theta = Q/k$ where Q is the activation energy and k is the Boltzmann Constant. For a given material θ and σ_0 are constants which relate the intrinsic physical behavior of the material. For the OS-3 material σ_0 has been measured at CPI and at the Argonne National Laboratory to be 6.187×10^7 $(\text{ohm-cm})^{-1}$ and θ 1.234×10^4 (K). By comparison a typical highly conductive zirconia composition has σ_0 of 1.62×10^6 $(\text{ohm-cm})^{-1}$ and θ of 1.20×10^4 (K). Thus for typical geometries components of OS materials or zirconia must be heated well above room temperature to have appreciable conductivities, or equivalently, low impedances; the impedance must be low enough to provide a low-noise signal easily measurable by a voltmeter or other voltage measurement device. As may be seen, for any given temperature and geometry, OS materials are greater than 30 times more ionically conductive than zirconias, and this is an advantage in many applications.

Perhaps more dominant than the effect of temperature on the conductivity of the oxygen Nernst cell is the effect of the temperature on the behavior of the catalysis at the electrodes and the nature of the electrode/electrolyte interface. There is a vague "threshold" temperature for a given sensor at which stable EMF's due to concentration differences/changes are generated within a usefully short time. At lower temperatures, using present common electroding systems, Nernst oxygen sensors develop and exhibit a number of non-Nernstian behaviors, including "parasitic" voltages which appear though both sides of the electrolyte are under exposure to the same oxygen partial pressure! Some of the behaviors here are not well understood in the field of electrochemistry, and the hypotheses presented by some researchers are beyond the scope of this report. We simply note most extant zirconia-based Nernst sensors must be heated to temperatures above 700 °C to provide stable voltage output of theoretical magnitude given known oxygen partial pressure. In contrast, earlier studies at CPI have demonstrated OS-based sensors may be operated at ~ 600 °C. Lower temperatures may be achievable for sensors of either material given development of other, novel, electrode systems. [3]

Elevated temperature operation solves some problems but adds others. One such added difficulty is due to further aspects of the chemistry and catalytic reactions at the electrodes. For example, if carbon monoxide (or ANY combustible) is present in a gas sample which also contains free oxygen, the electrodes not only catalyze the reduction of the oxygen, but the reaction of the free oxygen with the monoxide to produce carbon dioxide (or with the combustible to form by-product species) as well. The electrochemistry becomes complicated by these reactions, and the EMF generated no longer corresponds to the oxygen concentration present. [4]

The high temperatures required for operation also lead to difficulties in hermetic sealing. The Nernst cell configuration requires that the electrolyte must form an impenetrable boundary between the

reference and sample regions. Any leakage and interchange of chemical species between the sample and reference sides other than the ion interchange through the electrolyte will poison the reference and/or sample concentrations and the cell voltages will not relate to what one is attempting to measure. High temperature sealing of materials is a still-developing frontier of technology; we will discuss some of these challenges below. The problems of forming hermetic seals at high temperatures have strongly influenced the design of Nernst oxygen sensors.

Our discussion above disclose some of the shortcomings of the Nernst oxygen sensor, i.e. it requires a reference gas of known oxygen partial pressure, it does not reliably measure oxygen partial pressure in ALL situations, there is a temperature dependance to the measurement and sensor behavior, and elevated temperatures are required for operation. Nevertheless, within all these limitations, Nernst sensors have found wide, successful application in a large number of situations: they are routinely used in automotive carburetion control, industrial furnace and kiln control, and quantitative gas analysis. We have felt, and continue to feel, that the unique and "less restrictive" properties of OS materials over zirconia-based materials might broaden the base of application.

IV. ORIGINAL PROPOSED CONCEPT AND ENVISIONED AREAS OF DEVELOPMENT

Our proposed OS sensor design might be contrasted with typical designs of zirconia sensors. Zirconia as a material has a high compressive strength, a very high sintering temperature (melting point ~ 2600 °C), a moderately high thermal expansion (~10 x 10^{-6} m/m-°C), and a relatively low thermal conductivity (~2 W/m-K). [5] Due to the high sintering temperature, geometries which may be produced in zirconia using present ceramic technology have been limited to relatively "simple" forms with relatively "robust" dimensions -- e.g. "thick" tubes, plates, pellets and disks. It

may be noted that the thicker the element, the lower the ionic conductance of the part at a given temperature; to increase the conductance for the sake of sensor operation then requires an increase in the temperature of operation. Further, the added thickness (and length -- see below) add to the materials costs for the sensor.

Partially due to the limits on geometries which may be formed, and partially to avoid the problems and demands of high temperature sealing (discussed below), a zirconia sensing device is often a single, seamless piece (e.g. a tube) of material which is extended from a heated region used for the sensing (a portion of the tube is placed in a furnace) to a lower temperature manifolding joint (an O-ring compression fitting or a compressed graphite seal). The manifolding joint is required because the sensor must have access to a reference gas. Length is generally required to give the joint sufficient thermal stand-off from the hot sensing region so that the seal joint does not deteriorate.

Figure 1 embodies the concept CPI initially proposed for the OS material miniature sensor. We felt this design was sound based upon a number of facts we felt were well-proven at the time of our proposal. First, measurements on the OS-materials from two universities indicated that the thermal expansion of these materials was ~5.2 x 10^{-6} m/m-°C at room temperature, which closely matched the expansion of the metal alloy Kovar (specially developed for and commonly used in glass-metal sealing applications). This expansion was also quite close to the expansion of common, inexpensive electronic substrate/structural ceramics which are readily pressed in a variety of complex forms from powders. Next, the technology for sealing such ceramics to Kovar is well-developed and routine. Finally, in preliminary tests CPI had found readily available ceramic adhesive materials which joined and seemed to seal small test structures of OS-materials to samples of the substrate/structural ceramics.

The novel concept presented in Fig. 1 was built upon the foundation of the thermal expansion match between the materials just listed. The OS sensing element could be quite small since other materials could be used for the bulk of the construction. The ease of forming and machining the other materials promised that complex shapes could be used, if required, in the sensor. The ceramic/ refractory properties of the OS materials, themselves, promised to ease the production of OS parts since they could be readily pressed from powders in any variety of required shapes and dimensions and fired at rather low temperatures.

Given the small size and lowered working temperature of the sensing element and the good thermal stand-off characteristics of the other materials, we envisioned that a small internal heater could supply the electrolyte heating requirements. The small size and practicality of forming complex structures in the manifold ceramics made it easy and reasonable to include a thermocouple in the design to monitor the temperature necessary to interpret Nernst cell readings. Finally, the small size and the low cost of all the materials suggested the cost of the complete sensor would be quite low.

A further vision for the design of Fig. 1 was that the bottom of the tube could be sealed and the cavity filled with a gas of known oxygen partial pressure (e.g. 100% pure oxygen). In this manner the sensor could have been rendered independent of the partial pressure of oxygen in surrounding air (the reference used in the open-ended tube configuration), and the sensor would be freed from manifolding to be used as a completely self-contained device which could function in many different environments where supplying a reference would be impractical (e.g. oxygen sensing in a mine shaft).

A prime concern for the development of the concept in Figure 1 and its evolution into the "sealed reference" device was that of the required hermetic sealing of the sensing element to the other

components. Hermetic seals for high temperature use are not necessarily straightforward: such seals are subject to various deleterious aging and chemical changes promoted by elevated temperature. Further, a high-temperature seal must experience the large temperature swing and subsequent thermal expansion shock involved between room temperature startup and heating to operating temperature; this is compounded if the seal must withstand the rigors of on-off cycling operation. Great care must be exercised to match the thermal expansion characteristics of dissimilar materials which are to be joined for high temperature use, or to use seals which are non-rigid (malleable or slip fit).

As was mentioned earlier, all available information at the time of our proposal indicated an excellent expansion matching existed between the OS materials and commonly available metals and ceramics which had been perfected for hermetic sealing in the electronics industry. Thus, it seemed quite certain the design of Figure 1 was feasible. The only question remaining regarded how these seals would hold up during aging and cycling in the chemistry of exhaust environments. Therefore, we planned that seal integrity over time would be rigorously tested on our prototype devices during the course of this contract.

V. SENSOR HEATING AND RELATED DESIGN MODIFICATIONS

As we considered our first working design of Fig. 1, we eventually realized that the external placement of the heater required that the heater leads pass external to the Kovar tube or through the sensor head. The former case would complicate the sealing of the Kovar tube to the manifold and the passage of the heater leads to the outside world, and the latter case would require a more complicated hermetic sealing of the sensor head. The design of Fig. 2, with the heater internal to the sensing head was proposed and adopted.

As a part of contract work, we began investigating the engineering of heater design. Worst-case estimates made at the time of proposal, based on Kovar conduction alone without considering convective transport by surrounding gases or radiative transfer, indicated a heater of only 6.7 W was required to support 600 °C operation. To allow for the other heat transport mechanisms, we decided to over-design, and began considering how we might achieve a heater of 10 W output within the space limitations of Fig. 2. A complex set of inter-relationships was discovered; we discuss these below.

Our original design was that the overall sensor o.d. be 3/8" (0.375"). Consultation with G.B.C. revealed that the limits of inexpensive pressing/forming technique required the "collar" wall thickness to wall length ratio be no smaller than 1:5. Given a heater device 0.250" high, the wall thickness could be no less than 0.050", and to this thickness had to be added another ~0.050" to safely form the long, tiny holes required to encapsulate the thermocouple leads and the thermocouple head. The final estimate was that the collar wall had to be minimum 0.100" thick, thus reducing the heater to 0.175" o.d. and 0.250" long, while still retaining a hole of significant size in the center for air/reference gas exchange with the sensing disk. We took these constraints to the engineering departments of several commercial electric heater companies. At the time, none of these companies produced any heating cartridges or devices of approximately the 0.175" o.d. x 0.250" long size which operated at our required temperature and wattage. Further, the engineers contacted felt designing a heater to meet our needs would be "difficult".

Custom heater design by these companies was out of the question given the financial limits of our contract. One attractive type of heater which might have been provided through professional design is the thin-film "meander track" platinum heater, but the printing of such thin-film tracks is beyond current CPI ability. Therefore, we began investigating the design of inexpensive, traditional, high resistance wire heaters on our own.

Several resistance wire manufacturers were contacted and samples and design literature were obtained. We discovered that there are numerous considerations in heater design: heater lifetime is affected by wire thickness, thermal cycling (including use of A.C. as opposed to D.C. currents), environment, total power output and heat dissipation/operating temperature, and heater support and geometry. Regarding the latter point, as example, our manufacturing reference books indicated that if a coil were used, certain width/length ratios for the coil were preferred; but it was unclear whether this preference was merely to ease manufacture, to prevent mechanically over-stressing and embrittling the wire, or to prevent concentrated heat loads which might somehow shorten heater life. One looming consideration for us was also the availability of materials in the small quantities needed for this research program: as we checked resistance wire suppliers, we found our selection was extremely limited. This factor did help narrow the number of variables with which we might have dealt.

We performed simple tests in which we passed A.C. and D.C. currents through samples of various resistance wire alloys. The tests were conducted in air and the wire was formed into various configurations: e.g. straight lengths, bare coils, coils enclosed in mullite holders, and potted coils cemented to OS parts. These tests were not exhaustive and systematic, but did indicate that we could achieve heating of the amount desired using small coils. We also found these simple coils could sustain heating over long periods of time ... at least as long as the 7 days spanned by our longest test. A few test coils did fail and gave us indication that the coiling process occasionally weakened points in the wire which led to early heater failure. Potting in various ceramic adhesives and in OS materials was tried, but we experienced a higher failure rate in potted as opposed to unpotted coils.

Despite the higher failure rates, we adopted the use of potted coils in the program for several reasons: First, coiling seemed the best method to get the desired heating power into the desired

space. Further, potting with a ceramic adhesive/potting agent specifically designed to coat heater coils seemed necessary to provide electrical insulation of the electroding in the sensor from the heater. Finally, we felt it vital to have potting to aid in the heat transfer between the heater and the sensor disk.

We also performed many experiments on various methods of attaching low-resistance copper leads to the heater coil. We investigated the use of crimp connectors, wire bonding (electric welding), and high temperature silver brazing to do this. We initially found that high temperature silver brazing provided the best and easiest connection of copper leads to the resistance wire coil, and oven tests were performed at the highest temperature we first anticipated for sealing/construction firing. These tests demonstrated the braze joints could survive during the assembly process we had outlined to that point. Later, assembly/firing sequence changes had to be made given our final sensor design and seal methods, and none of the joining techniques we employed seemed satisfactory. Therefore lead and heating coil were left as one continuous piece of wire in final prototype assemblies, though the leads then also heated.

A 29 gauge (AWG) Kanthal A-1 alloy was selected as our heater "wire of choice" for the program. The 29 AWG size was readily available in sample quantity; the 6.82 ohm/foot resistance of the wire allowed constructs which could be packed into the volume we projected available for the heater, yet which would deliver the required 10W using reasonably low input current and voltage; Kanthal A-1 is a very inexpensive alloy; and this alloy is one of the most rugged and heat-tolerant alloys available.

As detailed earlier, our original 0.375" o.d. design in Fig. 2 constrained the heater to be a torrid ~0.175" o.d. x 0.250" long, and the hole in the center needed to be of sufficient size to allow ready exchange of reference gases from the body of the manifolding tube to the sensing disk. We considered various

schemes for placing heater wire in this volume with an eye toward the ease of manufacture, optimizing the conditions for heater lifetime, and keeping the input current/voltage requirements low. Given a 10W target and the 6.82 ohm/ft Kanthal, and also given a 0.5A target current input, we calculated ~5.87 ft. of wire would be required in the heater volume! This would have required extremely tight winding of the heater wire, with subsequent problems of insulating adjacent turns; further, we feared the tight packing might be deleterious to heater life-time. We found if we relaxed the constraints to 1A, 10V input, the length of wire required went down to 1.47 ft.; but even this length in the required volume made for a very cramped heater.

The constraints placed upon the heater volume and the resultant difficulties placed upon heater design prompted the evolution of a third design for the sensor: the "revolver bullet cylinder", as shown in Fig. 3. This design originated at CPI and was refined in consultation with GBC at their plant in LaTrobe, Pennsylvania. We relaxed the o.d. of the sensor from 0.375" to 0.500", thus making the volume available to the heater larger. Next, we moved the thermocouple to the center of the sensor and reclaimed the thickness which was added to the sensor head walls by the need to hold/encapsulate the thermocouple. The two tiny channels to contain thermocouple leads, which would have been difficult to mold, were eliminated by placing one larger diameter channel on the sensor axis to a piece of inexpensive, extruded, two-hole mullite thermocouple protector tube cemented into the assembly. Cylindrical channels were provided parallel to the axis to encapsulate the heater coils, thus providing uniform heat dissipation, electrical insulation, and support to the coils. The structure in this design had no single, thin, self-supporting wall. The overall volume for the heater was thus increased as the heater channels could be made fairly large in diameter and could be moved near the 0.500" o.d. of the assembly. Finally, the new design allowed space for a large number of gas-exchange holes between the outer heater coil channels and the thermocouple at the center. As it

was possible to leave the heater coils unpotted in this configuration (the channels in the ceramic for the heater provided electrical insulation), gas-exchange to the sensing disk could be further promoted through the heater channels themselves.

A final design prompted by sealing considerations changed this vision of heater construction; this final design is most logically discussed later below.

During the course of our initial design and test work, we were concerned about the stress on the sensor and heater which would be involved with simple "on/off" heater operation, and we did some research into the possibility of finding/ constructing a solid-state circuitry device which would ramp the heater over an adjustable time. Though we feel such a device is quite possible, we could not find plans or a device on the market, and we do not have the electronic design capabilities to realize our concept. Ultimately, we relaxed our voltage/current restrictions and used a Variac in the laboratory to provide an adjustable A.C. current to our sensor heaters.

VI. THERMAL EXPANSION STUDIES

Thermal expansion studies were prompted by the need to exactly match the expansions of the components involved in the sensor construction. Though the OS materials were "known" to have expansions close to those of Kovar, the electronic ceramics to form the bulk of the sensor head, and of the ceramic adhesives to be used, we wished to characterize the various materials exactly to select the precise components to be used and to tailor-formulate the electronic ceramic head to our needs (GBC has the capability to vary the compositions/thermal expansions of its pressed parts).

We at CPI devoted a large amount of energy, through several rounds of design, machining and construction, toward developing

an inexpensive mechanical dilatomer for in-house use in this and other programs. Samples of our prime candidate and other candidate ceramic cements and sealing materials were cast and were measured in these devices, as were samples of our various OS compositions. Examples of our measurements are provided in Figs. 4 - 6.

Our measurements upon our ceramic adhesives (e.g. Fig. 4) revealed that the adhesives underwent a previously undetected and unanticipated shrinkage at and above ~ 650 °C. As this behavior could have undesirable effects upon sealing, we devoted a considerable effort toward trying to understand and influence this phenomenon: different mixing and curing/firing procedures were utilized to create bars for dilatometric study. Further, we expanded our other OS compatibility testing of various adhesives/coatings, and variations on the methods of applying these materials.

Our measurements on the OS materials (e.g. Fig. 5) revealed that the various OS compositions had differing expansions. Parallel work on OS material conductivities and stabilities (below) led us to center our attention on the OS-3 material as the prime candidate for sensor use. Our early in-house measurements of thermal expansion on OS-3 yielded results consistent with the university reported findings listed earlier.

However, in the course of measurements using our in-house equipment, thermal expansions measured on GBC materials with our system differed from the expansions accepted at GBC (e.g. Fig. 6). This led us to seek comparison of our measurements with outside laboratories. Along with other samples, we supplied a bar of OS-3 to the laboratories of Harrop Industries and of the Orton Foundation. The independent measurements made are displayed in Fig. 7. Though these measurements do not completely agree with one another (no explanation is known for the disagreement), both measurements did differ greatly with the CPI in-house and preliminary university measurements; we became convinced the expansion of the OS-3 material (and

undoubtedly of all the closely related OS materials) was significantly higher than had been known!

A comparison of the average of the Orton and Harrop findings with the expansion of Kovar and of a typical GBC ceramic, Cerasil, is given in Fig. 8. (We will use "Cerasil" as the generic name for the ceramic to be used in the sensor head in the following bulk of this report. Initially, Cerasil 223U was the ceramic of choice for the sensor collar.) As may be seen, there are gross differences, completely unanticipated, and these differences had severe implications upon the sealing between the OS-3 sensor disk and the Cerasil body of the planned sensor. Thus began an even more arduous odyssey of search, rethink, and redesign than we had been or had envisioned conducting, as we searched for a compatible set of adhesives/sealants/sealing methods and design for the sensor.

VII. SEALING MATERIALS AND METHODS SEARCHES

Based upon our early understandings of the thermal expansion of the OS materials, and upon the consequent design arrived at in Fig. 3, we expended a great deal of effort in finding a supplier for Kovar tubing in the dimensions we desired. As we have often experienced in the course of this program, it is difficult to obtain small quantities of materials for research and prototype purposes at a reasonable price. A number of tubing suppliers were contacted before we found one supplier, A.T. Wall Co. of Warwich, Rhode Island, who could custom draw a small quantity of the 0.500" o.d., 0.010" wall tubing required for the design of Fig. 3. Once found, we placed an order as the lead times were 6-8 weeks and we did not wish to impede the progress of the program.

Further, based upon our mistaken expansion beliefs, we expended a large effort in initially surveying materials and methods available

for making high temperature joints between OS-3 and ceramics such as Cerasil. We even felt that we had found simple solutions to our joining/sealing problem in the course of our initial effort, but in retrospect it seems that our initial surveys were made on samples too small to show the effects of thermal mismatch and seal porosity well.

Because of the difficulty of finding the Kovar tube in the first place, the expenditure made in purchasing it, our continued desire to make the bulk of the sensor "head" of Cerasil, and because of our continued desire to use the sealing technology available to join a Cerasil component to Kovar, our thought was initially rooted toward maintaining the design of Figure 3 and finding some seal system which would bridge the expansion incompatibilities between OS-3 and Cerasil. It was envisioned a seal system might be devised which could flex and thus absorb thermal expansion differential without failure. We felt this might be realized in one of several ways: a one-component seal in which the component had some flexibility, in a "shimmed" seal where a flexible member was interposed between and bonded to the mismatched ceramics, or in a "graded" construct in which adhesives were applied in layers where one layer would match the expansion of the Cerasil, another would match the OS-3, and the in-between layer(s) would have an expansion(s) between those of the two ceramics.

Our initial sealing explorations fell into four broad categories: (1) Search of commercially available ceramic adhesives/sealants and techniques of application, (2) investigation of braze techniques for making joints between dissimilars, (3) investigation of "soft" sealing materials such as graphite, and (4) glass seals.

A. Search of Commercially Available Ceramic Adhesives/Sealants

High temperature ceramic adhesive and sealant products from four companies (over thirty products) and various methods of application

were surveyed in the course of this program. Our tests of ceramic adhesives/sealants went hand-in-hand with our knowledge/researches of thermal expansions. Some of our adhesive surveys were conducted before we realized the expansion of OS-3 was not matched to the other anticipated sensor components and consequently involved only the original sensor materials choices.

After we gained the clearer picture of the expansion of OS-3, we began to research thermal expansions through various published tables and GBC's knowledge of the ceramics it produces to find materials possibly more compatible with OS-3 while still retaining some compatibility with Kovar. GBC provided samples of several of its higher expansion materials, and these were included in the adhesives tests.

We found there was no simple compendium of thermal expansion information for various materials, and the extant data which was available was often very incomplete and reported in a variety of ways. Because of this difficulty in finding information, we often resorted to the use of "shotgun" empiricism, testing adhesives upon specific materials we were able to obtain within a promising category. Further, as sources indicated there might be better materials matches than Kovar and Cerasil for OS-3, our thinking evolved and we began to consider departure from our originally envisioned materials. As an example of our empirical approach and our changes in thinking, we discovered that the OS-3 expansion was in the generic thermal expansion range listed for 400-series stainless steels and inconels. We obtained small samples of specific 400-series steels and inconels and performed bonding tests between OS-3 and these materials, varying the adhesives and methods of adhesive application used. Thus the matrix of our tests became quite broad and involved.

For typical first-round tests we would bond small pieces of OS-3 to the candidate substrate using candidate ceramic adhesives and application methods, fire the system to make the adhesive bond,

and then thermal cycle the system. There was considerable variation of the application methods tried. Most often, the ceramic adhesive was applied by itself between the elements to be joined, but graded layer application using several adhesives was also attempted. We also tried bonding thin copper shims between OS-3 and substrate with adhesives; we hoped shims in a sandwich construct would absorb expansion mismatches. We prepared the OS-3 and substrate materials in a variety of ways: pre-moistening of ceramic substrates with water (to aid in adhesive penetration into ceramic pores), pre-oxidation of metal substrates, and nickel plating of metal substrates were all tried.

As may be seen, with over thirty products tested in a variety of combinations and under a variety of conditions it becomes cumbersome and of questionable value to report the detail of the initial screening tests. In broad strokes, therefore, our tests included attempts to bond both bare and platinized OS-3 to alumina, mullite, steatite, Cerasil, Kovar, stainless steels 304, 347, members of the 400-series including SS446, inconel, and the glass-sealing alloys "42" and "52". The metals were tested in "clean", pre-oxidized, and nickel-plated states.

Candidate combinations of materials discerned from first-round tests then had to pass two criteria not well checked by initial screening: (1) Initial screening was done using small pieces bonded at their faces whereas the sensor required bonding in a quite different and larger geometry, i.e. along a narrow periphery on a ~0.500" o.d. It was anticipated the actual application could be a quite different bonding situation than that provided by the screening tests. (2) Initial screening indicated only the ability of the adhesive materials to bond and did not test hermetic sealing characteristics.

We therefore made second-round "hermeticity" checks which simultaneously checked both criteria. For these checks, OS-3 samples were bonded in constructs which would allow a leak test, and we

made these constructs larger than those used in simple "adhesion" tests. We did find the effects of thermal expansion mismatch were demonstrated much better: In many instances we found the OS-3 part (e.g. disk) cracked during firing of the seal or during thermal cycling though no such mismatch had been detected during initial screening.

Many of these tests were conducted before we were able to receive pressed parts from GBC. As an example of how we conducted some hermiticity tests, we sawed OS-3 pellets of ~0.500" o.d. (originally produced for ionic conductivity and other properties tests) into thin disks using a Buehler Isomet saw. We then corsetted the ends of short sections of metal tubing to slightly less than the diameter of these test disks, coated the interior of the corset and the edge of the disk with some candidate adhesive/sealant paste, inserted the OS-3 disk, and fired the assembly. In some instances, we performed two-step applications in which an adhesive was applied and fired, then overcoated with a candidate sealant and re-fired.

The leak tests were performed in three different ways:

(1) The simplest method was to connect the construct to a cylinder of pressurized helium gas using a hose, apply a few psig pressure of helium to the seal, and immerse the sealed end of the tube in a beaker of water. This was a room temperature test only but gave immediate indication of whether a candidate seal had formed.

(2) A mass spectrometer leak detector sensitive to helium was used to test in either "pressurized" or "vacuum" mode. In a "pressurized" test the construct to be tested was pressurized with helium as in (1) above and the mass spectrometer was used to sense escaping helium. In a "vacuum" test, the test piece was attached directly to the mass spectrometer system and a vacuum was applied. Helium gas was sprayed around the piece under test, and would enter the mass spectrometer through any leak.

Either test could be performed on candidate seals at sensor operating temperature by inserting the seal end of the test piece into a controllable oven. Once at temperature, the part could either be pressurized and a metal tube "sniffer" attached to the mass spectrometer could be inserted into the oven to capture escaping helium, or the part could be placed under vacuum and helium could be fed into the oven to surround the part. The latter method was used more often as the former is best suited to situations in which the "sniffer" may be easily moved all about the surface of the part -- the restricting confines of the oven and oven door made this difficult. However, we have had certain concerns about the suitability of our vacuum testing at oven temperature.

Though some seals might have been hermetic under normal low pressure differential circumstances, such as those of actual sensor application, the necessary vacuum applied by the leak detector subjected the seal to a 15 psi differential. This "abnormal" differential prematurely caused seal failure in some tests, particularly those involving glasses. In fact, we found it necessary to design and construct a special trap/filter to interpose between test pieces and our leak detector, as one failure occurred in which an OS-3 disk was "sucked" into the leak detector's delicate interior mechanisms.

Further, we began to question the suitability of the use of helium as a detecting agent. For example, solid glass at room temperature has some permeability to helium, though glass is impermeable to the larger gas molecules that make up air and exhaust gases. We speculated the situation may have been worse at elevated temperatures, and that readings of helium leakage might actually have been readings of helium migration, totally unrelatable to air leak rates.

(3) As a partial solution to our concerns in (2) above, we would pull a vacuum on a test piece at temperature for a given length of time, and then close the test piece off from the vacuum pump.

We timed the interval between pump close off and "leak up" of the test part, hose, and pump manifold to a certain pressure as registered by a vacuum gauge attached to the manifold. Using the same equipment and timing a number of trials we could thus get a qualitative indication of how a seal was holding against air at various temperatures. Our implicit assumption here was that "outgassing" from the evacuated equipment and connecting lines would be nearly constant.

From such tests we discovered there was a marked distinction which had to be made between a ceramic adhesive and a ceramic sealant. Most of the materials commercially available for high temperature bonding were adhesives only, and were actually quite porous to gases. Each manufacturer offered only a few items as "sealants", out of the dozens of items those manufacturers supplied; and these sealants were intended as overcoatings to be applied on top of a separate adhesive bond. We tested the overcoatings available at the time from our manufacturers and found none which were compatible with the hopeful OS-3/adhesive/substrate combinations we investigated.

Most of the adhesives tested in and of themselves were "rigid solids". One special category of adhesives we tested and which should be noted were obtained from Cotronics, Inc., of Brooklyn, New York. These were high temperature adhesive bases filled with finely divided metal, and these adhesive systems have shown ability in some dissimilar joining applications to flex and absorb thermal expansion mismatch, much as a braze seal may. We tested a matrix of five liquid binders and two metal filled powders. Unfortunately, none of these mixtures proved useful in our situation, and some even chemically reacted with the OS-3, reducing elemental metals from the OS-3.

B. Braze Sealing

A GBC suggestion led us to investigate the possibility of using brazing methods to join our materials together. Some braze metal seals have inherent flexibility large enough to absorb thermal expansion mismatch, and metalization/brazing of electronics ceramics is done quite commonly. Contact was made with Latronics, Corporation, of Latrobe, Pennsylvania, and the Latronics engineer first consulted was quite enthusiastic and confident our thermal expansion mismatch problem could be solved. Several design approaches were CAD generated by Latronics, and the approach preferred by Latronics, as it was quite similar to assemblies Latronics routinely made, was to braze an alumina sensor body to the Kovar tube and to the OS-3. The joint with the OS-3 would utilize a thin copper shim to absorb expansion mismatch, and the alumina body would be so intrinsically strong that mismatch with the Kovar tube would have no deleterious effect.

The Latronics engineer began initial testing in the Latronics production ovens to determine OS-3 compatibility with Latronics processes and materials. Such tests had to be arranged between Latronics production runs, which delayed test progress several times. One initial test demonstrated OS-3 did not suffer thermogravimetric weight loss or loss of ionic conductivity during exposure to a nitrogen braze atmosphere in the Latronics ovens. "Before" and "after" weighings and conductivity checks were made at CPI for this test.

A test braze attempt was then made, and in this instance an interaction occurred between the OS-3 and the braze used so that the braze oxidized before wetting the ceramic. The engineer at Latronics began trying to obtain samples of other brazes, and began waiting upon the installation of a smaller research oven at Latronics which would allow him better control over the processes. While we waited, Latronics went through upper level management changes which had new priorities and cost-cutting programs: the engineer with

whom we were working was "let go" without warning to him or notification to us.

For a time there still seemed interest at Latronics for pursuing our problem; another engineer made some minor efforts at testing. But as time stretched on, the research oven upon which everything "seemed to depend" remained uninstalled and "definite dates" for installation were repeatedly rolled forward. We eventually dropped contact with this company.

We made some efforts toward contacting other brazing companies and joining technology resource organizations even during our abortive interaction with Latronics. We discovered through the Edison Welding Institute in Columbus, Ohio, and contacts at The Ohio State University that a program at the DOE laboratories at Oak Ridge had successfully brazed zirconia to cast iron, and that problems of oxidation of braze by the ionically conductive ceramic had been encountered and solved. We pursued establishing an interaction with the researchers at Oak Ridge, but were rebuffed on the basis that it would be difficult to make working arrangements between a private company such as CPI and the National Laboratory. Other contacts we made did not feel they had the expertise to work on our particular problem.

C. "Soft" Seals

Literature indicates that seals of graphite are used in some commercial oxygen sensors. Conversations were conducted with several manufacturers of graphite seals, and only one felt our sensor could be sealed using graphite. Our investigations into graphite sealing technology revealed simple graphite seals begin to burn if exposed to oxygen at temperatures >~ 500 °C; however, the one company claimed there were ways to engineer the seal and that they had the technology to provide seals for much higher temperatures. Unfortunately, this company could never remember us between our repeated

phone calls (we had to re-introduce ourselves to the same people each time), it lost our FAXes detailing our requirements, and in general left us with very bad impressions. We eventually dropped contact with this company.

We made several contacts to investigate the utility of R.T.V.'s (organic adhesive/sealing materials) in our situation and obtained a sample of one product used to make sealing joints with ceramics. We tested this and found it bonded very well with OS-3, and retained great flexibility. Unfortunately, though the RTV was a "high temperature" organic material, the temperature limit was only 250 °C, much too low for our application as we envisioned it.

D. Glass Seals

In retrospect, we did not investigate large numbers of possible sealing solutions with glass, and yet it was a glass which has provided the best sealing solution we have to date.

We were discouraged at the outset of the program from pursuing glass to OS-3 sealing because of the constraints imposed by the application, and we questioned (as did some glass experts) whether a glass could be found which would fit within those constraints. GBC tested some glasses fired in contact with OS-3, and found violent interactions at ~ 900 °C. GBC's interpretation of the results was that silicates (the basis of most glasses) reacted with OS-3, and the first concern was whether any glass at any high temperature could be used in contact with the OS-3. At the very least, this ~ 900 °C reaction posed an upper temperature limit to the sealing (melting) temperature of the glass. Even if the ~ 900 °C reaction were solved, an absolute upper temperature limit of ~ 950 °C was imposed by the melting point of OS-3.

The lower temperature limit was imposed by the 600 °C operating temperature for the sensor. The seal would have to have a reason-

ably high viscosity and could not be molten at this temperature if seal integrity were to be maintained. Preferably the glass would need to have a softening temperature of at least 650 °C. Thus, a softening-melting temperature window of only ~ 250 °C was fixed by the peculiarities of our application. This narrow window presented a problem: typically, glass softening and melting points are separated by several hundred degrees Celsius or more.

From the standpoint of thermal expansion matching we faced another dilemma. The relatively high thermal expansion of OS-3 needed to be matched by the expansion of the glass, but high expansion glasses generally tend to have melting points much lower than the envisioned 600 °C operating temperature.

Contact with a large sealing glass manufacturer yielded only a salesman with pat answers. We did find other, more helpful glass engineers during our search; but the consensus of these was that a special glass would have to be designed, and that this would involve a great deal of money in consulting fees and laboratory work with no guarantee as to results. At this point, most of our focus shifted to the investigations of other methods of sealing described in the sections above, though continuing to make occasional inquiries into glass seal technology.

As other sealing methods did not prove successful, we eventually found a small technical glass company through a GBC recommendation which took interest in our project. This company considered our needs, and suggested several glasses "from the shelf" which might meet our requirements. We gained samples of these, and immediately obtained encouraging results. We will elaborate further on this in Section IX below.

VIII. FINAL REDESIGN

Each failure and setback as we investigated and pursued different methods for joining and sealing the Fig. 3 concept for a Nernst oxygen sensor provided more information and time to reflect and re-think. As we examined the thermal expansion information we gathered, contemplated the design of Fig. 3, and saw the difficulties we were having at finding methods of strain-relieving the thermal expansion mismatches inherent, it occurred to us that the design of Fig. 3 was making our problems much too complex. We came to realize sealing could be simplified if thermal expansion mismatches were lessened or eliminated by re-design, and we proceeded along this line. A series of "final" designs for the sensor resulted, and these are presented in Figs. 9a-c. Fig. 9c. is the culmination, and the design we adopted when constructing our best prototypes.

Our first step toward simplification was to make <u>both</u> the sensing disk <u>and</u> the sensor ceramic body from OS-3. This eliminated the thermal expansion mis-match problem between the sensor disk and body which existed in the Fig. 3 design. Upon consultation, GBC expressed that they were quite confident they could form and sinter complex parts of OS-3 as they do with the "Cerasil" ceramics originally planned for use. The sensor disk and more elaborate sensor body remained two separate parts in GBC's production; but we found in simple tests at CPI that fired parts of OS-3 could be joined with an OS-3 paste "mortar" and then fired, and the joint would hold well.

As the OS-3 sensor body had an expansion behavior quite different from that of Kovar, we abandoned attempting to use the Kovar tube we had purchased. In the course of our literature studies we eventually obtained good thermal expansion information on various steels and found that stainless steel 446 matches the expansion of OS-3 closely (Fig. 10). SS446 is a ferritic stainless which has been widely used in high temperature applications (though our

impression is that it is being replaced by "newer" alloys); of course this high temperature usability fit well with our needs.

We were thus forced into another arduous search for a small quantity of thinwall tube. Through a round-about chain of inquiry, we eventually found a geiger counter tube company which used 446 tube and which could give us a supplier contact. This company also shared with us a technique for corsetting (constricting the tube o.d. at some point) tube. This company used such corsets in geiger tube manufacture to aid in making a seal to a ceramic plug endcap, and the idea of corsetting to aid assembly and sealing became a part of our sensor re-design.

The tubing supplier, when contacted, could do a custom draw of 446 tubing for us to our specifications provided we order a minimum of 100 ft. and pay set-up charges; this was far too expensive and wasteful for the confines and needs of this program. However, the supplier did have some small quantities of 0.630" o.d. x 0.010" wall material "on-the-shelf". As this was reasonably close to our 0.500" Fig. 3 target we enlarged our sensor head design for the second time from our original intent, and purchased a quantity of this new o.d. material.

This final enlargement of the diameter of the sensor head eased the constraints on the heater to be incorporated into the sensor head even more. Also, we decided we could ease the restrictions placed on the current/voltage to be applied to the heater, thus allowing the use of heater geometries containing shorter lengths of wire and consequently of lower resistance. Upon a suggestion from GBC, our final design removed the complexities of the "revolver bullet cylinder" concept and placed the heater in position for better thermal contact with the disk; the heater coil was designed as a "range-top" and was placed in a "C" shape immediately underneath the sensor disk. We found we could easily supply all needed power to this coil using a Variac power supply operating at ~20 VAC (maximum output of the Variac was 10A at 140 VAC).

Our redesigns retained the thermocouple at the center of the assembly in the interests of space; we also thought this position might more reliably sample the "working" temperature of the sensor disk. Originally, the sensor body was to be of two identical parts ("collars") with the disk joined and protected in the middle. Upon suggestion from GBC, the sensor body was slipped into the tube so that the sensor body was flush with the tube end and the sensor body protected. Finally, "flanges" were added to the bases of the collars to provide a smaller contact surface between the assembled body and the tube, giving the heated disk better thermal stand-off from the tube and the heat loss path the tube provided.

Though the design of Fig. 9a. was the "final" design, and GBC's production of parts was planned around this, we found the components could be assembled in different ways as various needs became evident. In order to more easily see how components and seals were behaving, we assembled the parts for some test sensors according to Fig. 9b. As we gained experience in sealing and realized the disk did not need great protection, we made a last simplification to the system: we corsetted the tube at the very end and used this to form one seal rather than having the two seals of all previous designs. This concept is presented in Figure 9c.

IX. FINAL SEAL MATERIALS AND CHARACTERISTICS

As discussed in section VII above, a search path eventually led to a helpful supplier of a sealing glass. The supplier examined our thermal expansion data on OS-3 and our other requirements, and initially offered two candidate glasses. Our supplier mixed slurries of these glass powders in methanol so that the glasses could be applied as a paste to the desired joints prior to firing. One of the test glasses proved inadequate, but the other, V2B, immediately gave excellent results.

The first V2B/OS-3/SS446 hermetic seal test piece was found qualitatively "leak tight" in oven tests taken up to 650 °C (see VII.a. for seal test procedures), and this success directed most of our sealing investigations for the rest of the program. After the successful test of V2B, we continued only a modest effort investigating alternatives. A few more adhesive materials were tested and we made variations such as mixtures of adhesive materials with glass. These attempts met with varying success, yet to date pure glass seals have provided the best sealing solution for the sensor application.

We early noted several aspects of V2B use which required special investigation/precaution. First, the glass evidenced some slight reaction with the OS-3 material, so that the glass tended to yellow, but the reaction was not nearly as violent as that noted in GBC's studies with other glasses. We performed an experiment in which we placed some V2B on a piece of OS-3, fired, and then examined the result. We saw indication the glass did react with or "diffuse" into a volume of the OS-3 immediately around the V2B application. Second, and augmenting the first precaution, we found V2B interacted with platinum electroding if the glass came into contact with it: the electroding was changed from a matte gray to a shiny black. We concluded both of these phenomena might have implications to the ion conducting behavior of the system: to the intrinsic ionic conductivity of the OS-3 in the case of the OS-3/glass reaction, and to the catalytic ability of the electroding in the case of the electrode/glass reaction. Therefore we have felt V2B should be applied to our seals sparingly, and kept away from the electroded, sensing portions of the OS-3 disk in the assembly.

After the initial success with V2B we had the supplier perform a complete thermal expansion check on the material to assure ourselves of the compatibility of the SS446/V2B/OS-3 system. These data are presented in Fig. 11.

Early we noted the "working time" of the V2B/methanol paste was short, and the paste dried out quickly upon application. Our supplier was asked if the working time might be lengthened, and a V2B/isopropanol paste was mixed for us. Initially, the new mixture worked quite well, but we then ran into a time-consuming and puzzling mystery: after initially obtaining good-looking seals, later joints made with the V2B/isopropanol came out of firing blackened and bubbled.

We performed various tests and purity checks in conjunction with our supplier upon several different lots of glass/isopropanol mixture: we checked the effect of variations in firing conditions and procedures and performed other experiments as well. During the course of our investigation, our supplier had us try another glass, VS9, in both methanol and isopropanol bases. The results were the same: all isopropanol-based pastes led to blackened and bubbled seals, and we could not isolate a cause.

We finally abandoned trying to find the cause of this problem, took a practical tact, and used only methanol based pastes for the remainder of the program. However, our supplier urged us to retain the use of the VS9 glass as it was a composition they produced much more regularly than V2B and yet was not much different from the V2B in composition. Our checks demonstrated VS9 performed as well as V2B in terms of compatibility with SS446 and OS-3; apparently thermal expansion was not much affected by the slight compositional difference, and we assumed other characteristics were not much affected either. We consequently adopted VS9 as our seal material of choice.

As implied from earlier discussion, V2B and VS9 are glasses which melt/soften/solidify within the restricted band of temperatures required by the OS-3 sensor. That is, these glasses both melt below the ~ 900 °C possible chemical reaction limit (and consequently below the ~ 950 °C OS-3 melting point) yet these glasses remain significantly solid at the ~ 600 °C sensor operating tem-

perature so that the sensor remains sealed. One of our tests demonstrated a V2B seal remained intact against full atmospheric pressure (we used the intermittent evacuation/leak-up method of testing at temperature as outlined above) over the course of 7 days at 600 °C; however, other tests and experience demonstrated the V2B seals should not be taken much above 600 °C if the seal were to be subjected to pressure: we observed mixed results at 650 °C, with one test showing seal improvement and another showing seal decay. We have been advised by our supplier the "softening point" of V2B is 680 °C, and as glass viscosity varies logarithimically with temperature, even small excursions above 600 °C sensor operation may have large effect on the seal. Our semi-quantitative leak testing was all performed upon V2B, but our experience has indicated VS9 behaves similarly to V2B.

We found the final assembly concept in Fig. 9c. promoted easy formation of a very uniform and good seal. The amount of glass used had to be controlled to prevent flow onto the sensor's outer electrode, but the inward folded portion of the SS446 tube helped gauge the amount of material being placed into the seal and helped retain the glass where it was needed.

X. ELECTRODING AND LEAD ATTACHMENT STUDIES

As a subsidiary part of this program we performed studies to find optimum materials for catalytic electroding, conduction of voltages, and attachment of signal leads to the sensor. Through prior studies CPI had already adopted a particular platinum ink (A31) which, when fired, deposits a porous platinum electrode surface providing the catalyzation of oxygen and the conduction of charges at the OS electrolyte surface. In these prior studies CPI developed the methodology for applying and firing that ink. However, during this program we continued to attempt to improve upon what we had already developed.

As seal and sensor design evolved and we found that the sealing glass interacted with the A31 platinization, we realized it would be advantageous to apply the A31 to only the center of the OS sensing disk, away from the seal. This would also conserve the expensive platinum. As we did not have screen-printing capabilities, we tested the possible use of a "wax mask" to prevent the spreading of the platinum paste to the edges of the disk during the room temperature application. This mask could then be burned off during the paste firing step. We applied a ring of a "high-melt" wax (~ 90 °C melting point) to the periphery of disks to be platinized, allowed the wax to cool, painted the center of the disk with the platinum paste, and then fired the system. The wax did restrain the platinum to the center, and the wax residue from firing could be readily dusted off. However, through repeated tests we noted the platinum coating produced was not of "usual" appearance in color or texture, and we began to fear the catalytic properties of the platinum layer might be affected. For this reason we stopped using the wax-masking procedure and began merely to more closely control the amount of the paste applied to the disk center so that the spread to disk edges was minimized. If there were spreading, we used emery paper to hand sand the platinization off of the disk periphery.

Our original designs required the deposition of a conductive strip from the electroding on the sensor's disk to a "potting hole" for a lead wire. This strip was required to be compatible with the platinum electroding, provide a conductive path over "edges" in the sensor design, provide firm attachment of a lead wire, to withstand the various firings during sensor assembly, and to withstand the 600 °C sensor operating temperature.

We had often used a "fired on" silver paste, D20, for making electrical attachments to ceramics prior to this program, and we tested this paste for use in the sensor program. We found that the material underwent shrinkage and "tearing" during the firing, that it did not have good adherence to the platinized OS-3, and that a

darkened "halo" formed around the paste in contact with the A31 electroding. The latter implied a reaction or migration of the silver paste into the electroding was occurring.

We called the maker of A31 for recommendations for materials to suit our needs, and obtained small quantities of an ink for deposition of platinum tracks, O5, and of two "fired on" silver pastes, A94 and A58. We test fired all three of these on OS-3 surfaces, across sharp edges. We found the O5 required multiple coats to yield a good conductive surface and the track formed had questionable adhesion to the OS-3; it did, however, evince conduction over edges. A94 and A58 both adhered extremely well and provided conduction over edges. The fired tracks of A58 exhibited some shrinkage and tearing, and, as with the D20, a darkened "halo" formed around the silver on the platinum electrode surface. A94 test stripes exhibited no shrinkage or tearing, and no interaction "halo" at the contact edge with A31. Initially, then, we adopted A94 as our striping/lead attachment paste.

Later, as the design and sealing of the sensor changed, we discovered that A94 could not be used as it could not tolerate the temperature of the glass sealing step. We re-visited the use of A58 as this material has a higher firing temperature, and found that further tests did not exhibit the interaction "halo" that had been observed at first. We speculate some slight changes in our firing procedures were of benefit.

We abandoned using a conductive stripe in the later sensor designs and made lead attachments directly to the A31 electroding using silver wire attached with silver paste; thus shrinkage and tearing of the paste used became a less important factor than the ability to adhere to OS-3 (A94 showed excellent adhesion). However, talks with the manufacturer did lead us to try dilution of the paste with its solvent, and we found that such simple dilution of the A58 did reduce the shrinkage tearing. We tried only one dilution adding ~20 weight percent solvent.

As we indicated in Section III. ("Theory"),the sensor electroding functions as the necessary catalyst for oxygen molecule to ion conversion, as the agent allowing the transfer of the resultant ions to the electrolyte, and as the agent conducting/supplying the electrons transferred in the various electrochemical processes at the electrolyte surface. The electroding therefore controls a number of processes, and its nature is key to sensor operation. In fact, a series of not well-understood phenomena seemingly associated with the electroding prevent Nernst sensor (both zirconia and OS) operation below ~ 600 °C.

Though CPI's adopted electroding system (A31) seems adequate for ~ 600 °C operation, the OS materials properties should allow sensors which operate well below this temperature; therefore, during the course of this program we made investigations into alternative electroding systems which might function below the ~ 600 °C "barrier". Our efforts included the investigation of the use of other platinum inks to make the electrode deposition and the use of metals other than platinum in the electrode. We tested these materials/approaches by coating the sides of test disks of OS material and making conductivity tests, as well as heating the test disks and watching for the appearance of spurious signals.

We also made some tests of a proprietary coating applied for us by S.P.S. Badwal of C.S.I.R.O., Division of Materials Science, Melbourne, Australia. This researcher has successfully lowered the operating temperature of zirconia sensors using electrodes of materials other than platinum. Unfortunately, Dr. Badwal damaged our test parts while handling and applying his coatings, and our results with his system were inconclusive.

Finally, we investigated the possibility that "partial reduction" of the OS electrolyte might have a good effect, aiding catalysis/ charge transfer and thus lowering operating temperature. We have found the OS materials are chemically reduced when immersed in high temperature reducing atmospheres (e.g. pure hydrogen) with

no contact to an oxygen source. The reduction "metalizes" the OS material as the reducing atmosphere removes the OS cations and leaves behind the metals contained in the OS structure. We attempted to control this "metalization", trying to form a semi-conducting surface layer on OS parts. Using a special test chamber and apparatus we built, we made measurements of OS conductivity during the exposure to the reducing atmosphere and also tested for the effect of exposure upon the behavior of the spurious voltages. We found no useful gains from the metalization procedure, but we did discover if the reduction of the OS-3 material were not carried beyond ~5% weight loss a re-exposure of the OS-3 to oxygen (air) at temperatures as low as ~ 300 °C would reverse the reduction and rejuvenate the material.

XI. IONIC CONDUCTIVITY STUDIES

We performed checks upon the ionic conductivities of the various OS materials both to help make the initial selection of which material to use and then as a quality control check upon GBC production of parts. This has been accomplished using a CPI designed and constructed test chamber. This chamber was tubular and was inserted into a muffle furnace. The front end of the chamber was allowed to protrude through the fire bricking at the front of the oven into room temperature; this provided an access which was sealed with a face plate, teflon ring, and sealing clamp system. Gas inlet and outlet tubes led into the rear and from the front of test chamber. Silver voltage/current measurement leads were fed into the chamber through the face plate using mullite thermocouple tubes sealed to the plate using compression O-ring fittings. The leads, themselves, were sealed into the mullite with a vacuum sealing wax melted to the ends of these tubes. The face plate, O-ring compression seals, and wax seals were kept cool by a directed air stream from a fan. Heat load onto the face plate from the interior was diminished by an interior radiation baffle. Conversely, this baffle kept the face plate cooling from affecting

interior temperatures. A sample platform was attached to the face plate, and this supported the baffle, as well as held several samples in the chamber hot zone. The silver voltage/current lead ends were held to the electroded samples by pressure from weighted, short sections of mullite tube. These sections of tube were used to electrically insulate the steel weights (placed on the tops of the tubes) from the samples and leads.

Typically our procedure was as follows: The samples (usually disks) were mounted, a small forced air flow (or other atmosphere) was introduced into the test chamber using the inlet/outlet tube system, the sample was brought to test temperature, and a voltage (with a resultant current) was applied to the sample using two leads pressed against opposing sides of the sample. The voltage applied was measured using a high impedance voltmeter or chart-recorder. Current flowing in the leads was measured by placing a precision resistor in series with the sample in the circuit, noting the voltage drop over this precision resistor, and back-calculating using Ohm's Law. Typically, we fixed the voltage at the sample power supply to ~1 volt, and resultant currents and voltage drops over the sample were measured at various oven settings. Temperatures were determined using a platinum thermometer placed next to the samples.

In this manner we found the OS-3 composition had one of the higher ionic conductivities of the OS materials. Ionic conductivity data measured as above for typical OS-3 samples are displayed in Fig. 12. From other studies we knew that OS-3 is a more stable material against chemical reduction, and mechanically stronger, than the other OS candidates. OS-3 thus became the material of choice for this program.

More information regarding our ionic conductivity studies will be discussed in the "Conclusions" section of this report.

XII. MATERIALS DEVELOPMENT AND OS-3 PARTS PRODUCTION

As related earlier, delays were incurred in the development of sealing technique. These delays held up the early production of parts by GBC as the parts design depended upon the seal design. As we have reported, these delays also fortuitously provided CPI and GBC the time to re-think and re-design the sensor head assembly, and we see the resultant final design as being better than those originally envisioned from a number of standpoints.

Once final re-design was settled upon, GBC began the process of tuning the details of that design to enable the production within the limitations of their state-of-the-art methods and equipment. This latter process of fine-tuning, die design, and die fabrication was delayed at GBC for a number of internal reasons.

Once, again, however, the delays had long-term benefit. During the course of this contract, CPI has had other contracts to further develop and improve the OS materials and their processing. As an outgrowth of one of these it was discovered that ceramic powders processed using vibratory milling could be fired in the laboratory into parts approximately twice as strong (Young's Modulus measurements) as parts fired from powders produced using ball milling. As the powders originally given to GBC for pressing and forming were ball milled, but had remained un-utilized due to the delays, we were able to provide GBC with new, vibratory milled powders for a side-by-side comparison with the ball-milled materials in the manufacturing environment.

The introduction of the vibratory milled powders to GBC resulted in some unexpected difficulties which caused further delays toward final production of parts: GBC found that the different powders fired at different peak temperatures. Given a firing curve to optimize the fired density of OS-3 parts (this curve was derived from independent rate-controlled sintering studies), GBC found vibe-milled parts came out of the oven shaped as expected while

ball-milled parts were somewhat melted and slumped! When GBC lowered the peak firing temperature in an effort to reduce the slumping/melting in the ball-milled powder parts, the ionic conductivity checks at CPI revealed that the ionic conductivity was adversely affected. Finally, GBC did not find a qualitative difference between the strengths of parts from ball milled powders and vibe milled powders. Rather, both types of parts could be chipped rather easily, and the chips were always concoidal (shell-shaped) with very smooth, specular fracture surfaces. Since we expected parts of vibe-milled powders to be of greater strength, the lack of the strength increase was a troubling puzzle.

A great deal of time and effort went into attempting to understand and work around these behaviors and findings, and a meeting and several phone conversations were held between representatives of GBC, CPI, and a rate-controlled sintering/ceramics processing expert to search for explanations and processing optimizations. One possible explanation for the somewhat "frail" nature of the OS-3 parts was the presence of internal stresses in the ceramic; therefore, GBC devoted time to studying the effects of various firing curves, attempting to anneal the OS-3 ceramic parts. These firing curve studies were also to search out a new firing schedule to optimize part density while remaining below peak temperatures where the part would melt/slump. Further, GBC had to spend time in an investigation to find the best "parting agent" or substrate to use upon which parts might be fired, this as the OS-3 parts (especially ball-milled) were found to stick readily to most firing surfaces.

The various discussions and researches at the time of our work on this program produced very little in-depth explanation of the observed behaviors of the materials. No explanation could be found for the difference in firing behaviors of the two powders; possibilities of contamination in one of the powder batches were dismissed after discussions with the powder suppliers. All tests and experience indicated the concoidal fracture behavior is an

intrinsic property of the fired OS-3 material. However, at this time of final report, we find there may be an ominous explanation having to do with the quality of the work provided by our OS-3 powders supplier. We leave this to the "Conclusions" section at the end of this report.

Despite the mysteries, it was possible to derive a path upon which to proceed for final parts production for this program. The quantities of OS-3 powder available for this program, in either the ball- or vibratory-milled forms, were limited. Therefore, we elected to make the sensing disks of the vibratory milled powders; these could be fired at a higher temperature to avoid the problems in conductivity CPI noted were present in lower temperature fired parts. Since the "collar" parts were not required to be ionically conductive, and since no qualitative strength/fracture difference was found between GBC parts of ball- or vibe- milled powders, we utilized the ball-milled powders to produce the collars and fired these at lower temperature to prevent slumping/melting. Thus, the bottom-line benefits of having introduced the vibratory milled powder to the program were (1) it solved the dilemma encountered in the GBC production of the sensor disk, i.e. that the part had to be fired at a higher temperature for the sake of ionic conductivity, but parts of ball-milled powders would have melted and stuck to the GBC firing substrates at such higher temperatures, and (2) we were able to produce a larger number of parts than we would have been able using the ball- or vibe-milled powders alone.

In the course of the vibe-/ball-mill powder studies, GBC also performed a number of preliminary pressing/ press-adjustment studies and expended much labor in order to obtain flawless parts. Particularly, meticulous adjustment of the dies and pressing machine had to be made to eliminate cracks in the walls of the sensor collar and to preserve the integrity of the "parapet" provided for the contact between the internal electrode and the silver signal lead.

XIII. ASSEMBLY PROCEDURES

During the course of the GBC production studies and press adjustments a number of "scrap" imperfect parts were produced which were useful to us in our sealing and heater development and testing. Beginning with these parts, we began evolving our final assembly methods and procedures as we tried different sealing methods and ways of placing the parts (as per Figs. 9a. - 9c.). This evolution continued when final GBC parts arrived, and we derived our final prototype design (Fig. 9c.) and assembly procedure:

a. The sensor disk is platinized using the A31 paste. The amount of paste used is kept to a minimum and applied to the disk center to keep the paste away from the edges to later prevent the sealing glass from contacting the electroding. The proper application requires experience as the paste viscosity drops during firing and it will "run": seemingly small amounts of paste will flow to the disk edge. The electroding is fired using CPI proprietary methods. Once both sides of the disk are electroded, any electroding within several millimeters of the disk edge is scraped away using a grit paper. Care is taken to prevent touching the remaining electroding with one's fingers.

The interior electrode must extend from the center of the disk to a radius corresponding to that of the location of the "parapet" (see below) on the "collar". Alternatively, and preferably, a "tail" track may be extended from a smaller, circular inner electrode spot to a radius corresponding to the location of the parapet.

b. A 30 turn coil is fabricated of 29 AWG Kanthal A-1 wire, leaving ~7 in. lead length on each side of the coil. The end loops of the coil are bent outward so that the leads will pass perpendicular to and through the coil axis.

c. The coil and the interior of an OS-3 "collar" are wetted with distilled water. A small amount of A71 potting adhesive is spread into the coil recess area of the collar. The leads of the coil are passed through the lead holes in the collar base (at the ends of the coil recess) such that the leads protrude through the base of the collar. The leads are pulled through until the coil is nestled into the A71 and the coil recess. A71 should penetrate between the coils. More A71 is added to the sides and top of the coil to completely cover the coil, taking care that the A71 does not go over the level of the collar wall or into the center of the collar thus blocking the reference gas exchange holes. The A71 is allowed to cure 24 hours at room temperature.

d. The heater coil leads are passed through the holes of a 1/32" hole x 1/8" o.d. x ~6" long two-hole thermocouple protector mullite. The wires are drawn through the mullite so there is a minimal amount of lead wire showing between the collar base and the mullite.

e. OS-3 paste is applied to the top of the collar wall and to the A71 on top of the coil, to a level slightly above the level of the signal lead "parapet" but not to a level or in an amount which will eventually block the hole in the parapet. The sensor disk is then pressed against the top of the collar so that positive contact is made between the OS-3 paste and the disk, and so that the disk adheres against its weight given the slight stickiness of the OS-3 paste. If a "tail" track were used from the inner electrode on the sensor disk, the disk must be oriented so the tail is in contact with the hole in the parapet. The hole must remain clear of OS-3 paste. The assembly is loaded into a laboratory oven, with the sensing disk flat on the oven floor and the lead wires/mullite tube pointing up. The assembly is fired using the CPI proprietary optimum OS-3 densification firing curve, modified by truncating at a peak temperature of 850 °C to prevent a deleterious high-temperature thermal expansion mismatch of the A71 potting and the OS-3 collar.

f. A short coil is fashioned on the end of a 0.010" dia. x 2" long silver lead. The o.d. of this coil must be less than the i.d. of the hole in the parapet; a small diameter wire is useful as a mandrel upon which to wrap this coil. The coil is then dipped in A58 silver paste thinned using 20 weight % solvent, and finally inserted into the hole in the parapet. Using a wire probe to contact the inner electrode via a reference gas exchange hole, a VOM is used to check the electrical continuity between the silver lead and the inner electrode of the sensor head. Assuming continuity, the part is loaded into the oven again disk down and fired to peak temperature 850 °C. An air flow is provided into the oven. Occasionally we have noted an apparent interaction of the A58 and OS-3 resulting in a dark "stain" through the collar bodies. The reaction is non-destructive and is minimized using CPI proprietary A58 application and firing methods.

g. A type K thermocouple with leads ~12" long is fabricated of 0.010" chromel and alumel wire using a wire bonder. A short piece ~3/8" long of 1/16" o.d. x 1/64" hole i.d., two-hole, round thermocouple mullite tube is cut. A small slot is cut into one end of this along the line defined by the two holes. This slot should be wide and deep enough to accept and recess the bead of the thermocouple. The thermocouple leads are passed through the holes in this mullite "header" and are drawn down so that the bead nestles in the slot and below the end of the tube.

h. The thermocouple is coated or dipped into A52 ceramic adhesive and then inserted into the central hole of the sensor assembly. A small dab of A52 is placed onto the egress of the short piece of inner electrode lead from the assembly. The assembly is placed with the disk flat down, and the A52 is allowed to set at room temperature for ~4 hours.

i. A ~12" length of 0.010" silver wire is pulled through one hole of a ~6" long, four-hole, 1/8" o.d. x 0.020" hole i.d. thermocouple protector mullite. A short length of the silver wire is left

extending from one end of the mullite. The leads of the thermocouple potted in the sensor head assembly are passed through two of the remaining holes in the four-hole mullite. A jeweler's brazing torch is used to fuse the short tail of silver wire from the tube to the inner electrode lead protruding from the sensor head. The four-hole mullite is drawn down to completely shield the thermocouple leads, and the silver lead is gently pulled taut. The silver lead remaining exposed is folded down against the collar (between the heater leads) and along the sides of the four-hole mullite; this is then overcoated with A52. The assembly is allowed to set several hours at room temperature for the A52 to harden.

j. The two mullite tubes are bound together using wraps of high-temperature wire, e.g. short scrap lengths of heater or thermocouple wire. Care is taken to position the thermocouple tubes and lead such that the head assembly has a natural tendency to remain perpendicular to the two mullite insulating tubes.

k. A ~6" long x 0.630" o.d. x 0.010" wall piece of SS446 tubing is lathe cut and squared, and one end is folded in perpendicularly ("corseted") to ~0.450" i.d. The interior of the tube at the corset is wire brushed and cleaned with acetone.

l. An amount of VS9 glass is applied uniformly around the inner surface of the corset. The sensor head/lead assembly is inserted into the non-corseted end of the SS446 tube, pressed against the VS9 glass paste application, and then held pressed against the paste using a spring loaded ram which attaches to the open end of the tube (a special, CPI-designed and constructed device).

m. Assemblies prepared as above are inserted into an oven specially designed and constructed by CPI for firing the glass seals. Up to eight sensor assemblies are inserted through the oven base, such that the sensors are vertical and the flow of the melting glass under gravity will be uniform around the seal

surface. The sensor tube base and leads protrude from the oven base and may be cooled with an air flow. The seals are fired using a controlled time-temperature curve. An air flow is also admitted into the oven. Peak firing temperature is 850 °C.

n. There are several options available for making the lead connection to the outer electrode. For the purposes of our laboratory tests, we always made a loop of 0.010" silver wire with a short tail bent perpendicular to the loop. The loop diameter was made approximately the diameter of the A31 outer electrode. This loop was dipped in A94 and placed on the top of the sensor so that the A94 contacted and flowed onto the edges of the A31 electrode. The assembly was fired vertically as in "l." above, with an air flow; peak temperature was 600 °C. After firing, we extended the short tail with a length of 0.010" silver wire which we fused to the tail using a jeweler's torch. One might equivalently use the SS446 tube as a lead by painting a stripe of A94 from the A31 electrode to the tube corset. If necessary the SS446 contact point may be cleaned with grit paper to remove any oxidation from previous firing steps. Another option is to make a braze connection of the outer electrode lead to the side of the SS446 tube. This connection should be made well away from the seal/sensor head area to prevent overheating the seal or ceramic parts.

Examples of the final parts produced by GBC and of our resultant prototype assemblies are pictured in photographs A2 - A6 in the Appendix A.

XIV. SENSOR TESTS AND RESULTS

Early in the program we began testing the use of OS-3 in the "Nernst sensor disk" geometry that we envisioned and achieved in the final prototypes. Our first attempts at testing Nernst performance were prior to having discovered the V2B/VS9 sealing solution. For these early tests we designed and constructed a

test frame which clamped electroded disks of OS-3 between the ends of two tubes, and a crushed alumina fiber felt was used as a packing in the joints. Reference gas (air) was fed into one of the tubes; the other tube was hooked to a gas handling train which supplied gas mixtures containing various partial pressures of oxygen. Both tubes contained a small tube on the interior, and the whole arrangement was manifolded such that the test and reference gases were directed to the disk OS-3 sample through these small tubes, and then exhausted along the interiors of the larger, containing tubes. Thus the gases were continually refreshed at the OS-3 sample. A commercial Thermox oxygen analyzer was hooked in series with, and preceding, the test frame in the gas train. This allowed the oxygen partial pressure in the test gas to be known via an accepted "standard". (In the Thermox, this is a heated zirconia Nernst sensor tube). The arrangement of tubes was placed into the interior of a small, controllable tube furnace to provide heating of the disk, and a thermocouple placed near the disk monitored the temperature. Voltage across the disk was monitored using leads attached to the disk electroding and passing out through the alumina felt seal washers. The arrangement allowed us to calculate the voltage expected to be generated across the OS-3 test disk given the Thermox measurement of the oxygen partial pressure of the sample gas and the temperature of the test disk from the thermocouple. (Eq. 1).

Despite our effort and care in constructing this device it never worked satisfactorily as the alumina felt washers leaked too badly for Nernst cell measurements. It was used briefly for some amperometric sensor studies (Section XV below) and then abandoned.

Upon our discovery of the V2B sealing glass, but prior to the production of any parts by GBC size-matched to our SS446 tubing, we electroded and sealed disks into the ends of two corseted tubes using the glass. Wire attachments were made to the electroding; the inner electrode lead was passed through the side of the SS446 tube and sealed with glass. Again, the gas train and Thermox

system was used: the tubes were manifolded to the system using a special adapter fitting. The manifolding (again using a small tube contained in the larger sensor tube) allowed a continual flow of fresh sample gases to be directed against the interior electrode of each test sensor disk. When each tube was under test, the outer electrode was left in unrestricted contact with ambient air, a thermocouple was attached directly to the outer side of the sensor disk using a small amount of A52, and the disk-end of the tube was placed into the center of a controllable tube furnace.

Again (Eq. 1) we were able to calculate theoretical voltage outputs for the test disks for the various situations to which we subjected them. The voltages actually measured tracked with changes to oxygen partial pressures and reversed in polarity as the ratio between the sample and reference (air) oxygen partial pressures became greater or less than 1. However, the voltages measured were considerably less than that expected through our calculations for any given oxygen partial pressure.

We conjectured that one factor perhaps influencing our poor results was that the electroding on the disks had been applied using our "wax mask" technique for localizing the platinization. We noted there was a visible difference between wax masked electrodes and electrodes applied without using the technique, and feared the visible difference might indicate changes affecting catalytic performance. We abandoned the wax mask technique for the rest of the program.

Further, we felt we still had problems with non-hermeticity; this time not due to leaks through the seal, but due to the disks fracturing during testing. This was possibly due to the fact the disks were not manufactured to fit closely into the SS446 tubing. Rather, the disks were sliced from pellet samples designed for other CPI tests, and the resultant disks were ~0.1" smaller in o.d. than the i.d. of the tubing. To seal these disks required a rather thick seal. Though the glass seems well matched to the other com-

ponents in thermal expansion, we conjecture there was enough of a difference that when the seal was thicker a large strain was generated.

Our primary battery of tests began with the arrival of parts from GBC pressed to our design. Our first assemblies and consequent tests were made using imperfect parts from test pressings at GBC, and we assembled these in the manner of Fig. 9b. These assemblies/tests pointed out areas of design and construction requiring improvement, particularly that it was difficult to make the two seals required in the Fig. 9b. design, either simultaneously or consecutively. (See also Section VII.) Our designs and procedures evolved into the Fig. 9c. assembly using the final, flawless pressed parts from GBC.

Further, our first test devices were constructed without incorporated heaters and thermocouples as a simplification as we sought to solve the issues of sealing and performance first. A next level of prototypes then incorporated the type K thermocouples, and finally heaters were included in the last several prototypes.

We tested our various assemblies in the CPI oven testing chamber, and for this we constructed a special face plate to accept the assemblies. (This chamber was previously described in conjunction with our measurements of electrolyte ionic conductivity.) The modified face plate/access port had an O-ring compression fitting brazed to it which sealed to our 0.630" o.d. sensor tubes. The tail end of a sensor for test could be passed through the access port at this compression fitting, with the sensor protruding several inches into the interior of the test chamber. The tail end of the sensor hung out of the oven and compression fitting, thus the interior of the sensor had access to air, and the various sensor leads exiting the tail were accessable. These leads were hooked to a terminal strip to ease attachment to measurement instruments. A second small compression fitting in the face plate accepted a mullite thermocouple protector tube. This tube was used

to allow passage of a silver hook up lead for the sensor's "outer" electrode, and the end of the tube was sealed with vacuum sealing wax. The tube also served to hold a platinum thermometer and its leads as we tested prototypes which did not contain the type K thermocouple.

The O-ring compression fittings and wax seals were cooled during testing with a directed air flow from a fan. A piece of high temperature alloy sheet was cut so that it could be slipped over the sensor tube and mullite lead-carrying tube, and thus serve as a radiation baffle to reduce the heat load upon the access port plate and further assist in keeping the O-ring seals cool. This baffle was positioned mid-sensor tube into the oven interior and several inches from the access port plate.

The test chamber was placed in an oven, and oven heating was used for tests of heaterless devices. Testing of devices containing the coil heater was conducted with the oven off.

As described earlier, the interior of the oven test chamber could be flooded with a continuously refreshed flow of gas mixtures provided from a tank farm/manifold system. A Thermox I oxygen analyzer could be hooked ahead of or behind the test chamber in the gas system, providing readings as a standard of the oxygen partial pressure present in the test gases.

A Hewlett-Packard Model 7132A two-channel chart recorder and Keithley Model 181 nanovoltmeters were used to measure thermocouple and sensor output voltages. These instruments were used in various combinations. Near the end of our program we utilized a Digital Equipment Corporation PDP11/23 computer and accessed the the Keithley nanovoltmeters via IEEE-488 interface to automate data collection.

The best experimental results obtained among our various tests are presented in Fig. 13. We have found the final heaterless proto-

types responded quickly to oxygen partial pressure changes when heated to ~ 600 °C, and changes in output signals tracked changes in oxygen partial pressure. Output voltages did reverse polarity correctly as sample gas oxygen partial pressure became greater or less than atmospheric (the ratio of the two becoming greater or less than one). Exact response speed was not quantified as the time involved to completely purge the oven testing chamber was not measured; however, initial change in prototype sensor readings seemed "immediate", given a time lag between the Thermox and the test chamber due to the purge of the interconnecting lines. However, as shown in Fig. 13, readings were never completely commensurate with theoretical expectation.

The output voltages we recorded were generally not stable over long periods. As an example, when pure oxygen was introduced as a test gas, we found sensor output peaked at some voltage approaching theoretical expectation, and then shifted over time to a value indicating an oxygen content lower than 100%.

Such behavior could be explained by leakiness of the seals, as corruption of the reference gas by onrushing sample gas would tend to change readings over time. To test this hypothesis, we fed the sensor head of our prototype with a tiny air flow; this was accomplished using a small diameter steel tube placed into the length of the prototype interior and terminating near the base of the sensor collar. A laboratory fan was connected to force the air flow down the tube. This provision for constant refreshment of the interior reference atmosphere did NOT improve sensor performance, and in one case the results obtained were even farther from theoretical than those recorded without the air flow!

We are therefore at a loss to explain our Nernst sensor results. We did note that prototype sensor performance improved as we developed better sealing methods; thus (despite the experiments to the contrary related in the preceding paragraph) seal leaks might still be implied as the main source of less than theoretical

performance. We found it very difficult to obtain "perfect" seals; nearly all of the devices tested did exhibit tiny leaks under pressure tests at room temperature. It does not seem logical to us that extremely tiny leaks appearing only under pressurization could lead to reference gas poisoning in low pressure situations, especially in those tests where the reference gas was constantly refreshed. However, such explanation must be considered a possibility.

It is conceivable that the A31 electroding was not behaving properly catalytically. However, other CPI studies utilizing this material have indicated no problem. We feared the seal glass/A31 interaction could create problems; but as we have related, we took special care to avoid that interaction, and saw no visible evidence of such interaction on our test prototypes.

Two final hypothetical explanations for the discord between our observed and theoretical results are that the Thermox I was not an adequate standard by which to gauge our measurements, or that the oxygen partial pressure in the test chamber was actually quite different than that recorded by the Thermox. These possibilities were suggested by certain experiments in which we first flooded the system with nitrogen, introduced some hydrogen for a brief time, and then switched back to either tank nitrogen alone (which contained some trace oxygen), or nitrogen mixed with a small amount of oxygen.

In these situations we found very discrepant behavior between the Thermox and the CPI prototypes. (Fig. 14). The presence of the hydrogen caused the test and Thermox sensors to give their highest voltage readings, indicating low oxygen partial pressures. The Thermox readings theoretically corresponded to less than approximately 10^{-20} atm. Upon the introduction of the nitrogen or nitrogen/oxygen after a period with some hydrogen, the CPI sensor responded and indicated larger oxygen partial pressures; at the same

time the Thermox would change very little and would continue to indicate very low oxygen partial pressures.

The lack of response of the Thermox and the presence of response from the CPI sensor when response was expected suggested some fundamental difference between the two sensors which might invalidate the use of the Thermox as a comparison standard for the CPI sensor. One obvious difference is that the Thermox I is a zirconia-based Nernst sensor operating ~ 140 °C hotter than the CPI sensor, at ~ 738 °C. As previously mentioned the presence of combustibles in gas samples in contact with extremely hot Nernst Cells can lead to combustion and consequent reaction of free oxygen in the gas sample, and the electrochemistry at the electrode becomes complex. Some process such as this may have been behind the behavior we observed, and the CPI sensors may have been indicating more correct values for the oxygen partial pressure than the hotter Thermox.

We have also thought it possible that the Thermox and CPI sensors were seeing true differences between the oxygen contents at the localities of these sensors. We speculated differences could perhaps exist due to the nature of the CPI sensor test chamber. The test chamber was composed of high temperature stainless steel; such metals form protective oxide layers under heating and the sample gases might have been interacting with the metal/oxide layers during sensor testing and oxygen might have been being adsorbed/de-adsorbed. In the Thermox, by contrast, the sample gases came into contact only with the hot zirconia electrolyte and platinization and such processes do not occur with these materials. We speculated that if adsorption/de-adsorption processes were occurring, they might have led to unexpected changes in the actual oxygen partial pressure present in the sample chamber and in the gases downstream from the chamber.

We made attempts to gain more evidence for our hypotheses by placing the Thermox both before and after the CPI test chamber in the

gas flow and repeating our hydrogen exposure/oxygen bleed experiment. The voltage-time records of the CPI sensor are shown schematically in Figures 15a and 15b. The data of Fig. 15a were taken with the Thermox placed first in the gas stream (the output from the Thermox feeding the CPI test chamber), and the data of Fig. 15b were taken with the Thermox placed after in the gas train (the output of the CPI test chamber feeding the Thermox. We found that the characteristics displayed in these schematics were very repeatable as hydrogen or oxygen were bled into the system.

As may be seen in the "Thermox" record, there were fine features or "plateaus" which would indicate brief leveling of the oxygen content inside the oven test chamber. These fine features were not present in the "Thermox downstream" record. We also found the Thermox readings with the "Thermox upstream" indicated lower oxygen partial pressures were achieved than with the "Thermox downstream", but it is difficult to consider these differences as great since the differences occur in the $\sim<10^{-20}$ regime. Other than these minor differences between the records of the two situations, the gross behavior was repeated.

We also made an attempt to lower the operating temperature of the Thermox to see if operation at the CPI sensor temperature would cause both sensors to behave similarly; we found we could not get reliable readings from the Thermox with the cell temperature lowered below ~ 700 °C.

The minor differences between the behavior of the system with the Thermox before and after the CPI test chamber do suggest some complex interactions of the sensors and test chamber with the system gases. The gross similarities of the behaviors are very strong, however. No mechanism is clearly revealed to us allowing us to understand the differences in response of the CPI sensor and the Thermox as oxygen is bled into the system after hydrogen exposure. Most importantly, we find no further clue as to why

the CPI sensor did not yield full theoretical voltages during our various tests.

We finally note that the introduction of the combustible hydrogen placed both the Thermox and the CPI sensors in a low oxygen regime in which electronic conduction was likely to occur. Though we speculate this might have something to do with the observed "hang up" of the Thermox readings as oxygen was bled into the system, we have no clear understanding how the electronic conduction mechanism would produce the observed results.

The results we have reported above were collected with heaterless assemblies. As mentioned, we found it difficult to obtain "perfect" seals as tested under ~5 psig pressures at room temperature. We found that hairline cracking often appeared in the sensor disks after several thermal cyclings.

The inclusion of the heater led to a number of further problems which we were not able to solve within the limitations of this program. The heaters failed on a significant fraction of our units after several hours. We also saw cracking of the sensor collar bases around the air exchange holes over time, and post mortem examinations also showed cracking of the collar walls. We did test some of these devices for oxygen sensitivity but could not obtain readings for a variety of reasons including noise pickup problems across the signal leads (possibly bad connections to the internal electroding), a bad thermocouple, and separation of the sensor head collar from the disk upon heating.

XV. AMPEROMETRIC SENSOR STUDIES

Over the course of our literature reviews for information relevant to the Nernst sensor configuration which was the central focus of this program, we came across several interesting and exciting articles relating the use of oxygen ionic conductive electrolytes

to form "amperometric" oxygen sensors. Because of the availability of OS parts and sensor test equipment we have conducted a minor effort in parallel with the Nernst Sensor study to investigate the use of OS materials in amperometric devices.

There are several different constructions for amperometric oxygen sensors, and several different schemes for making the "amperometric" measurements. Most commonly the oxygen conductive electrolyte is utilized as an oxygen pump. Rather than placing the electrolyte as a barrier between two regions of differing oxygen partial pressure and allowing ions to migrate "passively", resulting in a Nernst voltage across the barrier, amperometric sensors reverse the process and apply a voltage across the electrolyte to "actively" drive ions through the electrolyte. This "pump" is immersed in the sample gases, and there is no need for a reference gas. Further, the electrolyte must only be heated as much as is necessary to allow significant ionic conduction: the "spurious voltages" and electrode/electrolyte interactions noted in conjunction with (attempted) Nernst Sensor operation at low temperatures do not affect amperometric measurement.

In the most common amperometric sensor configurations/schemes of application, a partial barrier to oxygen molecules is placed over an electroded oxygen electrolyte (Fig. 16). Oxygen molecules penetrating the barrier from the sample gas are catalyzed into ions by the electroding, and all ions produced are swept through the electrolyte by a fixed voltage applied across the electrolyte. (Once on the other side of the electrolyte these ions recombine into molecules and are exhausted.) The number of ions swept through the electrolyte is directly related to the electrical current involved (Faraday's Law), and the number of molecules penetrating the barrier is directly related to the oxygen partial pressure outside the barrier (Fick's Diffusion Law). This chain of relationships leads to the fundamental concept of such sensors: that the current drawn by the sensor given a fixed applied voltage

is directly related to the oxygen partial pressure in the surrounding gas sample.

The "partial barrier" used in these sensors is required to cause the current drawn to be limited by the ions available rather than by the ionic conductivity of the electrolyte. Without considering the complexities of rates of molecular impact upon and reaction at the sensor electrode, the ionic current which may be drawn through an electroytic membrane without a barrier may be very large though the surrounding molecular concentrations may be very small. One may intuitively see the point by comparing the relative sizes of the Ampere and the Faraday.

From the standpoint of the convenience and expense of power supply and detection equipment, one wishes to have a sensor which has limiting currents on the order of milliamps. The current drawn through a coated electrolyte pump is reduced to smaller levels by the diffusion limited coating, and the upper limit for the oxygen concentration which may be sensed without "swamping" the sensor is increased. The amperometric sensor concept has largely been developed by researchers interested in the automotive industry; published research and fully developed zirconia devices have been designed to function in the ~1% to ~20% oxygen partial pressure range. Total currents flowing through these devices are kept on the order of ten's of milliamps to ease interface to microprocessors and detection circuits.

Nearly all of the published research and commercially produced devices of the amperometric type utilize restrictive barriers, either provided by a tiny orifice through a solid cover plate, a capillary channel, or by porous coverings. One would imagine limiting currents would exist for unrestricted devices if used in extremely low oxygen concentration environments; however, we have seen no theoretical or experimental work on the behavior of an unrestricted electrolyte in such an environment. Nor have we seen any theoretical or experimental work on a device which uses as a

"poor oxygen catalyst" electroding as the molecule/ion restricting barrier, which would also seem to be a logical approach.

A general mathematical description of amperometric devices may be derived as follows: If a voltage , V, is applied across the cell of Figure 16, the cell will produce a back EMF according to the Nernst relationship (Equation 1). The combination of voltages with the internal resistance of the cell, R_i, yields:

$$I = (V + EMF)/R_i \tag{3}$$

(Refer to Equation 2 for the factors influencing R_i.)

The external voltage tends to move ions through the electrolyte and thus depletes the oxygen at the diffusion layer/electrode/ electrolyte interface. The oxygen partial pressure at this interface, P_1', becomes less than that in the bulk surrounding gases, P_1, and a diffusion current of oxygen is set up through the diffusion layer which will tends to equilibrate the oxygen partial pressures between the interface and the bulk gases. The diffusional flux, G, in general is given by:

$$G = \sigma(P_1 - P_1') \tag{4}$$

where σ is a constant depending upon the diffusion constant of oxygen and the geometry of the aperture. At steady state, the current and the diffusional flux are related by Faraday's Law:

$$I/4e = G \tag{5}$$

Combining Equations 3, 4, and 5 then:

$$I=\{V+(RT/4F)\ \ln\ [1-I/(4e\sigma P_1]\}/R_i \tag{6}$$

Eq. 6 describes a behavior which may be broken into two regimes,

and there is a third regime imposed by the physics and chemistry of the situation, not described by the above equation.

The first regime is Ohmic. When V and I are small, such that the ln(...) term becomes 0, Eq. 6 reduces to $I = V/R_i$.

The second regime is the one utilized in operating the device as a sensor. In this regime the device saturates at a limiting current regardless of the applied voltage; as related in the general descriptions above, the ions available to be moved are limited by the diffusion rate to the barrier/electrode interface, and no further ions (current) may be moved regardless of the voltage applied. This saturation current is given by:

$$I_s = 4e\sigma P_1 \qquad (7)$$

The third and final regime of device operation is that where the voltage is raised beyond a certain limit, and excess current begins to be generated by factors not included in Eq. 6. One of these factors is the induction of electronic current; as in the use of the Nernst Cell, when P_1' becomes quite small a partial decomposition of the electrolyte can occur and electronic conduction begins. Another process which may occur is the electrodecomposition of oxygen-containing gas molecules in the sample gas, such as water and carbon dioxide.

The function of such a device is shown schematically in Fig. 17. One may readily see that if a fixed voltage is applied to the device (and the device is held at a near constant temperature), the saturation current is proportional to P_1. The behavior of a device of higher internal impedance is shown in Figure 18, and it may readily be seen that the effect of the higher impedance is to narrow the operational range of the sensor. [6]

One may readily see that molecules must be catalyzed and swept through the electrolyte at a rate at least as high as the diffusion

rate into the sensor in order to maintain the partial pressure differential across the diffusion barrier. Thus, on the intuitive level one may see the ionic conductivity of the electrolyte is one of the factors going into the device impedance while the diffusion is the other. From the discussion above, we may infer it is beneficial to use higher ionically conductive materials in order to lower the impedance of the device and thus broaden the operational range of the sensor. Here we believe the unique, high ionic conductivity of OS-3 (and the other OS materials) has great benefit: the lowest temperature of operation we have seen in the amperometric device literature was ~ 450 °C for a thin, screen-printed zirconia device with an internal heater. We would have every expectation of further lowering operating temperatures for a sensor made using the OS materials.

We have constructed devices using OS materials in several configurations which we have hoped might duplicate the diffusion limited pumping conditions for an amperometric sensor. The devices were of varying levels of sophistication, and none were optimized; we have obtained I vs. V behavior as in Fig. 17 in only one test instance. However, even with our most elementary devices we have consistently seen current variations vs. oxygen partial pressure changes, and this has been at device temperatures as low as ~ 160 °C.

We assembled and gave cursory testing to "sensors" formed of OS-3 disks overcoated with our porous ceramic adhesive materials, A52 and A71. Our tests were conducted in the oven test chamber already described in connection with ionic conductivity and Nernst cell testing. The devices were suspended in the test chamber from mullite tubes which carried the current/voltage leads to the device. The devices were thus completely immersed in the test gases with no reference gas supplied. The temperature at which these tests were conducted was around 450 °C, and various current measurements were made within a matrix of oxygen partial pressure variations (from "trace" to 1 atmosphere) and applied voltages (0 to ~1.5 V). The response currents measured were not greatly stable, and the

"saturated" I plateaus hoped for were not observed; however, the results were encouraging in that changes in current were noted at the different oxygen partial pressures.

In another crude attempt, we attached cover plates of thin sheet copper to OS-3 disks using A52. On these devices the cover plate had been pounded into a shallow dish shape so that a tiny volume was enclosed between the cover and the electroded face of OS-3 disk. A pin was used to punch a tiny hole in each of the covers. During assembly of one of the devices, we filled the volume under the shallow dome with alumina powder in an effort to further increase the diffusion path between surroundings and the inner, electroded face. The tests conducted on these were at temperatures ~ 430 °C - ~ 450 °C and ~0.8 VDC applied. The largest currents involved were on the order of several milliamps. The tests were again encouraging as we saw changes of current with variation in oxygen partial pressure. The device containing the alumina powder was particularly interesting as the initial responses to change were quite rapid. In several instances the current level did stabilize within ~5 minutes after a sample gas change.

Most of our effort in our investigations of OS materials in amperometric sensing were conducted upon OS multilayers which had originally been envisioned for use as ultraminiature Nernst devices. These multilayers had been constructed for CPI and were originally studied under DOE contract #DE-FG01-82CE-15908 between 5/82 and 5/83. As we reviewed the concepts of diffusion-limited amperometric sensors, we came to remember that one of the findings from that previous contract was that the multilayers WERE DIFFUSION LIMITED and did not function well as the intended Nernst devices. Remembering the diffusion limitation, we began to speculate these devices might find use as amperometric sensors.

The OS multilayer devices consist of ~19 layers piled ~3 mm deep with interposed electrodes. The electroding is offset to opposing sides with alternating layers, and this geometric arrangement is

shown schematically in Fig. 19 (Fig. 19 also pictorially includes a diffusion layer not present in the "bare" devices, but which is envisioned for final device development); each multilayer device may be considered as a single, thin electrolyte membrane of large surface area folded down upon itself. Overall, the devices are ~5 mm x 5 mm x 3 mm in size.

The original concept for application of these devices was that each might be placed in bulkheads separating sample and reference gases; the arrangement was to be such that one of the electrode access sides was exposed to the sample gas and the other to the reference gas. The bulkhead and device were to be heated. The sample/reference gases were expected to diffuse without impedance down the opposing electrode layers, and the device would then behave as a Nernst sensor. Testing of these devices indicated oxygen molecules/ions were not diffusing/migrating down the electrode surfaces into the device body and through the electrolyte as expected. "Diffusion limiting" was experienced even though several variations on electroding were constructed and tested, i.e. devices were constructed with conventional (dense) electrodes, "lacey" electrodes (small voids), and "infused" electrodes (most of the electrode layer space was hollow).

A mathematical argument (Appendix B) was constructed to consider whether amperometric sensing might be feasible using these devices which contain diffusion limitation at both the ingress and egress electrodes. The simple model did suggest the current through such a device would be proportional to the surrounding oxygen partial pressure. Further, it was reasoned the multilayer geometry of the device would be extremely efficacious as the parallel, thin layers should lead to an extremely low device impedance, the importance of which was noted above.

Our first test of the concept was conducted upon a "bare" OS-2 multilayer with "conventional" electroding. The device was held at ~ 213 °C. We immediately found that the current passing through

the device, 1 VDC applied, responded to changes in oxygen partial pressure. The responses were not stable over long periods, but if the slight drift were ignored, the responses did seem to track the changes recorded by the Thermox in both speed and features. Our results are recorded in Fig. 20.

We explored a number of variations in continued experiments. We used OS-2, -3 and -4 devices with both lacey and conventional electrodes, and we applied various overcoatings to the "ingress" sides of devices in order to attempt to influence diffusion and change device characteristics. Overcoatings used included A54 silver paste, A52 ceramic adhesive, and OS-3 paste. Behavior was recorded at various applied voltages and at various temperatures. Because of the volume of data we began to use Keithley Model 181 nanovoltmeters and an IEEE 488 interface to a computer to collect the data we generated. A sampling of our findings is presented in Figs. 21 through 24.

Fig. 21 records the interesting results for an OS-2 conventionally electroded device with no overcoating. The device was held at ~ 162 °C and 1.5 VDC was applied. As may be seen the behavior of current vs. oxygen partial pressure was fairly repeatable over several sweeps. This is not "standard" amperometric sensor behavior as discussed above, as the current is not linearly related to the oxygen partial pressure, nor could we obtain the "standard" I vs. V applied behavior for this device. However, we feel the extremely low temperature and approximate repeatability of the variations make this a notable result. We do not currently have a theoretical explanation for this result.

A compendium of results obtained at low temperatures for the device of Fig. 21 is shown in Fig. 22. This Figure gives further example of the current vs. oxygen partial pressure and an indication of the current vs. temperature behavior for these devices at low temperature. The current vs. temperature behavior for an OS-4 device is further explored in Fig. 23. In this experiment, the device was

held at at a fixed oxygen partial pressure of 1 atm. and the oven controller was set to various temperatures. Temperature (measured by a Type K thermocouple attached directly to the device) and current were sampled at a uniform rate as the oven heated; as may be seen by the "scalloping" the current was not completely stable at the oven set-points.

We could not obtain the "standard" I vs. V behavior for any of the bare devices tested. Consequently we concluded that the devices, though too diffusion limited to make good Nernst sensors, were not enough diffusion limited to yield the expected theoretical behavior for amperometric devices. As related above, we coated the ingress of various devices with various substances to influence the diffusion characteristics. An indication that we did influence those characteristics and began to achieve "theoretical" behavior is shown in Fig. 24 in which we have graphed I vs. V measurements for the device of Fig. 21 after its ingress had been overcoated with a layer of OS-3 paste and then fired. We expect that the OS-3 paste layer was porous, or perhaps allowed only tiny channels between the main body of the device and the overcoat. One may see in the Figure that there is a hint of the saturation plateau effect at very low oxygen partial pressures. The device was at ~ 384 °C in this test and the current levels were consequently fairly "large" (milliamps).

XVI. CONCLUSIONS AND AREAS FOR FUTURE DEVELOPMENT

We have seen that the prototypes for Nernst sensors created during this program suffered from a number of unexpected problems: difficulties in sealing, low intrinsic strength of the OS-3 structures we created, and difficulties brought by the inclusion of the heater to the unit were prime problems. We have further had the discouraging result that none of the units tested yielded full theoretical voltage output according to the Nernst Law.

However, at the conclusion of the program, we were made aware of information which may have caused some of the difficulties we have reported. Above, we reported that we introduced vibratory milled OS-3 powders into this program and ultimately made the sensing disks of our final sensors of these. Our introduction of these produced some puzzles in that we did not see a marked improvement in part strength as expected from the researches of our powders supplier. We did see a marked difference in the firing characteristics of parts from vibratory milled vs. parts from ball milled powders, a behavior which is not uncommon when dealing with powders of different grain sizes, but which may also indicate contamination. Our investigations at the time of the discovery of this dilemma yielded no clue to causes -- e.g. we questioned our powder supplier about the possibility of contamination and were assured there was none. Our ionic conductivity measurements did not seem to indicate any problem, within the limits of error and variation we had come to expect.

At this late date, our powders supplier has realized that some of the powders supplied to us for our various projects have been incorrectly calcined and not completely reacted. At this point we have no way of being certain which batches of these powders were affected nor how incomplete reaction would affect our results.

We have questioned why problems in the powders were not noted in our ionic conductivity quality control checks. We feel we have two explanations for this: Fist, in retrospect we realize we DID see slight departure of the conductivities of our parts from our ideal ionic conductivities for the OS-3 material. These seemingly slight departures were not great and seemed to lie within the accuracies of the equipment and methods we used. As example, our final comparisons have been made on the basis of logarithmic plots (e.g. Fig. 12); unfortunately the logarithmic plotting may obscure differences.

Second, we were not able to make "four-lead" ionic conductivity checks on the disks we used. In order to make "ecclesiastical" potentiometric conductivity measurements we must utilize pressed bars of material, which allow accurate measurement of (constant) cross-section and length and provide physical separation of the current and voltage leads. When performing the measurements upon our sensor disks we could not separate our voltage and current leads. Further, the two-lead techniques we used required certain lead corrections to be applied to our data reduction, or we assumed the corrections were insignificant, and the measurements were very sensitive to the thickness measurement.

If the materials used in this program were among those incorrectly prepared by our supplier, this might have an impact upon our ability to achieve full Nernst potentials with our prototype sensors. On the other hand, literature indicates a large degree of impurity may be tolerated in a Nernst Cell as long as the electrode/ electrolyte interface is not affected. [3] The incorrect preparation certainly would have impact on the structural strength of pressed parts, the thermal cyclability of those parts, and upon the thermal expansion of the material. It might be recalled we did obtain differing thermal expansion measurement results from independent, but quality, laboratories. Our powder supplier made the test bar for us, and if the bar were of incompletely reacted materials, perhaps this would result in the bar undergoing shifts in thermal expansion with each thermal cycling. Shifts in thermal expansion during thermal cycling may explain some of the difficulties we noted in part/seal life (i.e. sensor disk cracking after several cycles).

We remain confident that OS-3 may be utilized in a Nernst sensor operating at lower temperatures and of lower cost than a comparable zirconia sensor. We have learned a great deal about the properties of, and manufacturing of parts from, OS-3 over the course of this study. We have further learned a great deal about sealing this material into structures. We feel that a more robust design than

what we utilized might be developed and employed to great benefit, and the correct processing of vibratory milled powders may yet yield stronger parts. We feel that heater lifetime and design shortcomings could easily be solved using expert guidance. Similarly, we feel sealing problems can be solved given a dedicated program, and these may already HAVE been solved by the D.O.E./Oak Ridge Laboratories.

An exciting discovery made during this program has been that OS multilayer devices exhibit oxygen sensing capabilities at temperatures as low as ~ 160 °C. It is our hope that future programs will allow us to develop diffusion layers matched to these devices which will allow refinement of the device into a stable, sensitive sensor of extremely low temperature operation.

OS3 multilayer devices could be manufactured in quantities of millions per day using extant ceramic multilayer capacitor manufacturing methods and the price of production of a single device would be on the order of tens of cents rather than tens of dollars. (This technology could not be used to produce zirconia-based devices because of zirconia's very high sintering temperature.) If so developed, the extremely low temperature operation and extremely low price per device of OS3 Amperometric sensors would open new vistas in application of oxygen sensors, and would go far to solve problems existing in present applications.

References:

1. City Technology, Ltd., "Humidity Effects", Technical Information Sheet 11, Issue 2.98., London, England.

2. David C. Hill and Harry L. Tuller, "Ceramic Sensors: Theory and Practices", Chapter 5, pp. 286 ff.

3. Badwal, S.P.S., et. al., "Low-Temperature Behavior of ZrO2 Oxygen Sensors", Advances in Ceramics, Vol. 12, Science and Technology of Zirconia II, N. Claussen, M. Ruhle, A. Neuer, eds., American Ceramic Society, 1984.

4. H. Okamoto, et. al., "Non-Ideal EMF Behavior of Zirconia Oxygen Sensors, Solid State Ionics 3/4 (1981) p. 453-456, North Holland Publishing Co.

5. Private Correspondence with Ceramatec, Inc., Salt Lake City, Utah.

6. E. M. Logothetis, "Air to Fuel Sensors Based on Oxygen Pumping" Ceram. Eng. Sci. Proc., 8[9-10], pp. 1058-1073, (1987).

APPENDIX A. PHOTOGRAPHS.

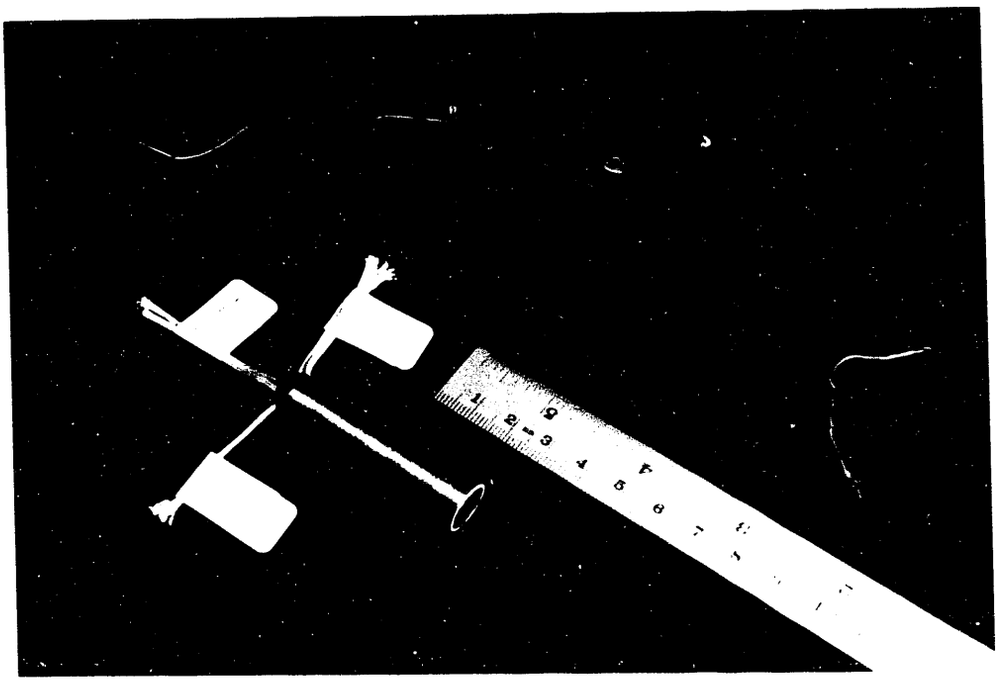

Figure A-1. Model of Early Sensor Concept.

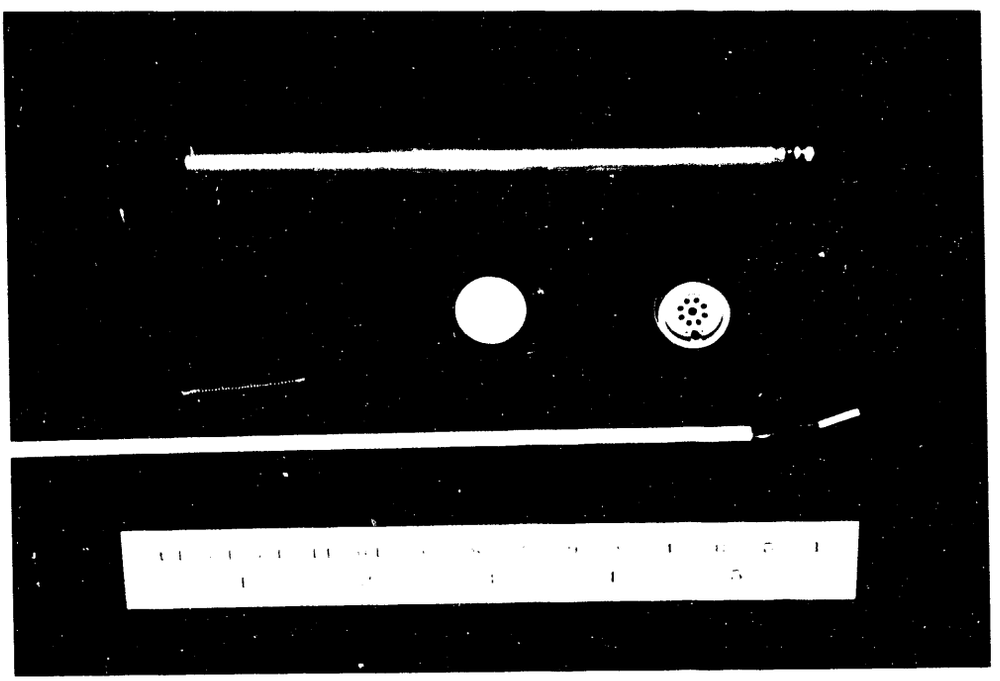

Figure A-2. Final sensor parts: Corsetted tube, heater coil, sensor disk (GBC), sensor collar (GBC), and thermocouple assembly.

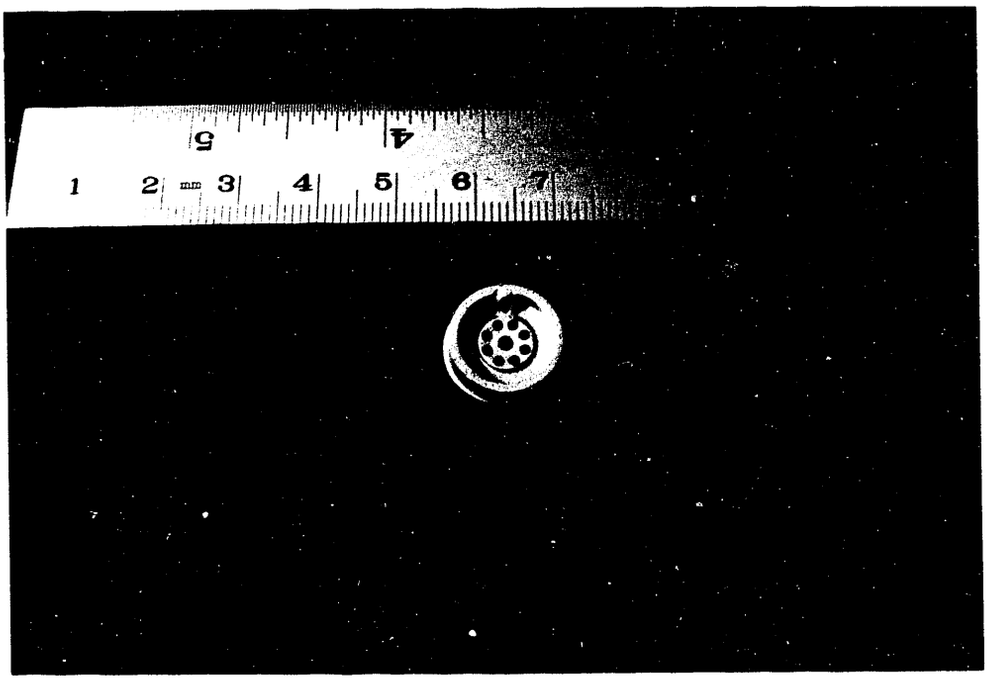

Figure A-3. Close-up of early GBO collar pressing (breakage at "parapet" was later remedied).

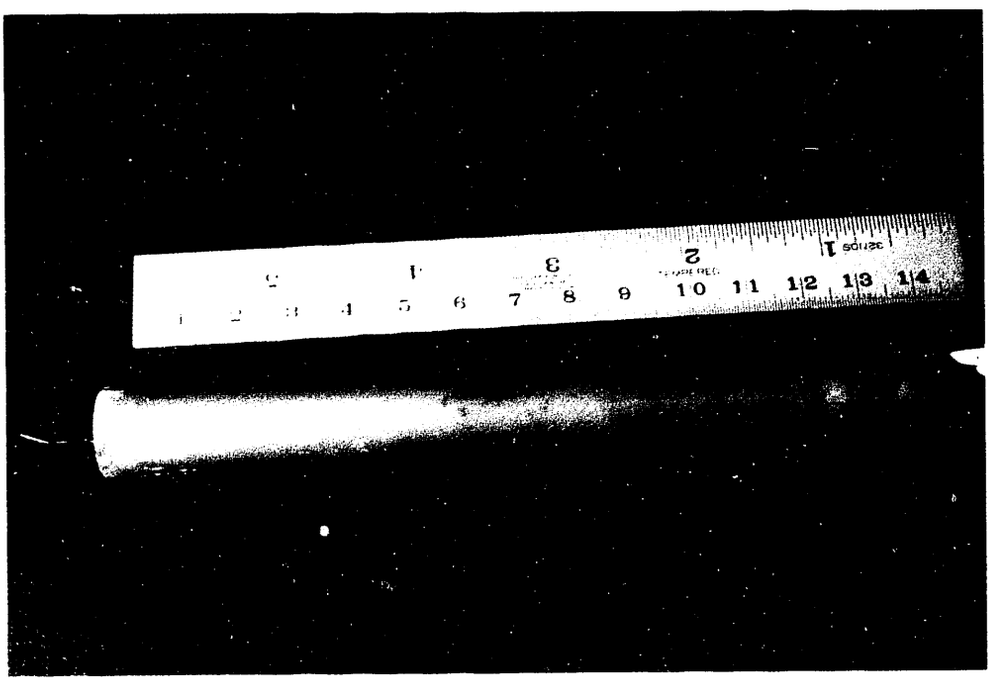

Figure A-4. Prototype Nernst Sensor, final assembly (side view).

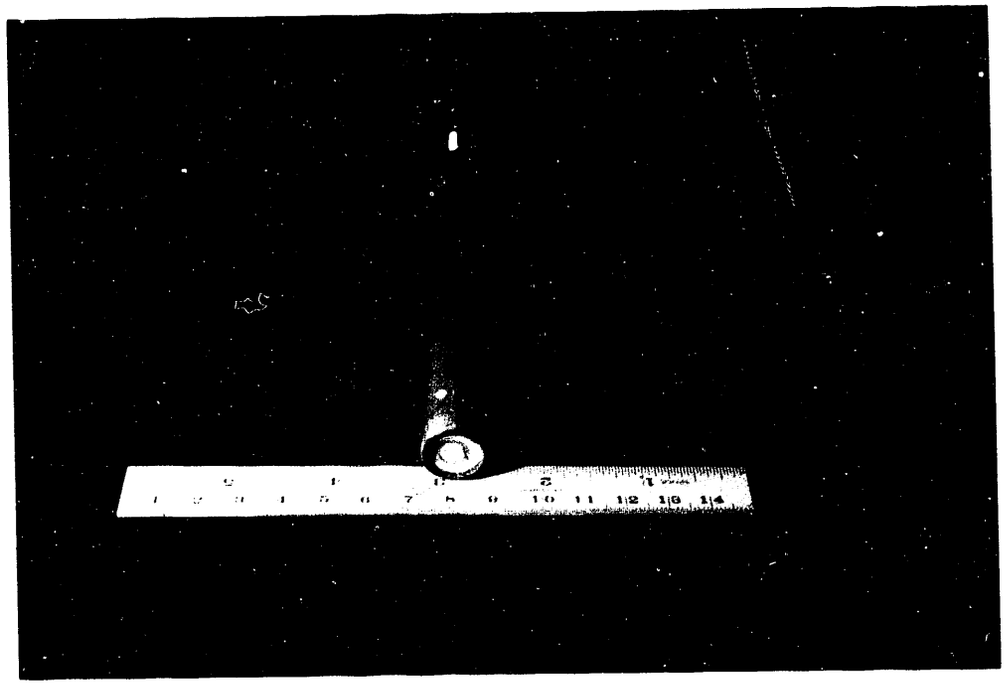

Figure A-5. Prototype Nernst Sensor, final assembly, end view.

Figure A-6. Prototype Nernst Sensor, final assembly, close view of glass seal, outer electrode and outer electrode lead.

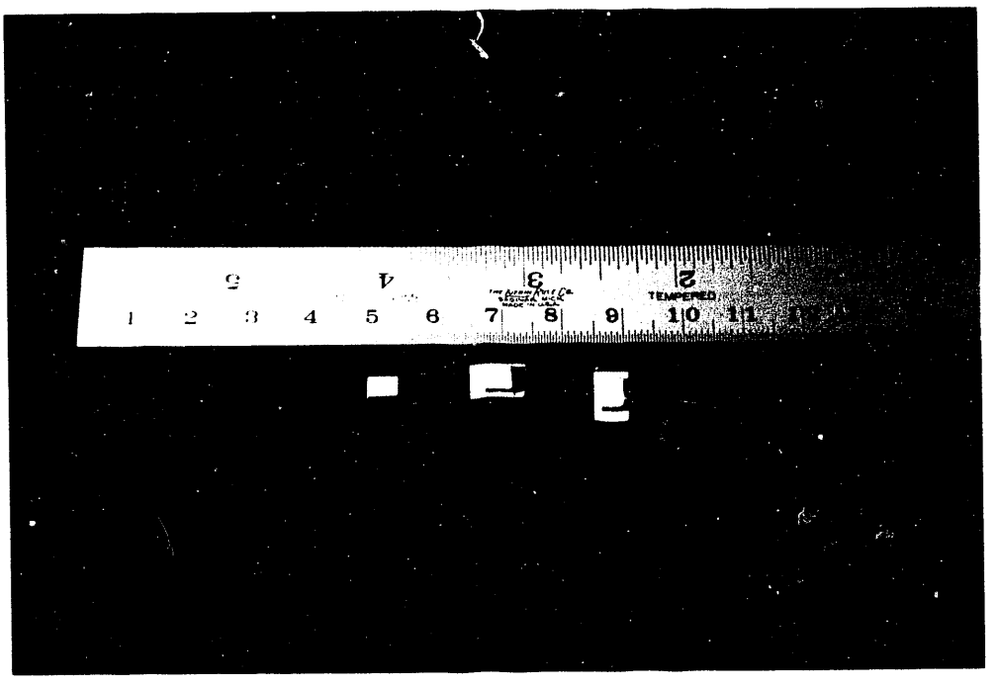

Figure A-7. CPI Multilayer Amperometric Sensors.

APPENDIX B. THEORETICAL DISCUSSION OF AMPEROMETRIC OXYGEN SENSING

An amperometric oxygen sensor based on a multilayer-capacitor type geometry was demonstrated in this program. The purpose of this appendix is to outline the broad theoretical picture of how this new type of sensor operates.

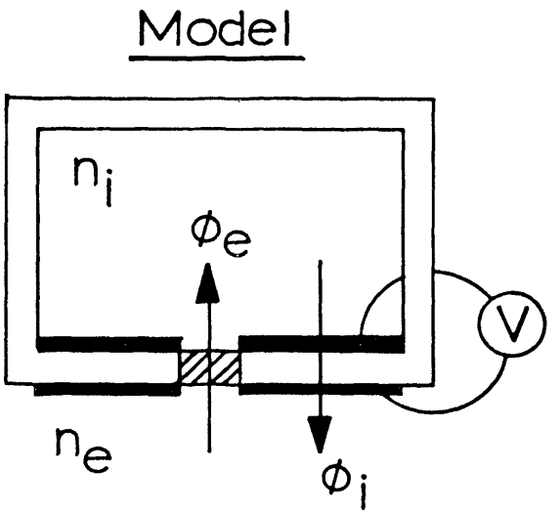

The cavity contains a density of n_i moles of O_2 per unit volume, and the infinite reservoir contains a density of n_e moles of O_2 per unit volume. A flux ϕ_i of O_2 moles is flushed out of the cavity by the applied voltage V, depleting n_i in the cavity. This depletion creates a concentration gradient, $n_e > n_i$, resulting in a flux ϕ_e of O_2 moles from the reservoir into the cavity. This ϕ_e flux takes place across a "diffusion plug", as shown, and the units of the ϕ-fluxes are moles per unit area per second.

At steady state,

$$-A_i \phi_i = A_e \phi_e \qquad \text{(B1)}$$

where A_i is the effective electroded area within the cavity and A_e is the cross-sectional area of the plug. The meaning of Eq. (B1) is that the flow of O_2 moles into and out of the cavity are in balance (i.e., the cavity concentration n_i is constant).

Problem: What is the relation between the current I due to the applied voltage and the oxygen partial pressure in the infinite reservoir?

A. ϕ_e Flux

Fick's first law applies

$$\phi_e = -D\nabla n \cong -D_o e^{-Q/kT}(n_e - n_i)/\delta \qquad (B2)$$

where $D = D_o e^{-Q/kT}$ is the diffusivity in units of cm^2/sec and δ is the characteristic thickness of the plug. A linear concentration gradient has been assumed, $\nabla n = dn/dx = (n_e - n_i)/\delta$ (i.e., the plug is at a constant temperature and D does not depend on n).

B. ϕ_i Flux

For possible low-temperature operation (~ 200 °C), the voltage-driven flow of oxygen may be limited by the $O_2 \rightarrow 2O^{-2}$ catalysis at the electroded surface within the cavity. If the cavity contains m_i moles of O_2, then the rate at which moles are catalyzed is given by the rate equation

$$dm_i/dt = km_i = k_o e^{-U/kT}\, n_i/v_i \qquad (B3)$$

where $k = k_o e^{-U/kT}$ is the rate constant and v_i is the volume of the cavity. A first-order rate equation has been assumed.

If there is sufficient voltage to "sweep" all the electrode-catalyzed oxygen from the cathode to the anode, then

$$\phi_i = (dm_i/dt)/A_i = k_o e^{-U/kT}\, n_i/v_i A_i \qquad (B4)$$

Finally, equating the steady-state fluxes from Eqs. (B2) and (B4) according to Eq. (B1), we have

$$k_o e^{-U/kT}\, n_i/v_i = A_e D_o e^{-Q/kT}\, (n_e - n_i)/\delta \qquad (B5)$$

C. Perfect-Gas and Faraday's Laws

The oxygen partial pressure in the infinite reservoir, p_e, is the quantity to be measured and is related to n_e by the (approximate) perfect-gas law

$$p_e = n_e RT \tag{B6}$$

The ionic current flowing due to the applied voltage is given by Faraday's law

$$dm_i/dt = I/zeN_o = k_o e^{-U/kT}\, n_i/v_i, \tag{B7}$$

where Eq. (B3) has been used and, as before, we assume the voltage is large enough to sweep all the catalyzed oxygen from the cathode to the anode.

The procedure now is straightforward: $n_i \propto I$ from Eq. (B7) and $n_e \propto p_e$ from Eq. (B6). Substituting in Eq. (B5) and re-arranging we have the final result

$$p_e/IT = \underbrace{\alpha e^{U/kT}}_{\text{Catalysis}} + \underbrace{\beta e^{Q/kT}}_{\text{Diffusion}} \tag{B8}$$

where

$$\alpha = Rv_i/k_o zeN_o \;\&\; \beta = R\delta/zeN_o A_e D_o \tag{B9}$$

It is interesting to note that the α/β ratio is

$$\alpha/\beta = (D_o/k_o) v_i v_p/\delta^2 \tag{B10}$$

where $v_p = A_e \delta$, the volume of the plug.

D. Observations

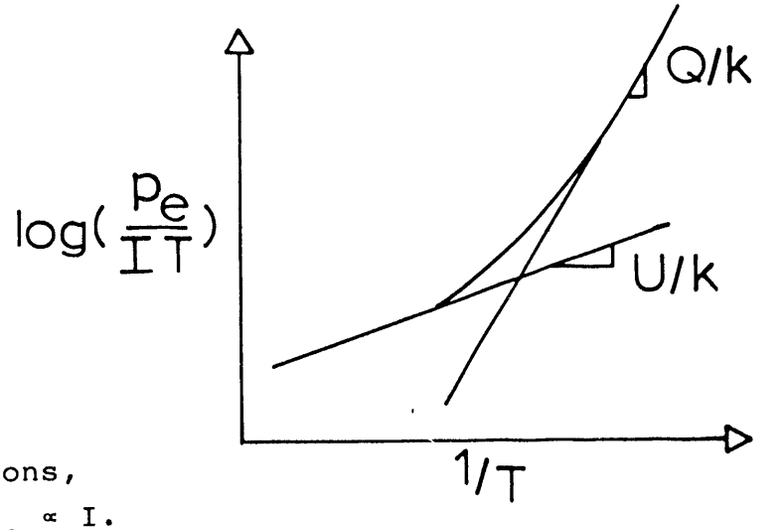

1. In the general case, Eq. (B8) suggest two regions on a $\log(p_e/IT)$ vs. $^1/T$ plot, and one suspects that Q > U, as showned.
2. Under isothermal conditions, Eq. (B8) predicts that $p_e \propto I$.
3. Whether catalysis or diffusion is dominant, Eq. (B8) predicts that $p_e/I \propto Te^{\theta/T}$ which is very strongly temperature dependent.
4. If the sensor operates in a temperature range where diffusion (or catalysis) dominates, then Eq. (B8) predicts a two-point calibration of the sensor -- same p_e at two different temperatures to determine β and Q/k (or α and U/k).
5. The voltage V enters the sensor operation as shown. For a given p_e, there are three regions:

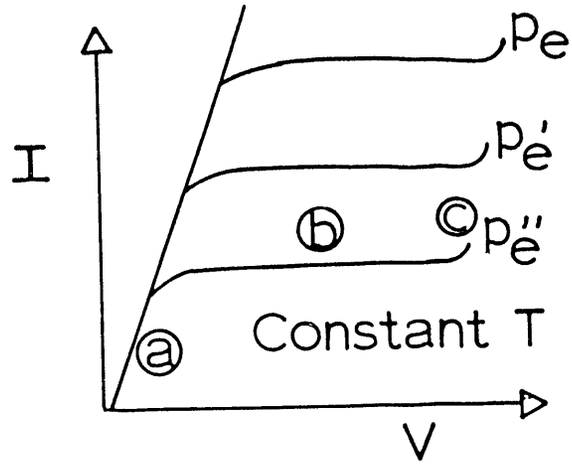

   a. I ∝ V -- in this region V is not large enough to "sweep" all the catalyzed oxygen from the cathode to the anode, and "ohmic" behavior occurs.
   b. Constant I -- Eq. (B8) applies in this region.
   c. I-V upturn -- Electronic conduction begins to contribute.

6. The reason why the OS3 "Capacitor" sensors operate at such low temperatures is that the multilayer structure involves thin ceramic layers arranged in parallel electrically, plus the fact that the oxygen ionic conductivity is ~ 30 times larger than zirconia. These three factors operate to lower the sensor resistance to the point that measurable currents result from small voltages at low temperatures (~ 200 °C compared to ~ 600-700 °C for zirconia).

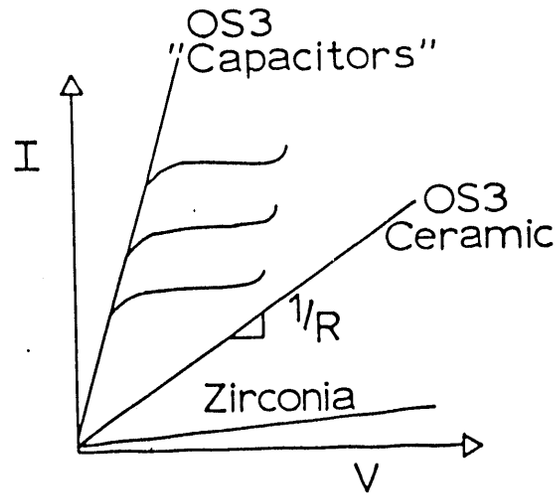

7.

Model Above

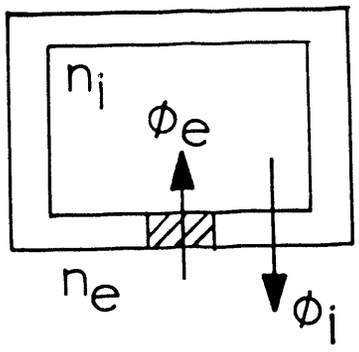

Capacitor Model

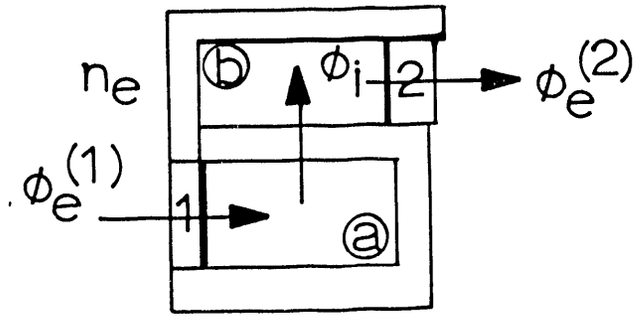

The model treated above involves one diffusion plug whereas the multilayer-capacitor design involves two plugs, as shown. At steady-state for the capacitor model

$$A_e^{(1)}\,\phi_e^{(1)} = A_i\phi_i = A_e^{(2)}\,\phi_e^{(2)} \qquad \text{(B11)}$$

because no O_2 moles are collecting in the a and b cavities or in the ceramic membrane. From Eq. (B2) we have for the ϕ_e fluxes from Eq. (B11),

$$D^{(1)}(n_e - n_i^{(a)})/\delta^{(1)} = D^{(2)}(n_i^{(b)} - n_e)/\delta^{(2)} \qquad \text{(B12)}$$

where the superscripts refer to the plugs and the two cavities, and we have assumed that $A_e^{(1)} \cong A_e^{(2)}$. If we further assume that $D^{(1)} = D^{(2)}$ (i.e., same temperature and that $\delta^{(1)} \cong \delta^{(2)}$, then Eq. (B12) yields the simple relationship

$$n_i^{(a)} + n_i^{(b)} \cong 2\, n_e \qquad \text{(B13)}$$

The meaning of Eq. (B13) is that the slight "vacuum" in cavity a (i.e., $n_i^{(a)} < n_e$) is compensated by the "overpressure" in cavity b (i.e., $n_i^{(b)} > n_e$). The important point, however, is that the first equality in Eq. (B11) is the <u>same</u> as Eq. (B1) (apart from a sign convention), and so Eqs. (B8) - (B10) apply to the capacitor model.

8. From Eq. (B8), $p_e/I = \beta T e^{Q/kT}$, which is a very strong temperature dependence. An important question is the relative <u>uncertainly</u> in a p_e-measurement that results from a uncertainty in measuring T. We find that

$$\delta p_e/p_e = (1-Q/kT)\delta T/T \qquad \text{(B14)}$$

In this diffusion-dominated case, $Q/k = 1.234 \times 10^4$ K, and we have from Eq. (B14) the following table

T, °C	$\delta p_e/p_e$
100	-32.1 (δT/T)
200	-25.1 (δT/T)
300	-20.5 (δT/T)
400	-17.3 (δT/T)

So for example, if at 200 °C (= 473 K) δT/T were ± 5% (i.e., δT = 23 °C = 23 K), then $\delta p_e/p_e$ would be ± 130%. If however, δT were ±5 °C, then $\delta pe/p_e$. would be ± 27. Therefore a <u>premium</u> is placed on the T-Measurement.

FIGURES

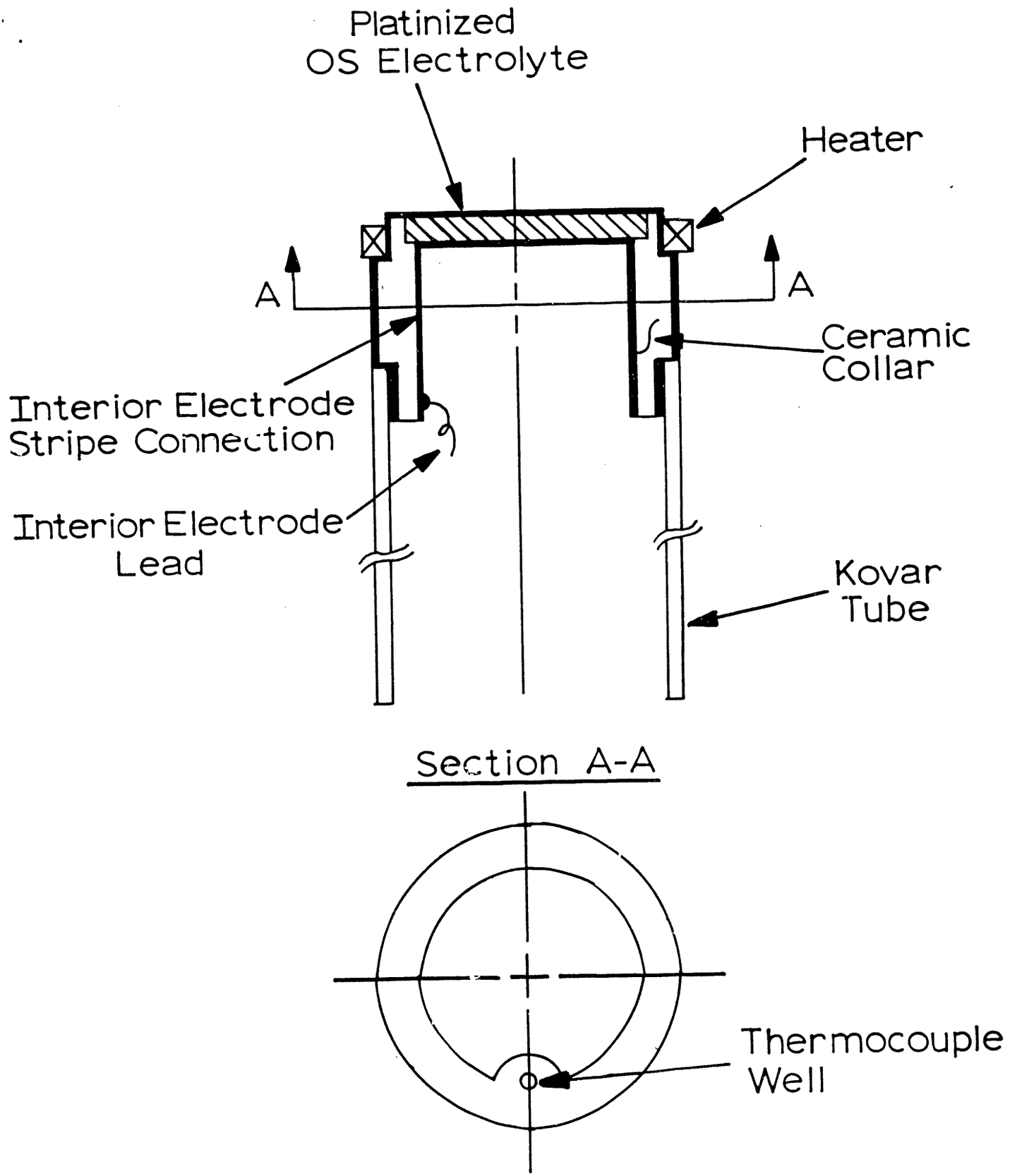

Figure 1: Original Working Design for CPI OS Nernst Sensor.

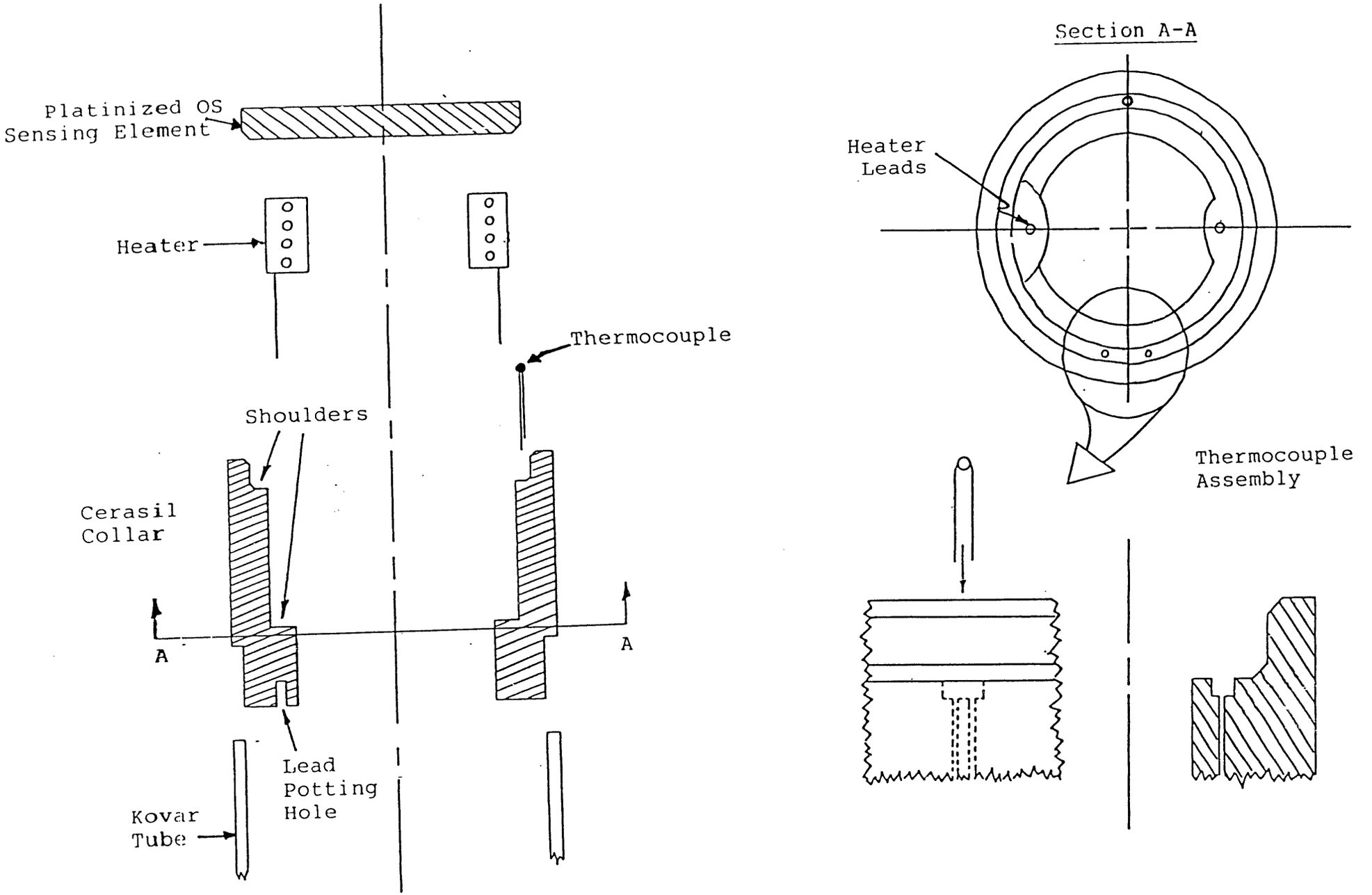

Figure 2: First Sensor Redesign.

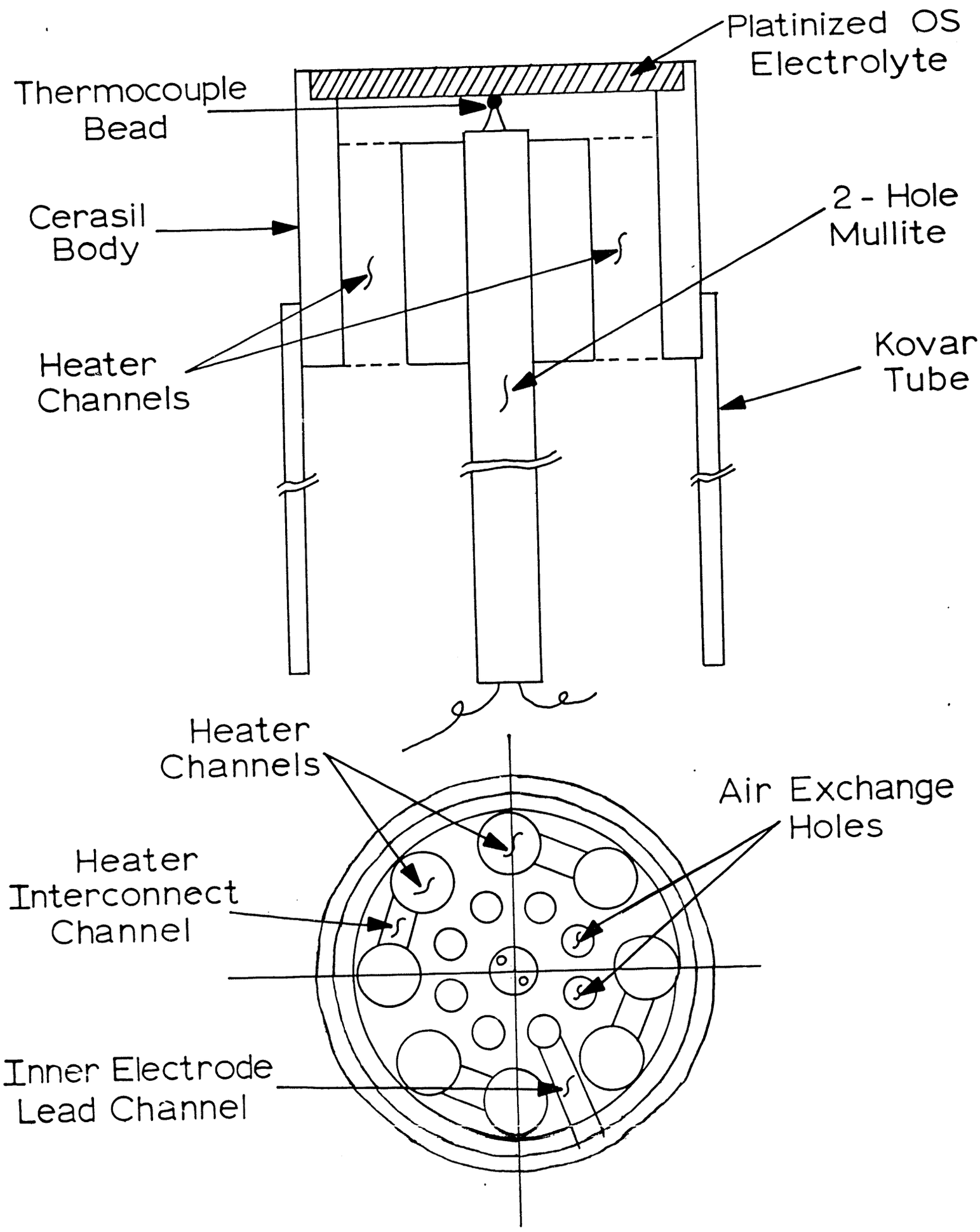

Figure 3: "Revolver Bullet-Cylinder" Redesign.

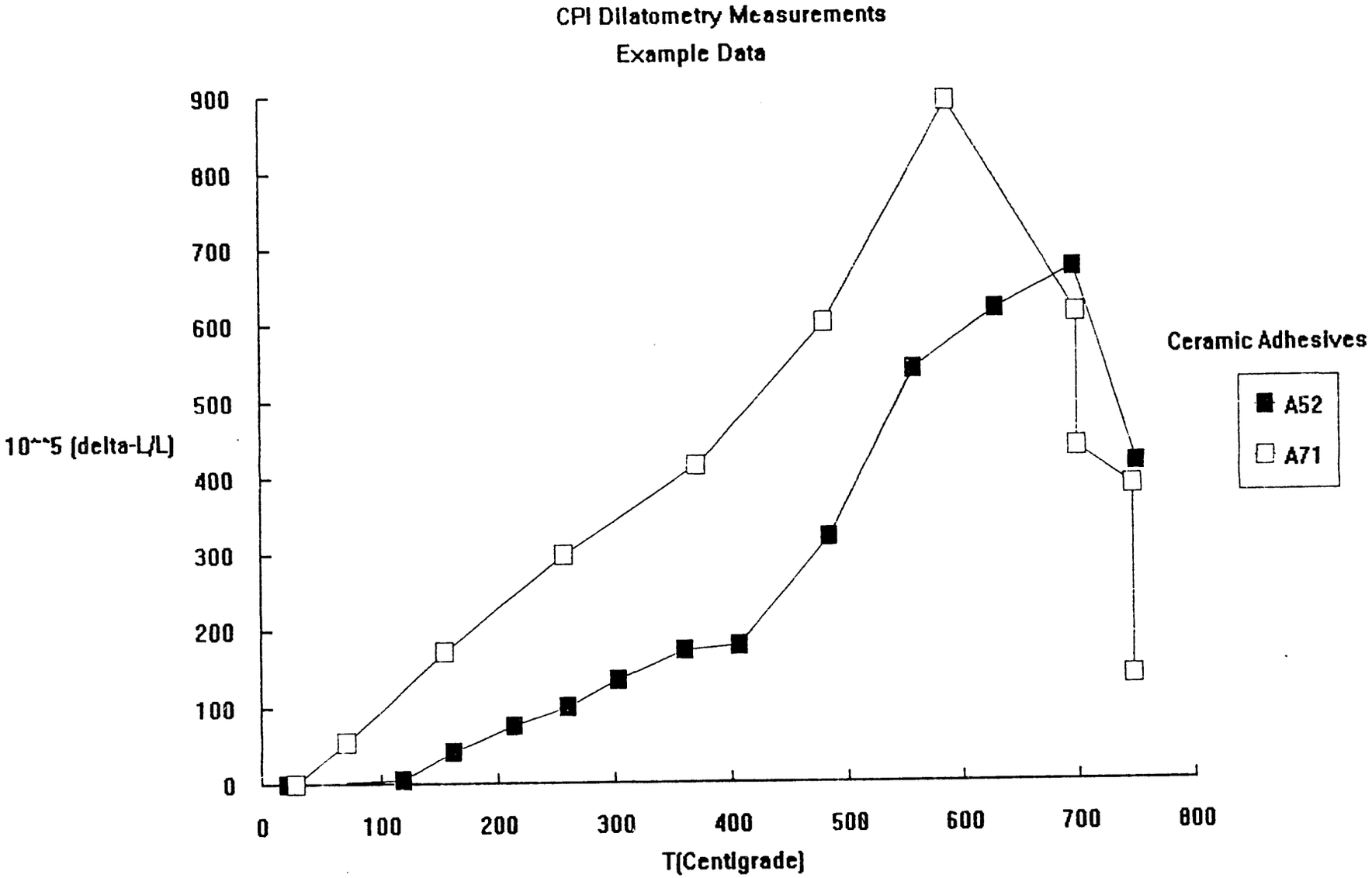

Figure 4: CPI dilatometry measurements on ceramic adhesives

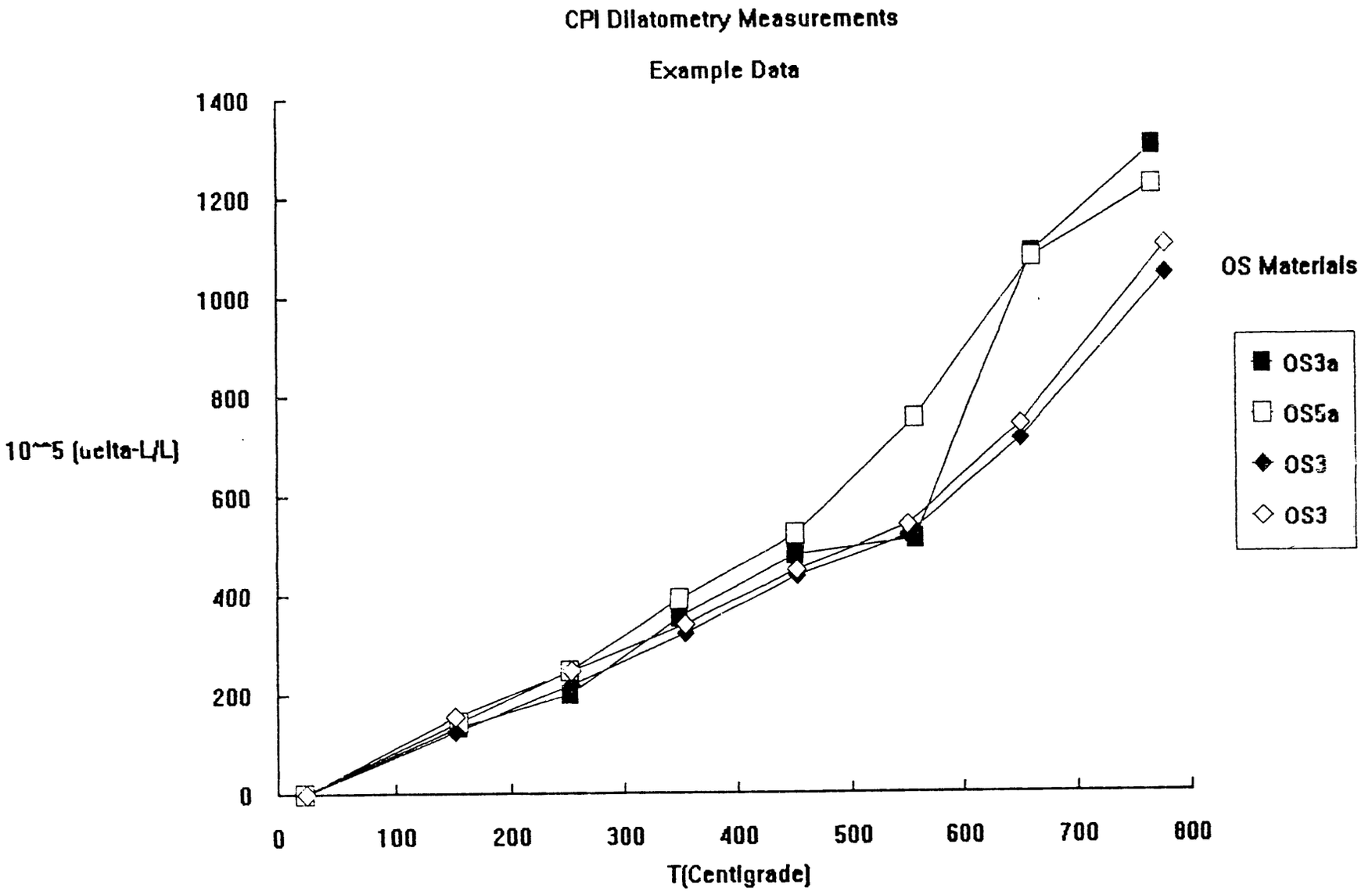

Figure 5: CPI dilatometry measurements on various OS materials

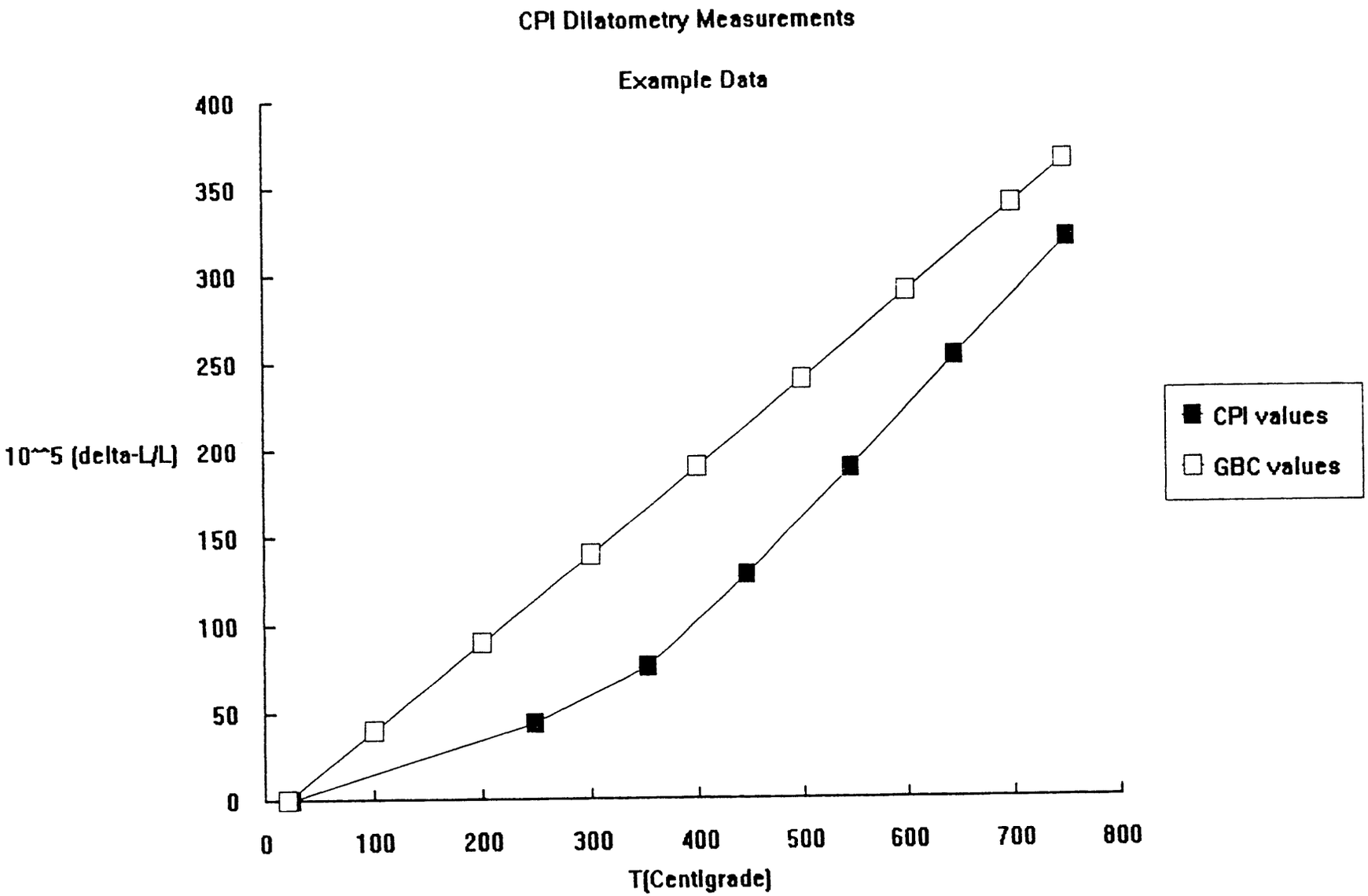

Figure 6: Comparison of CPI measurements and GBC accepted values for thermal expansion of Cerasil 223U

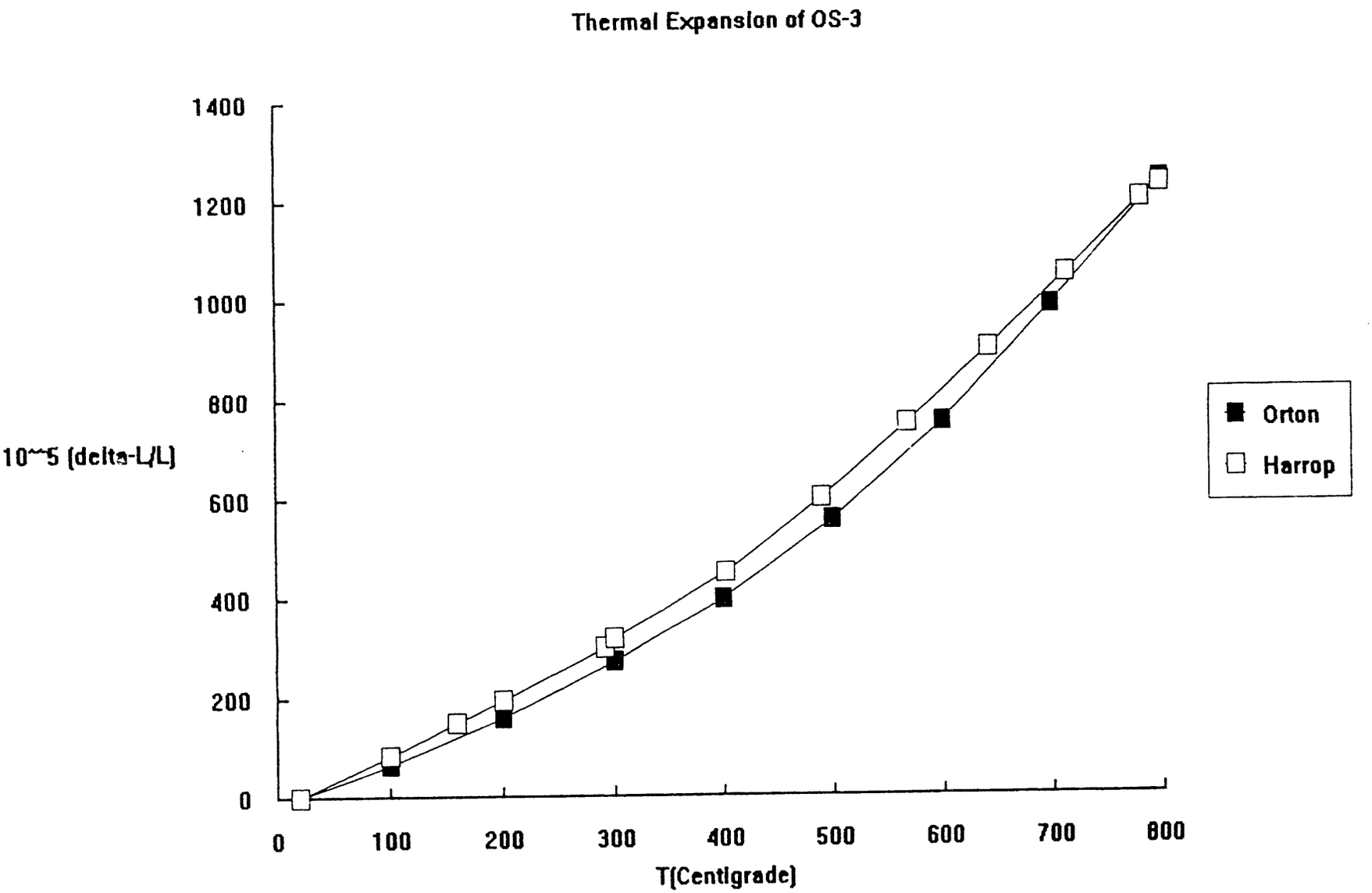

Figure 7: Independent Laboratory Measurements of OS-3 thermal expansion

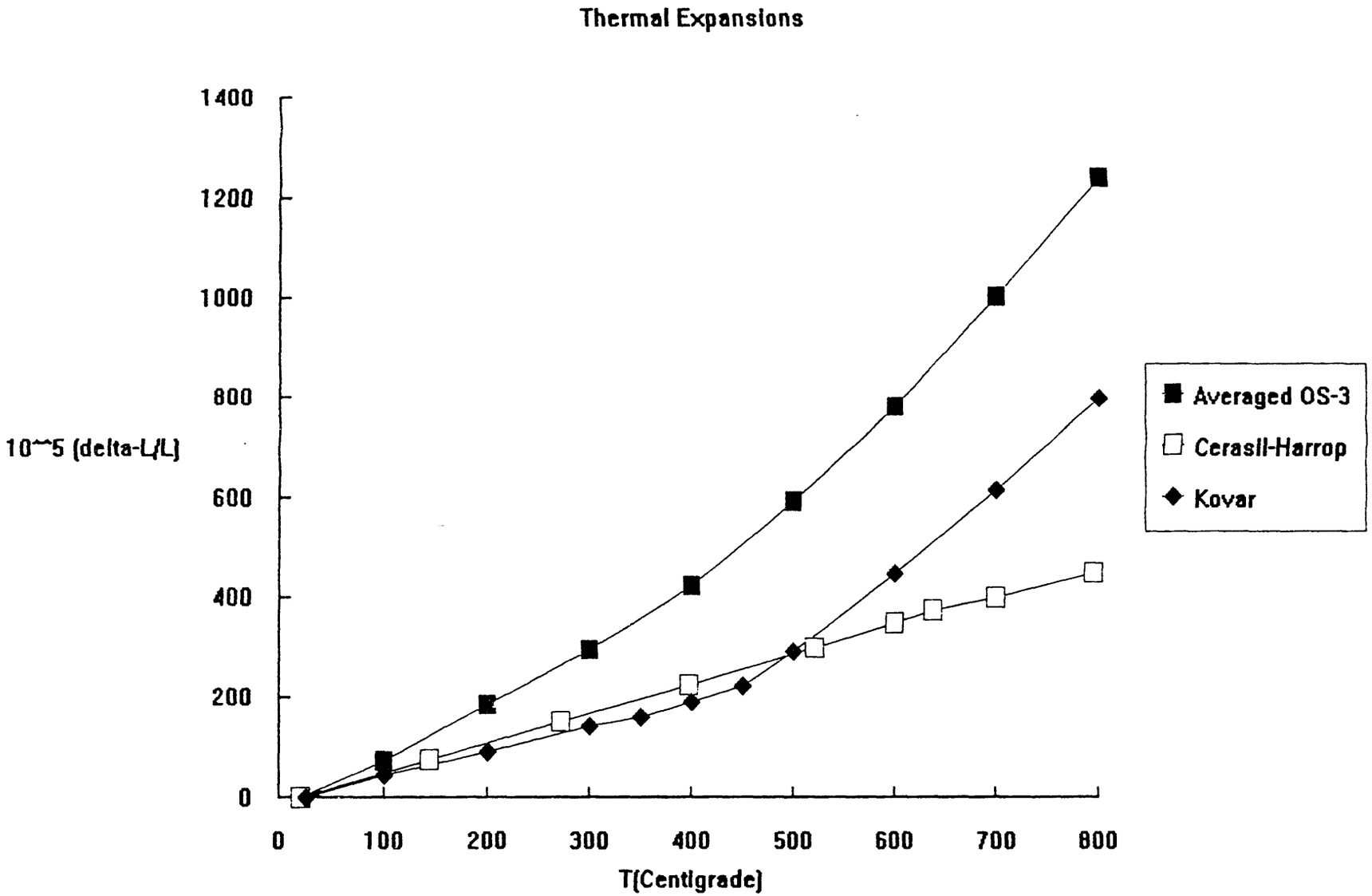

Figure 8: A comparison of the thermal expansions of the materials first envisioned for use in the minature sensor

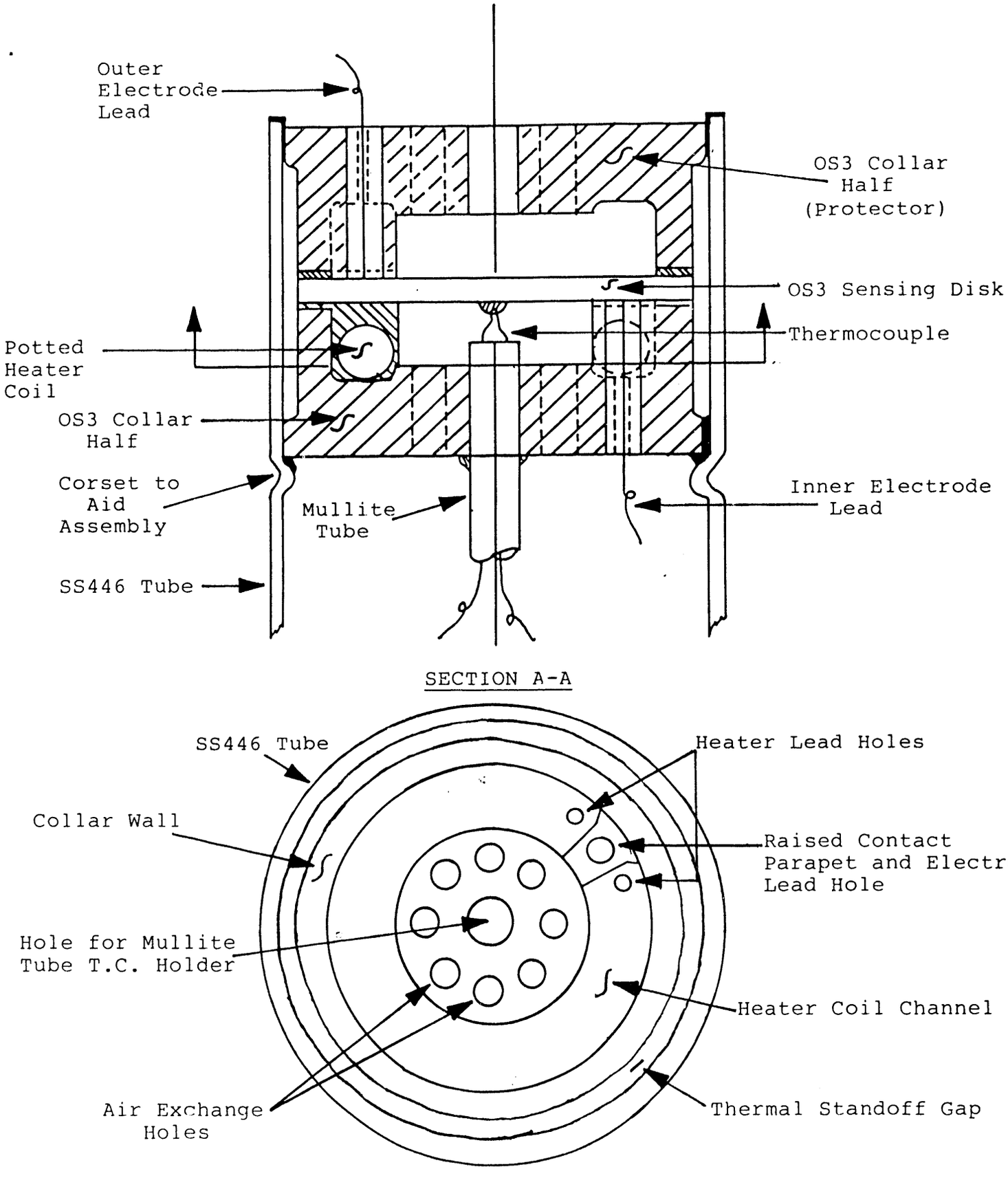

Figure 9.a. Final Sensor Redesigns, First Assembly concept.

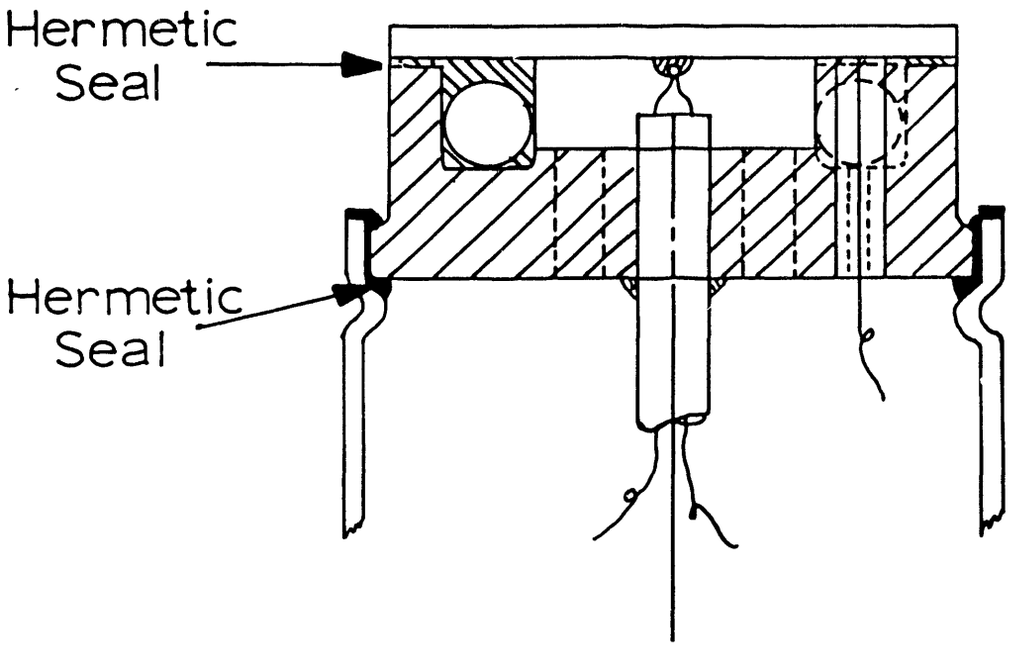

Figure 9.b. Final Sensor Redesigns, Second Assembly Concept.

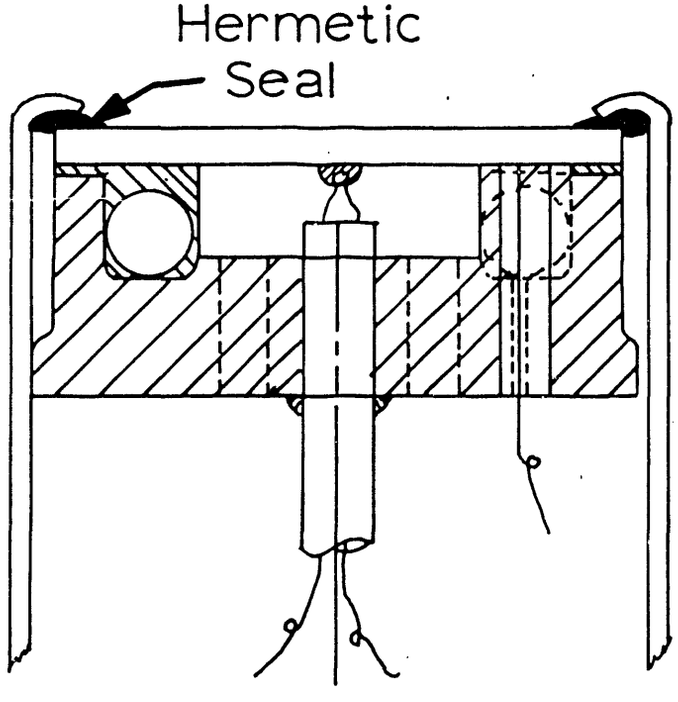

Figure 9.c. OS-3 Nernst Sensor, Final Assembly Design.

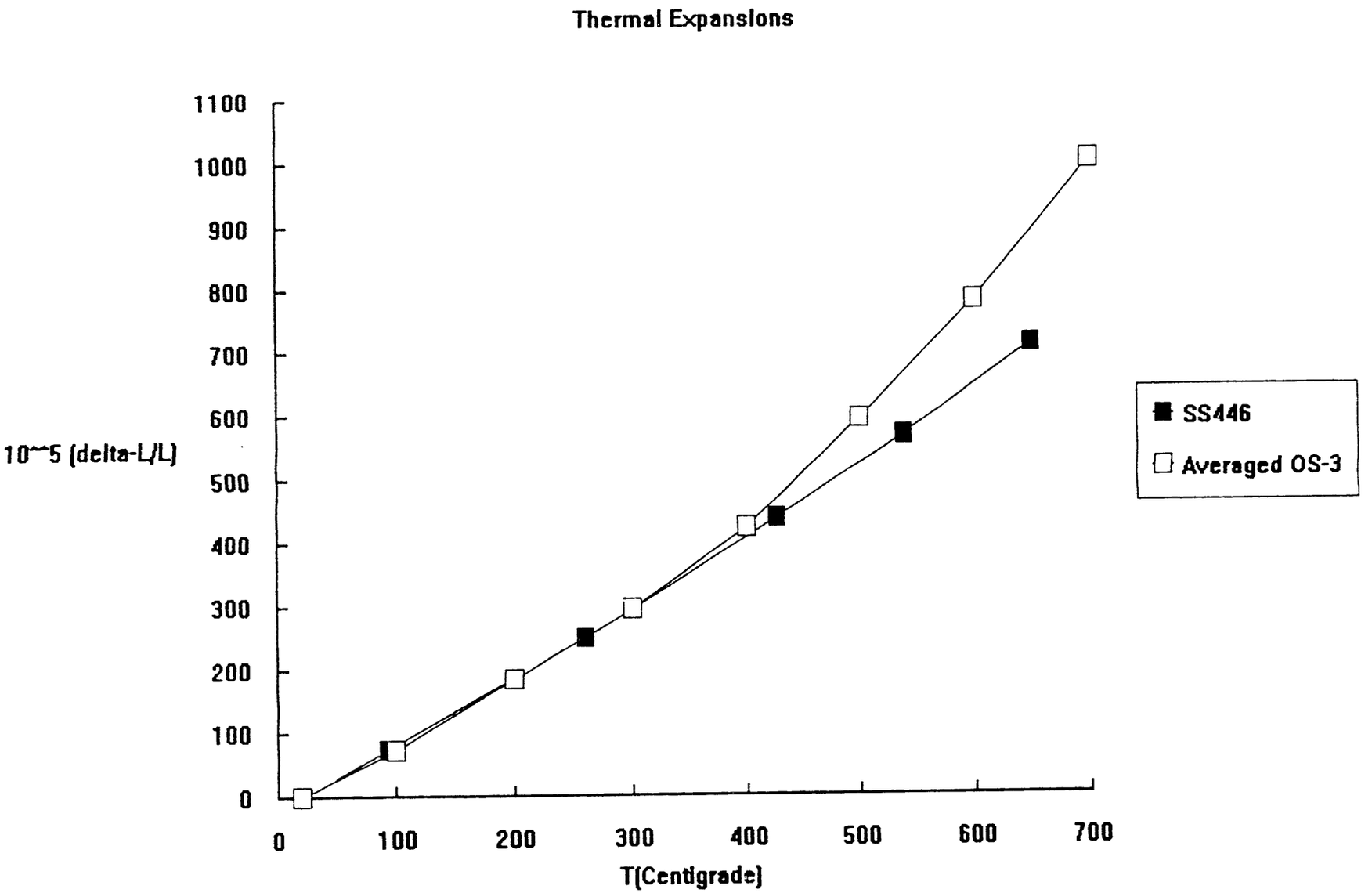

Figure 10: Comparison of the thermal expansions of OS-3 and SS446

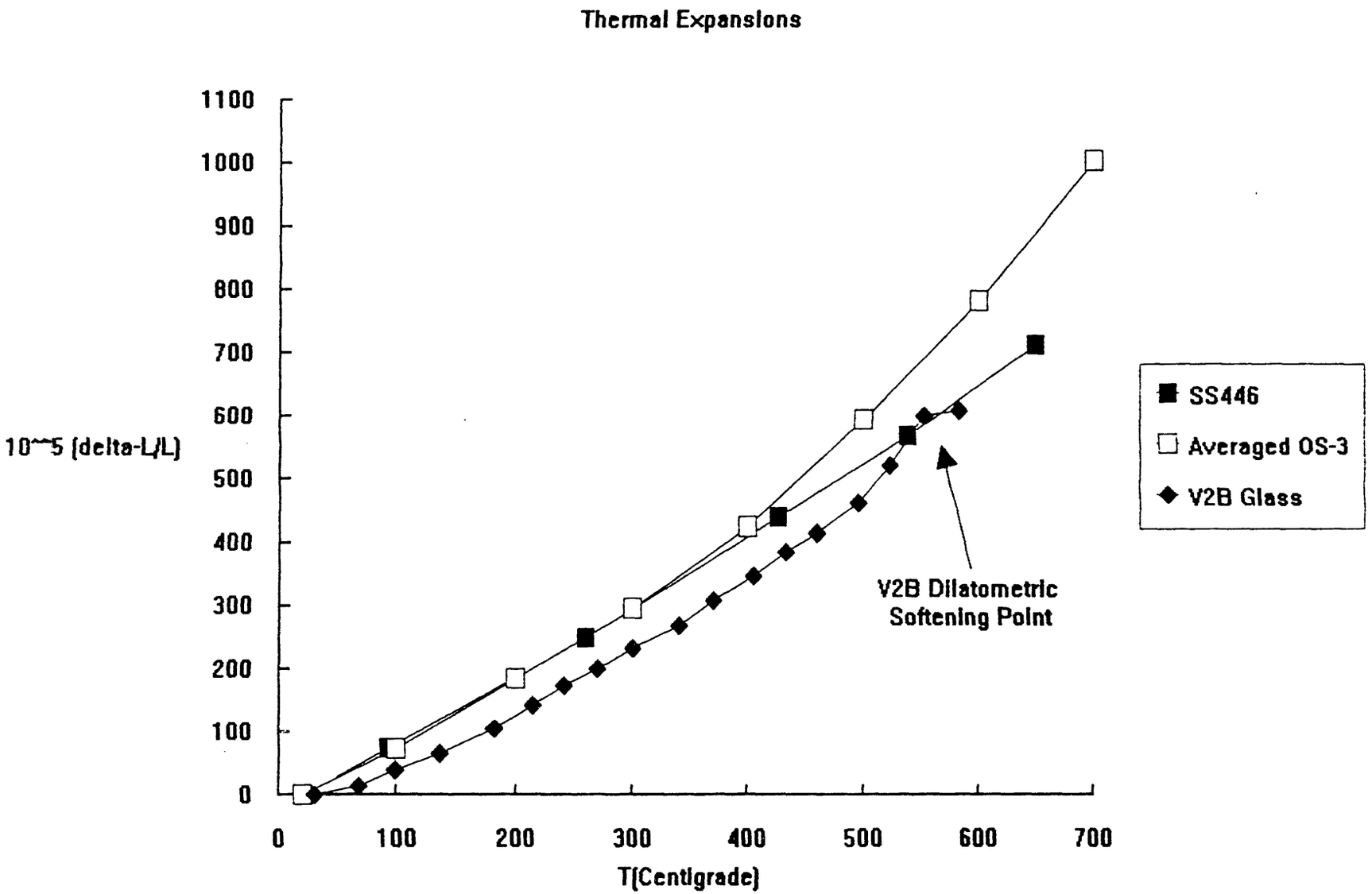

Figure 11: Comparison of the thermal expansions of the final sensor materials

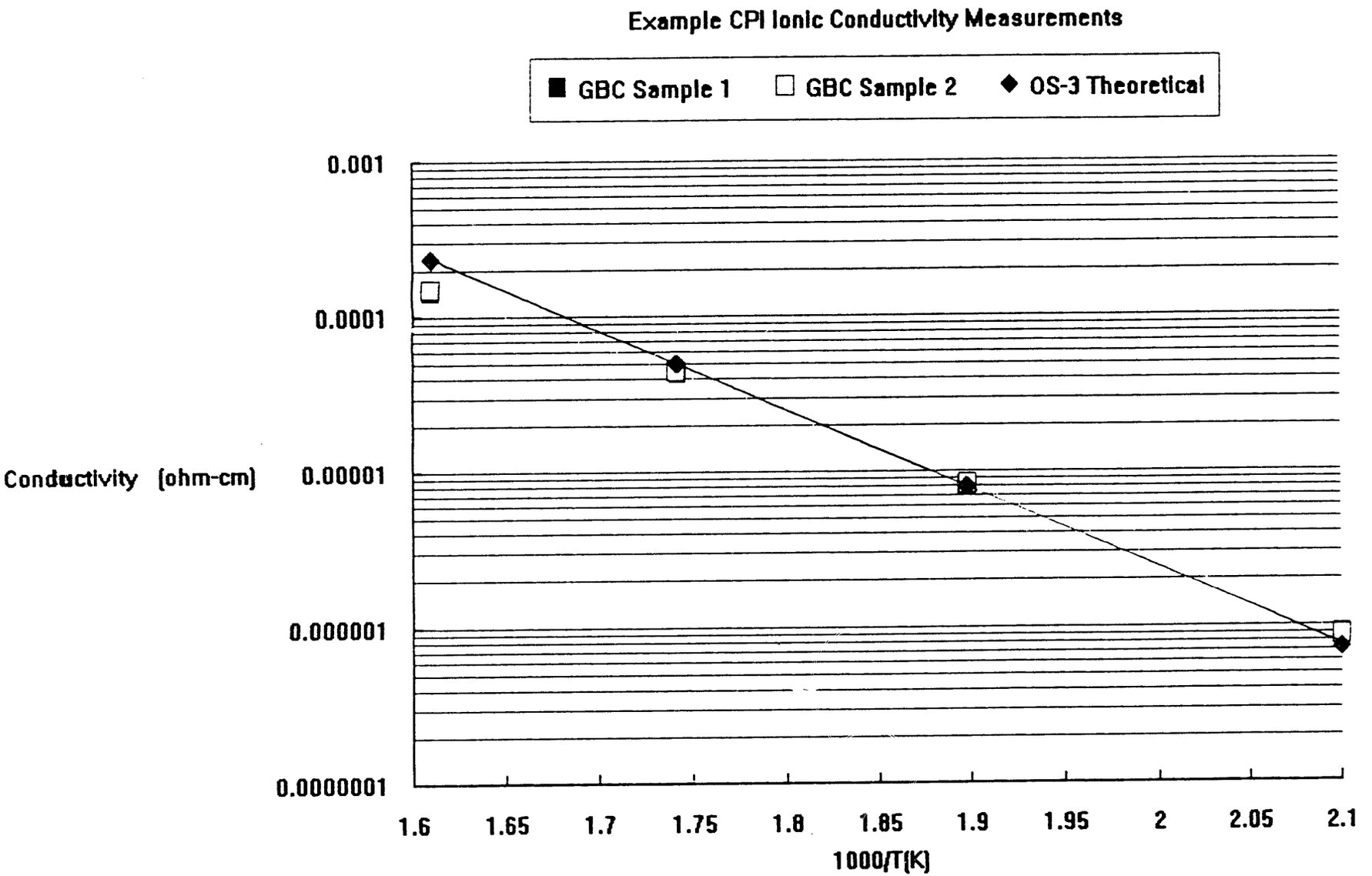

Figure 12: CPI Ionic conductivity checks on GBC produced OS-3 parts

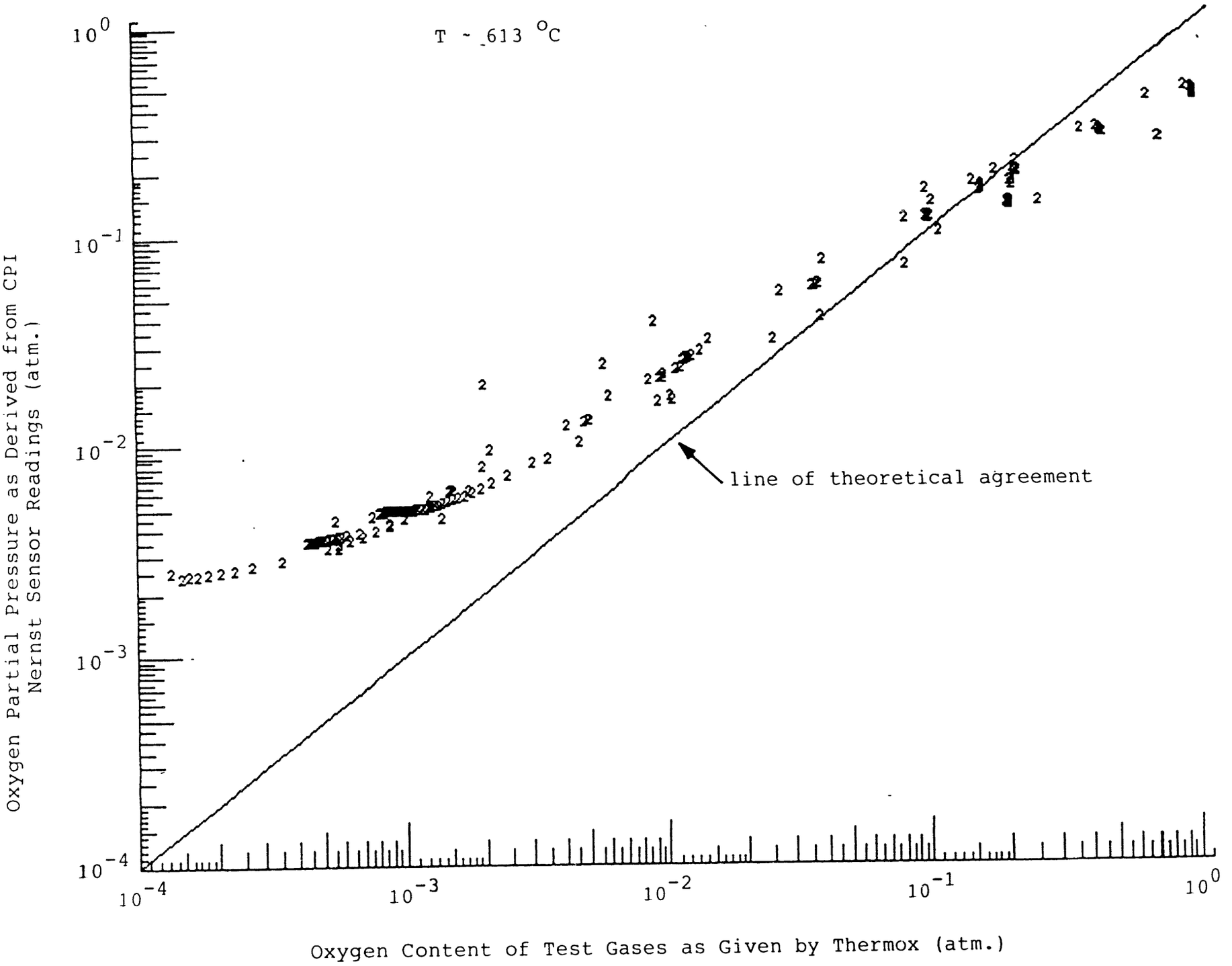

Figure 13: Example data from CPI OS-3 Nernst Sensor

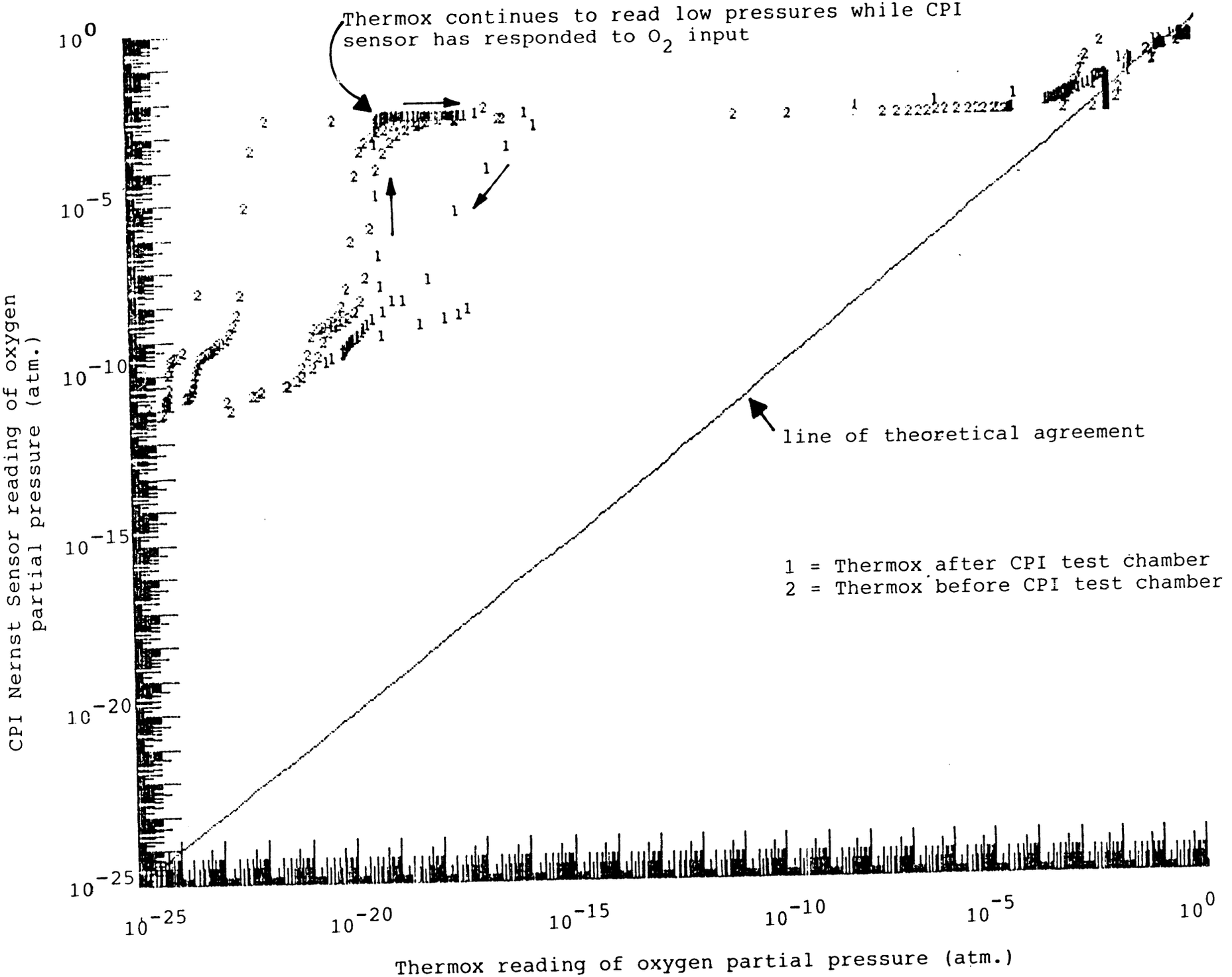

Figure 14: CPI Nernst sensor/Thermox responses to large shifts in oxygen partial pressure.

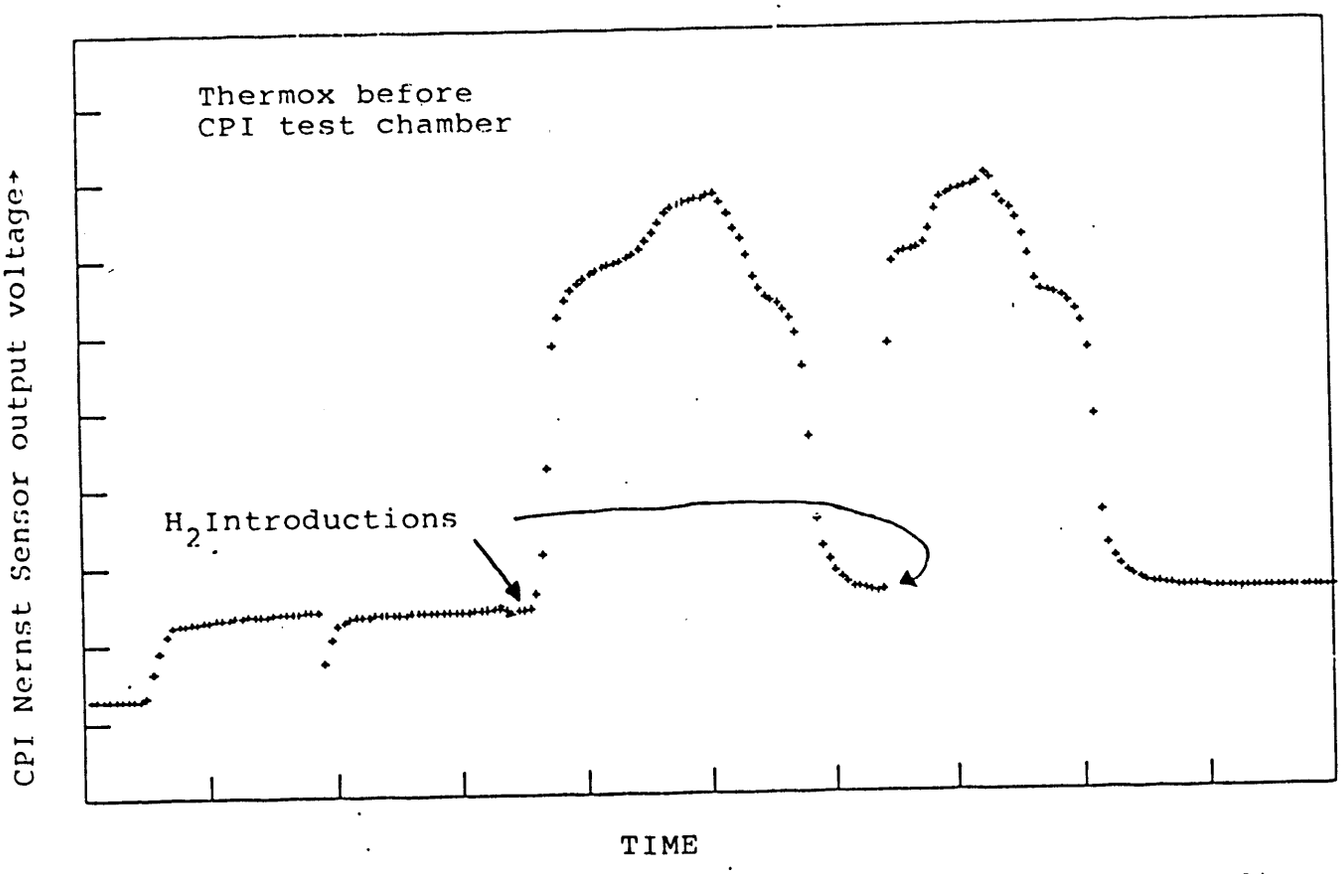

Figure 15a: CPI Nernst Sensor response test Thermox preceding.

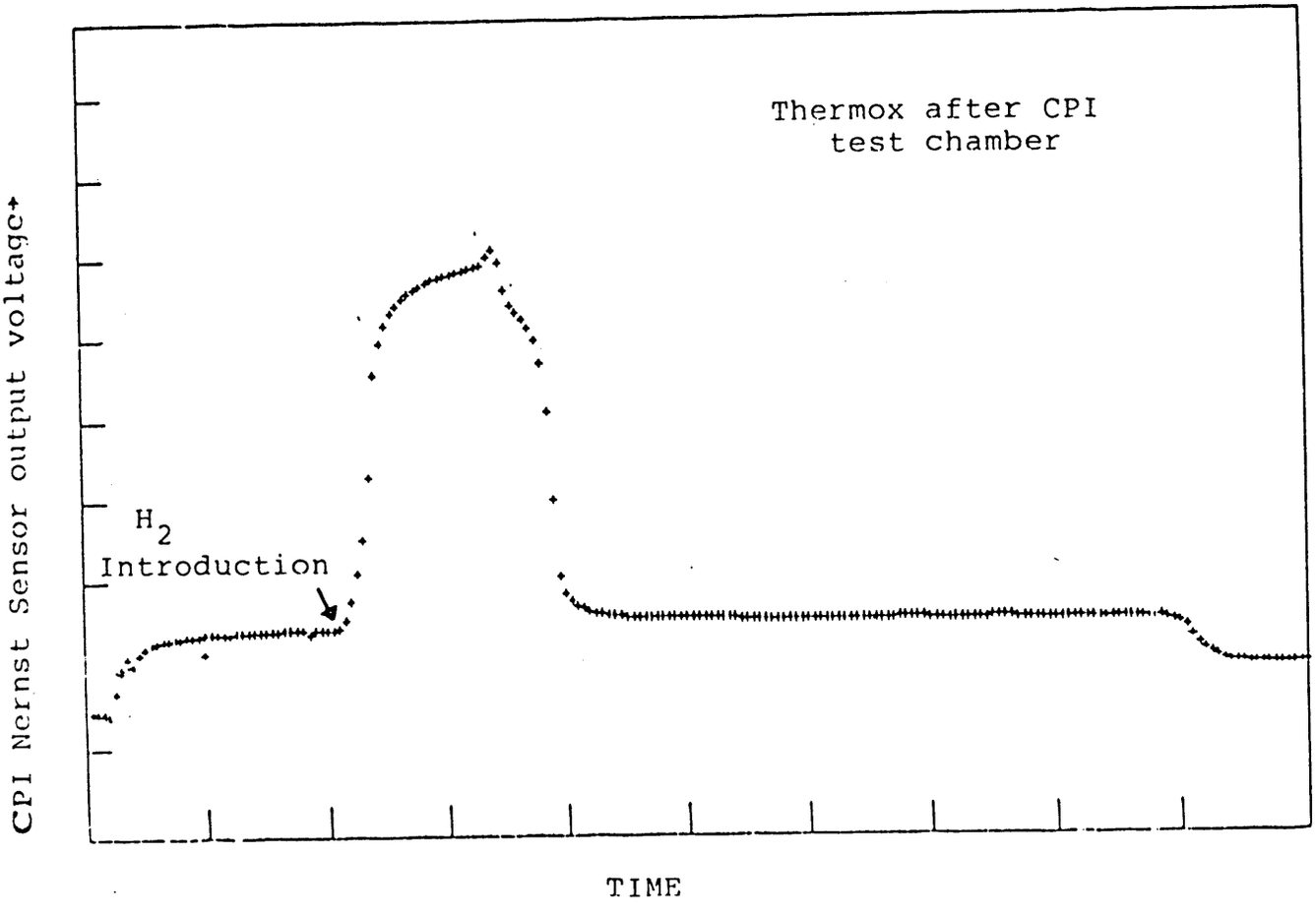

Figure 15b: CPI Nernst Sensor response test Thermox following.

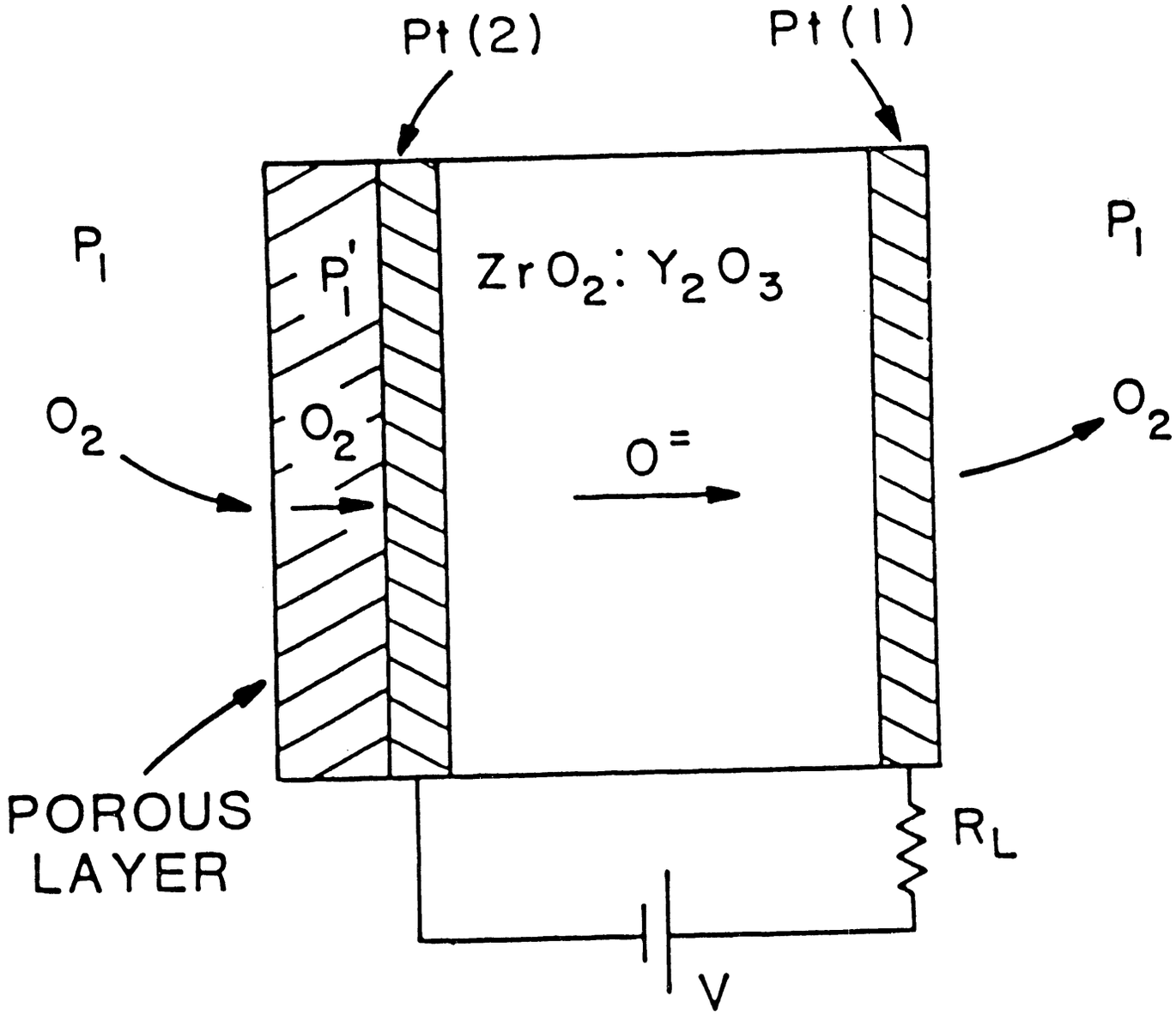

Figure 16. A Schematic of a single-cell O_2-pumping sensor with a porous layer on the cathode electrode acting as a diffusion barrier.

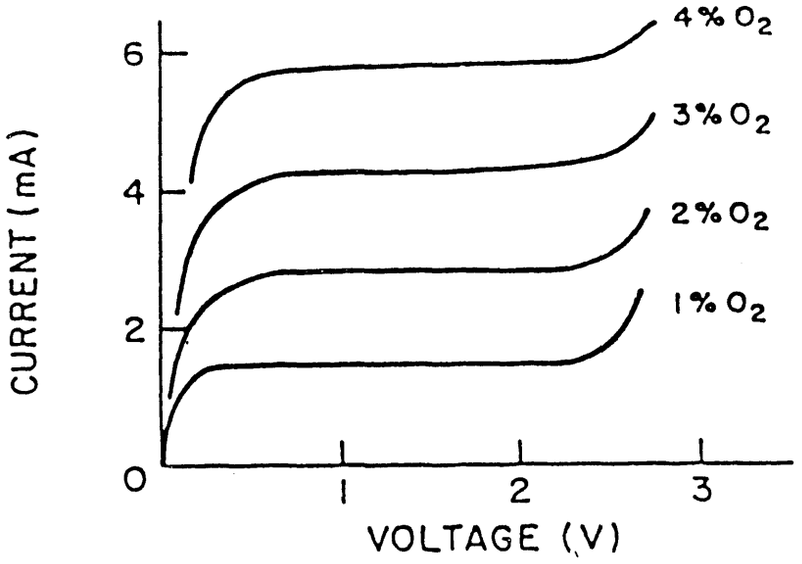

Figure 17. Current-voltage characteristics of a single-cell pumping device with low internal impedance exhibiting saturation currents over a wide range of oxygen pressures.

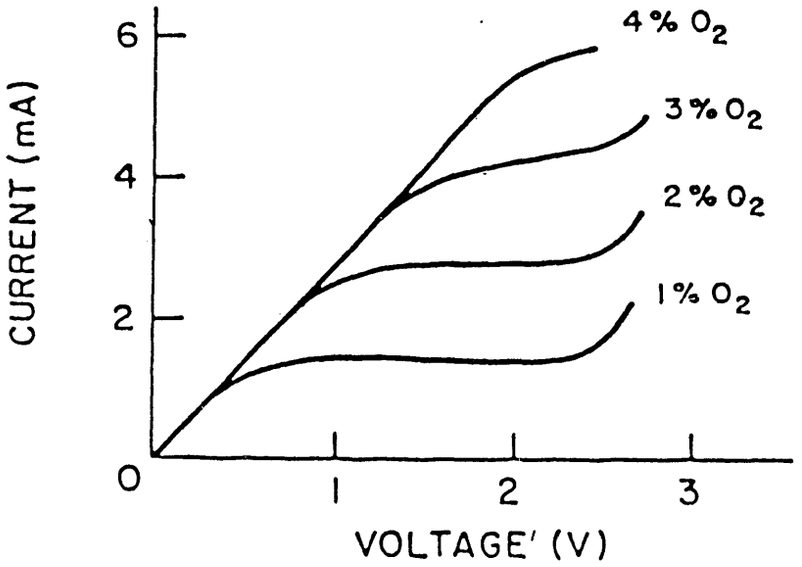

Figure 18. Current-voltage characteristics of a device with high internal impedance exhibiting current saturation over a narrow range of oxygen pressures.

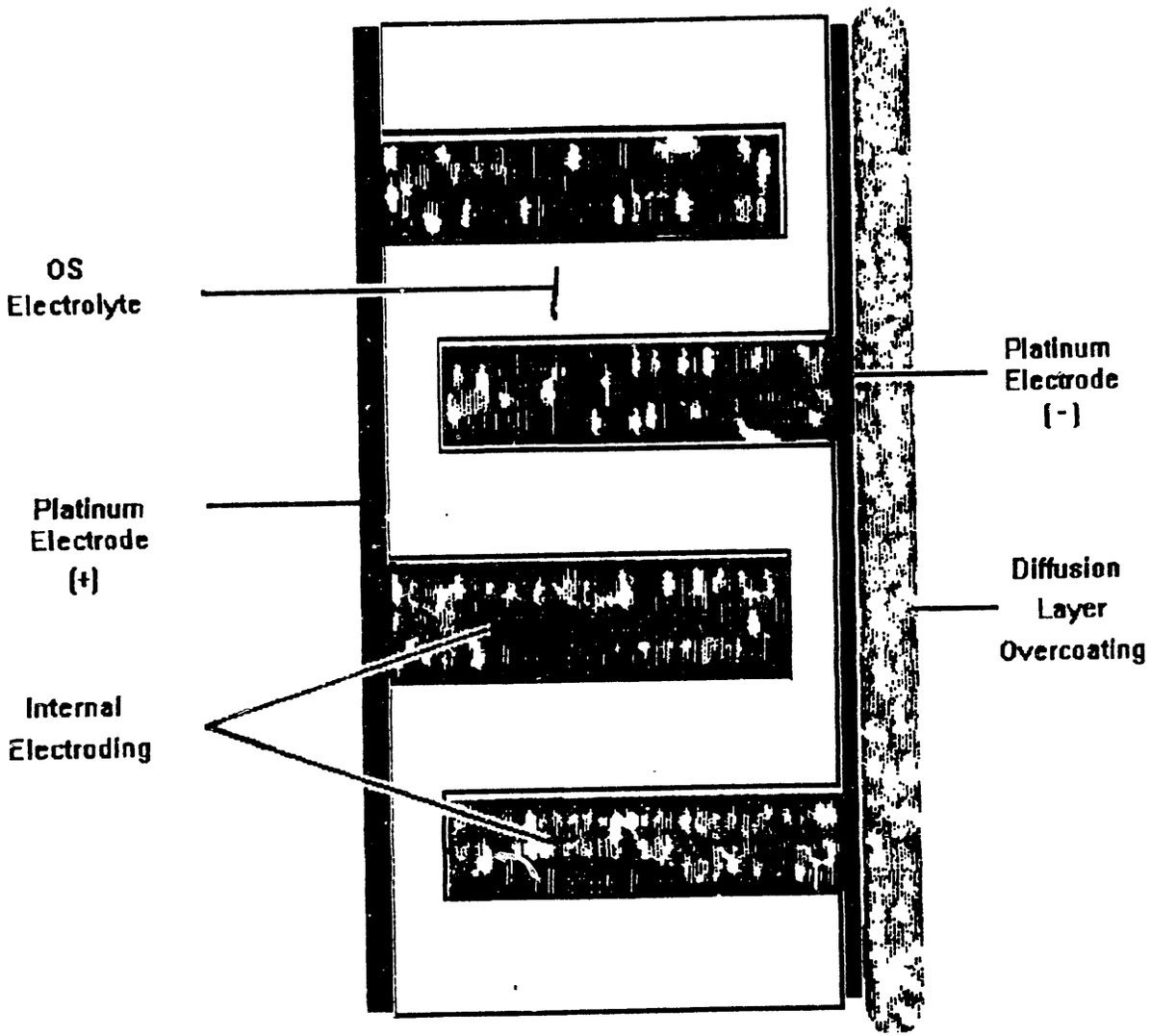

Figure 19: Schematic of CPI OS-Multilayer Amperometric Sensor

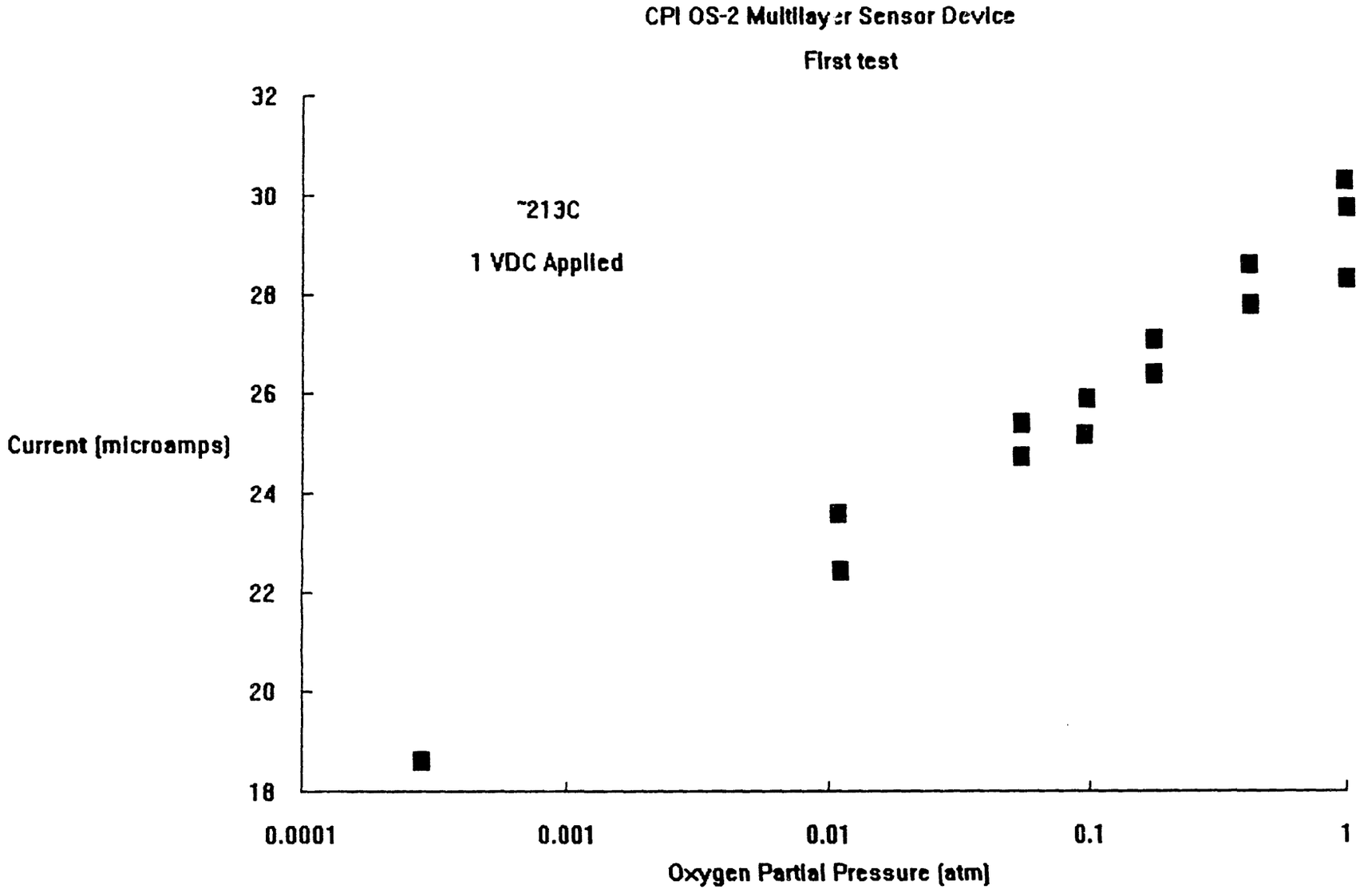

Figure 20: Current vs. oxygen partial pressure behavior for "bare" OS-2 multilayer amperometric sensor device

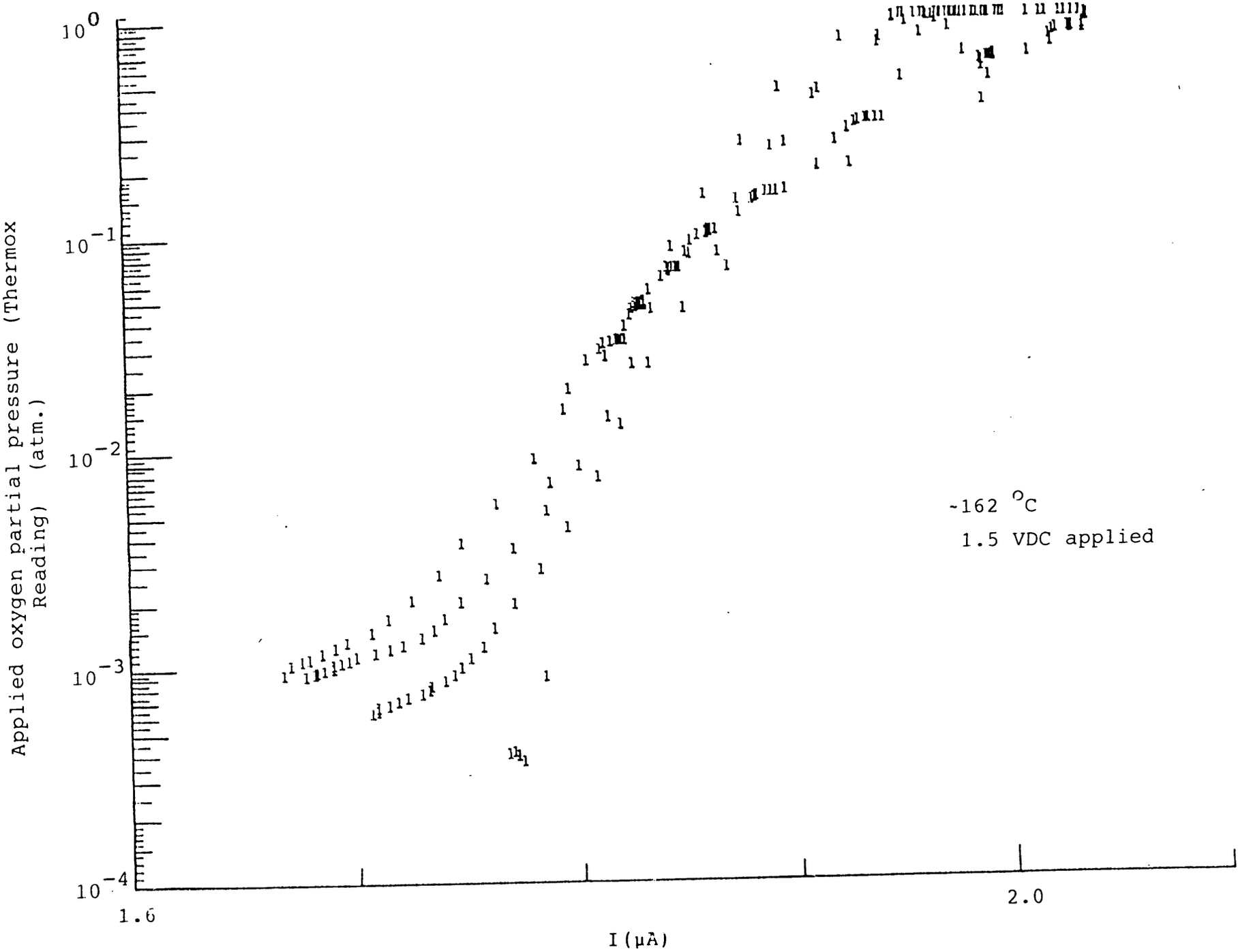

Figure 21: CPI amperometric sensor current variations with applied oxygen partial pressure.

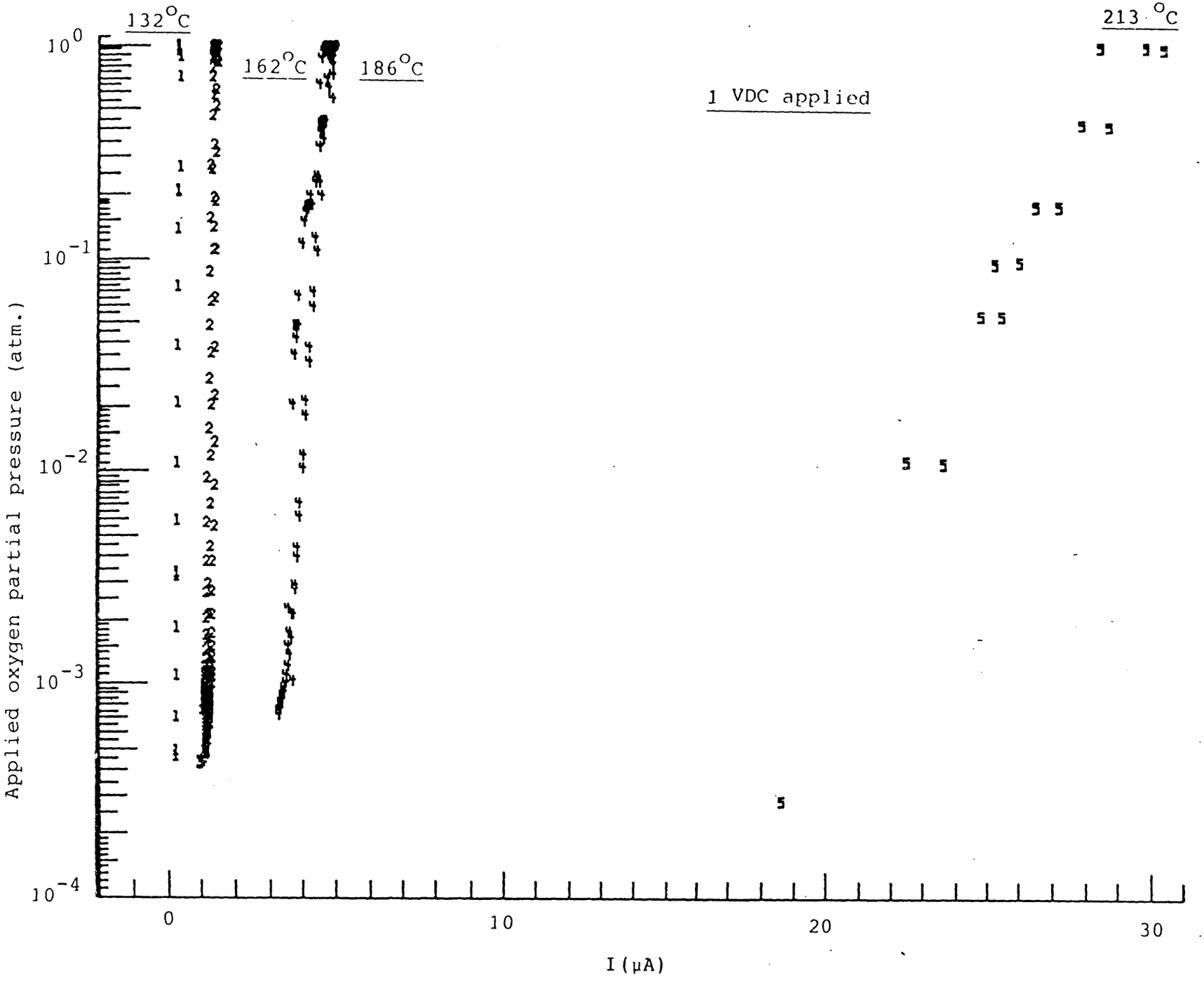

Figure 22: Applied oxygen partial pressure and temperature dependencies of current through CPI amperometric sensor.

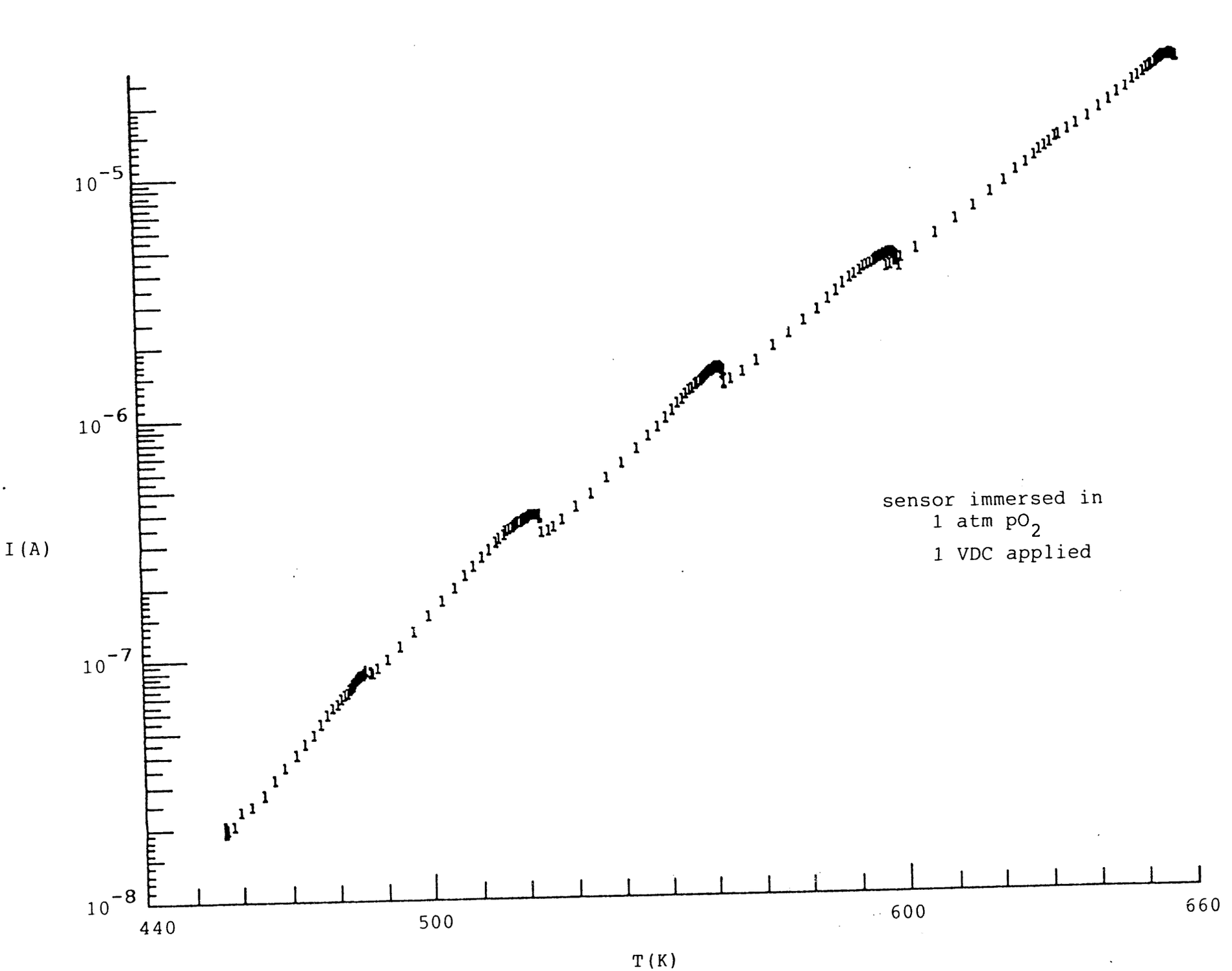

Figure 23: Amperometric sensor current vs. temperature, sensor in 100% O_2.

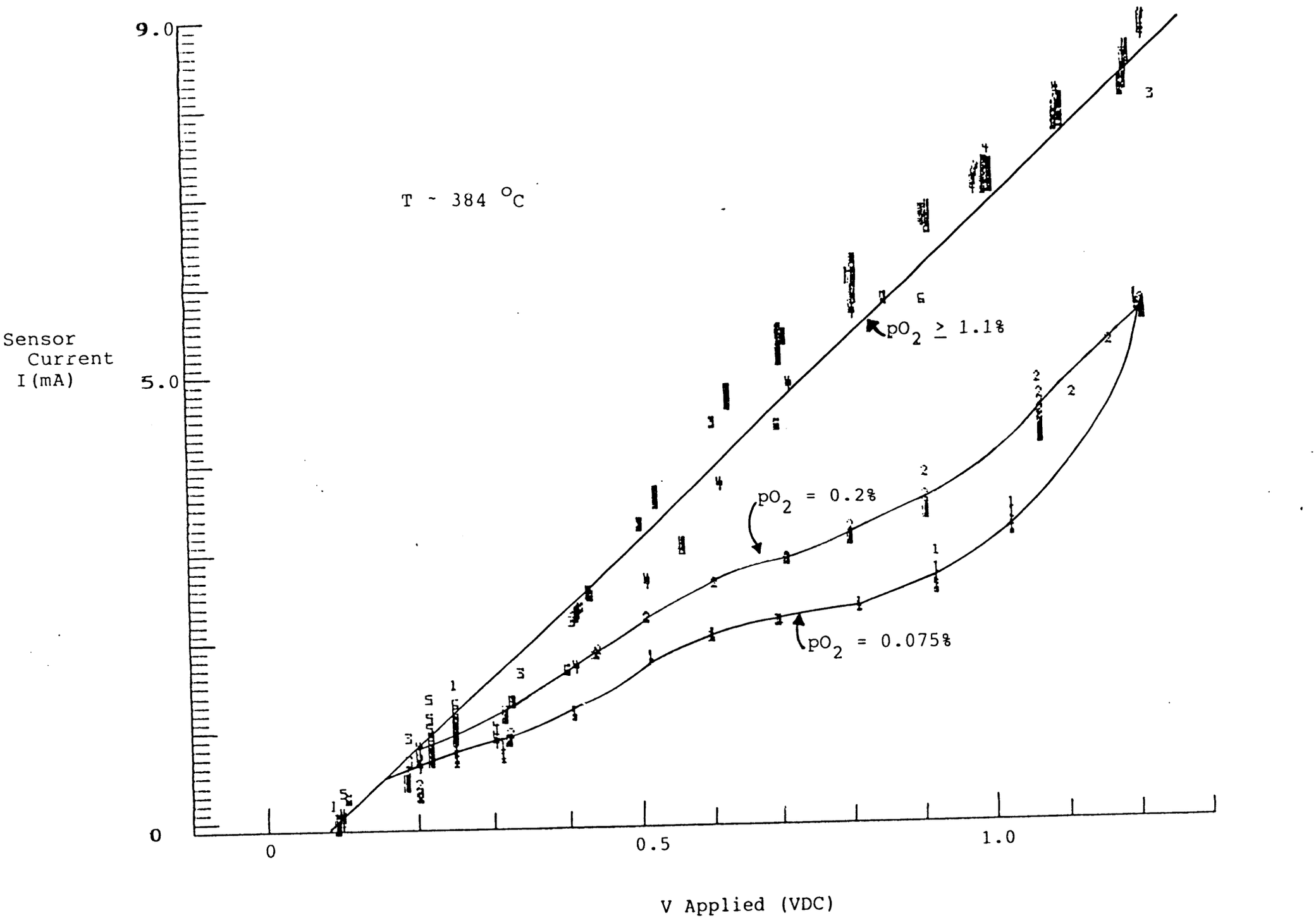

Figure 24: I vs. V Applied behavior for overcoated CPI amperometric sensor.

END

DATE FILMED

11 12 91